VOL 10
ISSUE 5
SEPT 2025

eMetN METEOR JOURNAL

eJournal for meteor observers www.emetn.net

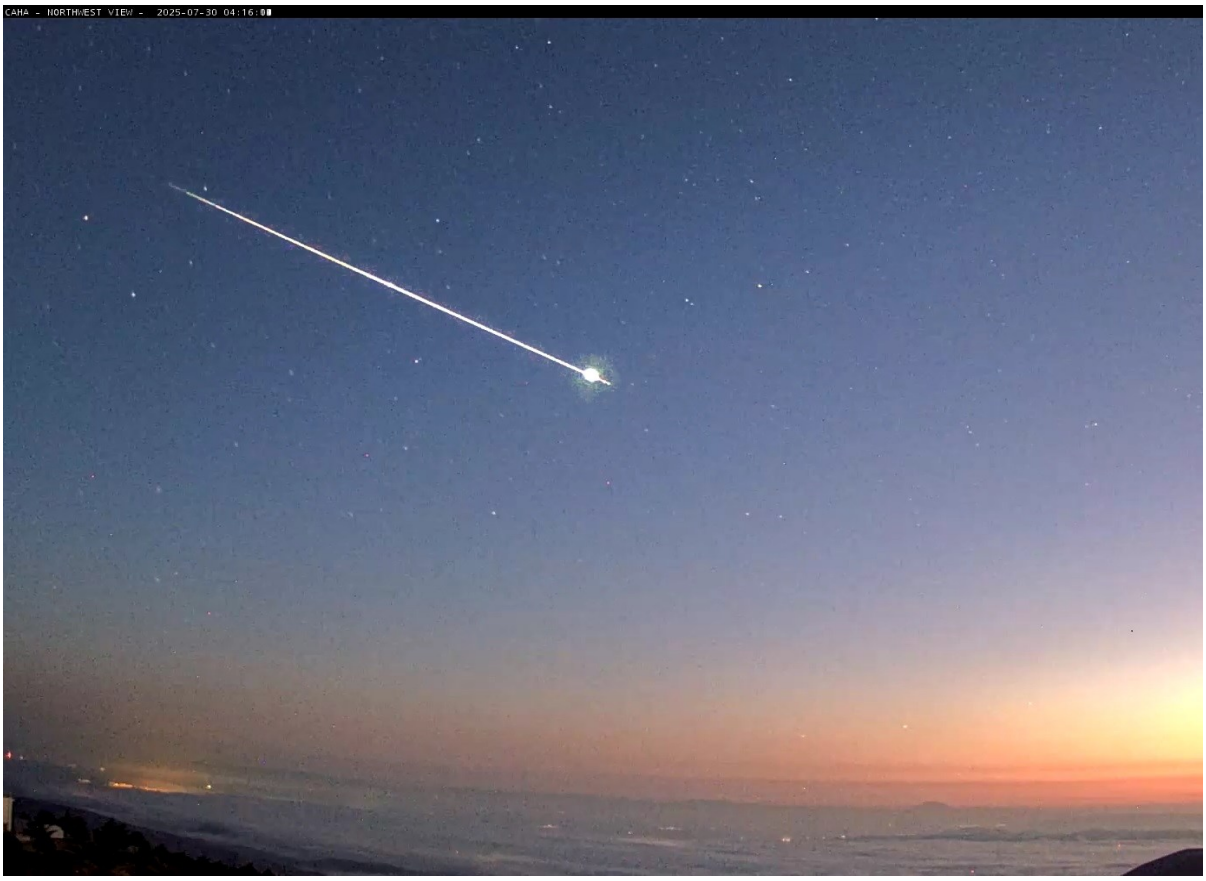

Alpha-Capricornid recorded over Spain on 2025 July 30, at 4:16:11 UT. (Copyright Jose Maria Madiedo).

ISSN 3041 - 4261

Contents

New meteor shower in Equuleus

Denis Vida[1], **Damir Šegon**[2] **and Paul Roggemans**[3]

[1] **Department of Earth Sciences, University of Western Ontario, London, Ontario, N6A 5B7, Canada**
denis.vida@gmail.com

[2] **Astronomical Society Istra Pula, Park Monte Zaro 2, 52100 Pula, Croatia**

[3] **Pijnboomstraat 25, 2800 Mechelen, Belgium**
paul.roggemans@gmail.com

A new meteor shower on a retrograde Halley-type comet orbit (T_J = 0.10) has been detected during June 15–30, 2025 by the Global Meteor Network. Meteors belonging to the new shower were observed between 85° < $\lambda_\odot$ < 99° from a radiant at R.A. = 319.4° and Decl.= +9° in the constellation of Equuleus, with a geocentric velocity of 56.9 km/s. The new meteor shower has been listed in the Working List of Meteor Showers under the temporary name-designation: M2025-O1.

1 Introduction

The GMN radiant map for June 2025 shows a weak concentration of related radiants in the constellation of Equuleus. 46 meteors of this meteor shower were observed by the Global Meteor Network[1] low-light video cameras on 2025 June 16 – 30 (*Figure 1*). The shower was independently observed by cameras in 22 countries across the globe (Australia, Austria, Belgium, Brazil, Chile, Croatia, Czechia, France, Germany, Greece, Hungary, Italy, Luxembourg, Netherlands, New Zealand, Portugal, Slovenia, South Korea, Spain, Switzerland, United Kingdom, United States).

The shower had a median geocentric radiant with coordinates R.A. = 319.4°, Decl. = +9.2°, within a circle with a standard deviation of ±1.2° (equinox J2000.0) see *Figure 2*. The radiant drift in R.A. is +0.66° on the sky per degree of solar longitude and +0.21° in declination, both referenced to $\lambda_\odot$ = 92.2° (*Figures 3 and 4*). The median Sun-centered ecliptic coordinates were $\lambda - \lambda_\odot$ = 232.75°, β = 23.72° (*Figure 5*). The geocentric velocity was 56.9 ± 0.7 km/s.

All meteors appeared during the solar-longitude interval 85° – 99°, with most events around 23–24 June ($\lambda_\odot$ = 92.2°).

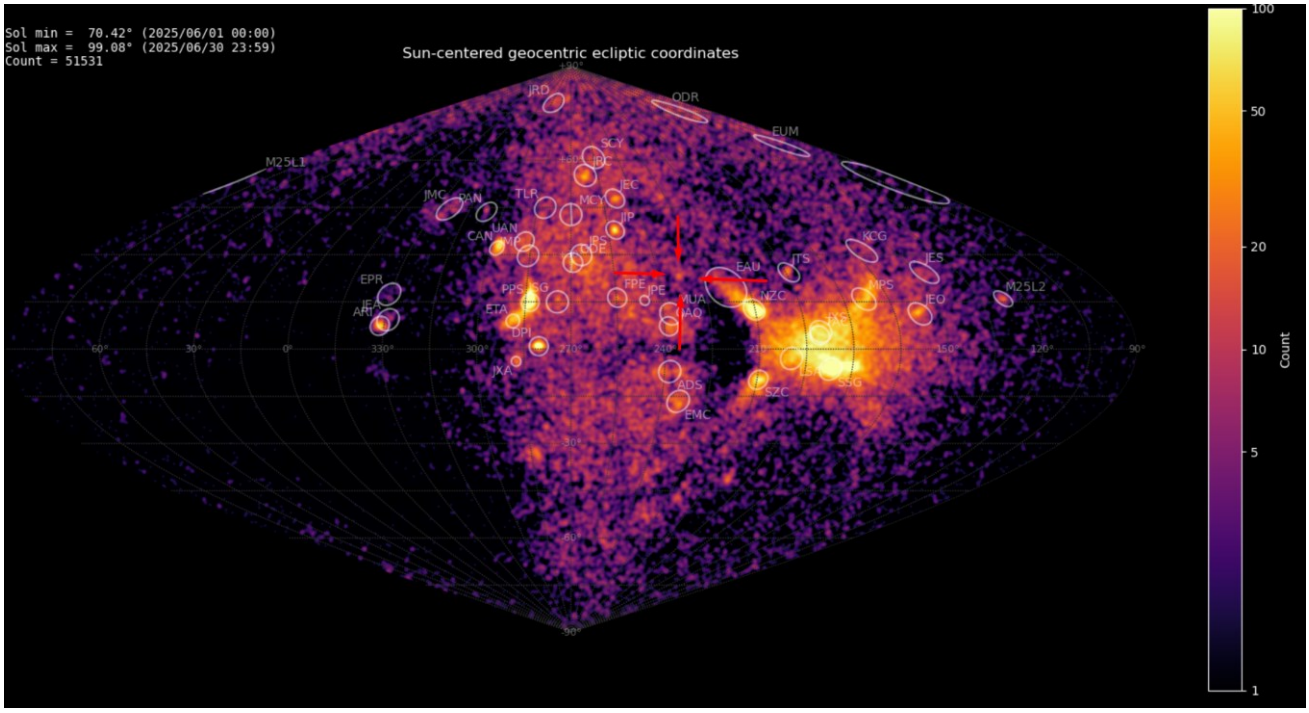

Figure 1 – Heat map with 51531 radiants obtained by the Global Meteor network in June 2025. A weak concentration is visible in Sun-centered geocentric ecliptic coordinates which was identified as a new meteor shower with the temporary identification M2025-O1.

[1] https://globalmeteornetwork.org/data/

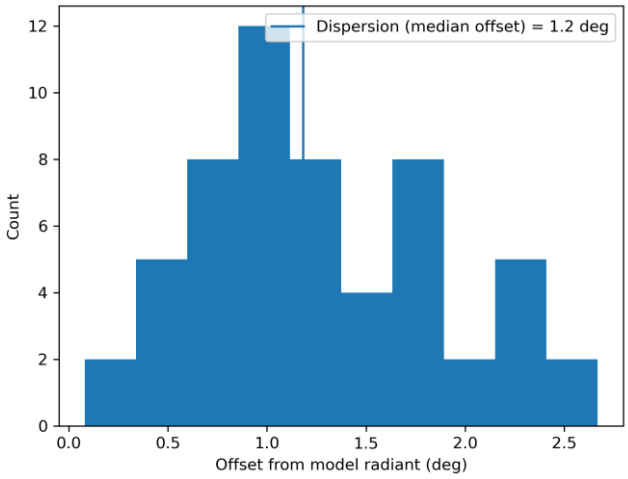

Figure 2 – Dispersion on the radiant position.

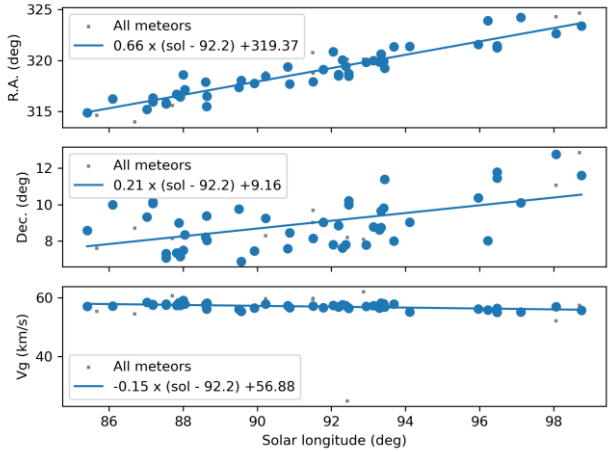

Figure 3 – The radiant drift.

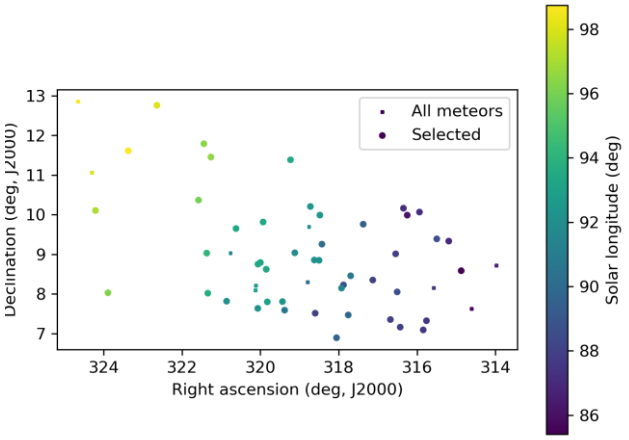

Figure 4 – The radiant distribution during the solar-longitude interval 85° – 99° in equatorial coordinates.

2 First detection

The GMN shower association criterion assumes that meteors within 1° in solar longitude, within 3° in radiant, and within 10% in geocentric velocity of a shower reference location are members of that shower. Further details about the shower association are explained in Moorhead et al. (2020). This is a rather strict criterion since meteor showers often have a larger dispersion in radiant position, velocity and activity period. Using these meteor shower selection criteria, 46 orbits have been associated with the new shower in the GMN meteor orbit database and the mean orbit has been listed in *Table 1*. This possible new meteor shower was reported to the IAU MDC and added under the temporary identification 2025-O1[2].

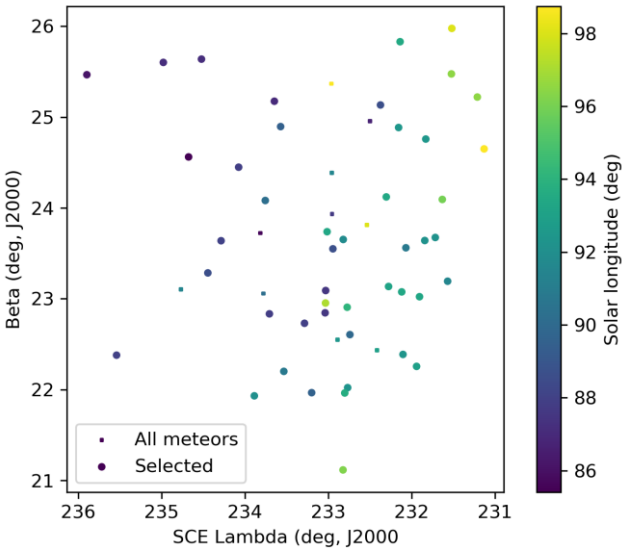

Figure 5 – The radiant distribution during the solar-longitude interval 85° – 99° in Sun centered geocentric ecliptic coordinates.

3 Another search method

Another method has been applied to check this new meteor shower discovery. The starting point here can be any visually spotted concentration of radiant points or any other indication for the occurrence of similar orbits. The method has been described before (Roggemans et al., 2019). The main difference with the method applied in *Section 2* is that three different discrimination criteria are combined in order to have only those orbits which fit the threshold for different criteria. The D-criteria that we use are these of Southworth and Hawkins (1963), Drummond (1981) and Jopek (1993) combined. Instead of using a cutoff value for the threshold of the D-criteria these values are considered in different classes with different thresholds of similarity. Depending on the dispersion and the type of orbits, the most appropriate threshold of similarity is selected to locate the best fitting mean orbit as the result of an iterative procedure.

This method resulted in a mean orbit with 45 related orbits that fit within the similarity threshold with $D_{SH} < 0.20$, $D_D < 0.08$ and $D_J < 0.2$, recorded 2025 June 16 – 30. The plot of the radiant positions in equatorial coordinates, color coded for different D-criteria thresholds, shows a stretched trail in Right Ascension from about 314° to 324° due to the radiant drift (*Figure 6*), see also *Figure 3*.

Looking at the Sun-centered geocentric ecliptic coordinates the radiant drift caused by of the Earth moving on its orbit around the Sun is compensated and a more compact radiant

[2] https://www.ta3.sk/IAUC22DB/MDC2022/Roje/pojedynczy_obiekt.php?lporz=01731&kodstrumienia=01234

becomes visible (*Figure 7*). The blue dots with $D_{SH} < 0.25$, $D_D < 0.105$ and $D_J < 0.25$ as well as the green dots with $D_{SH} < 0.20$, $D_D < 0.08$ and $D_J < 0.2$ display a large dispersion and may include sporadics. To reduce the risk of contamination with sporadic orbits, in the second method only orbits with $D_{SH} < 0.15$, $D_D < 0.06$ and $D_J < 0.15$ are considered. *Figures 8 and 9* show that these radiants appear on top of an evenly distributed sporadic radiant background. The diagram with the inclination against the longitude of perihelion (*Figure 10*) shows quite a lot dispersion on the longitude of perihelion Π.

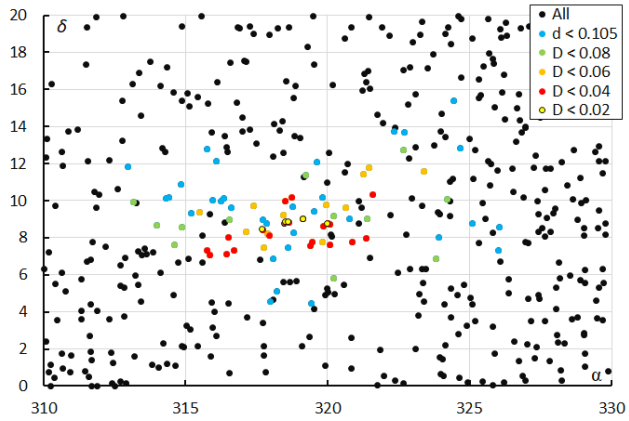

Figure 6 – The radiant distribution during the solar-longitude interval 85° – 99° in equatorial coordinates, color coded for different values of the D_D orbit similarity criterion.

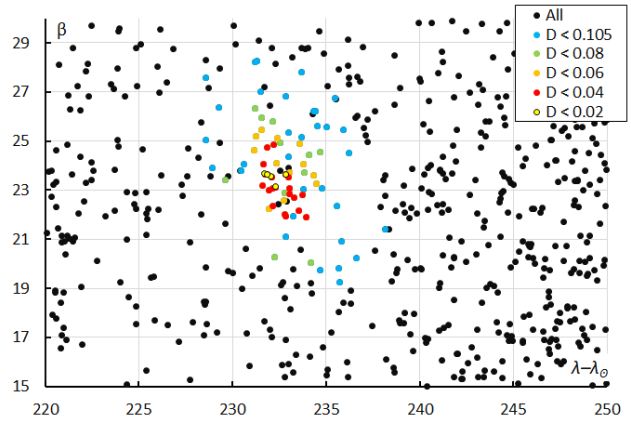

Figure 7 – The radiant distribution during the solar-longitude interval 85° – 99° in Sun-centered geocentric ecliptic coordinates, color coded for different values of the D_D orbit similarity criterion.

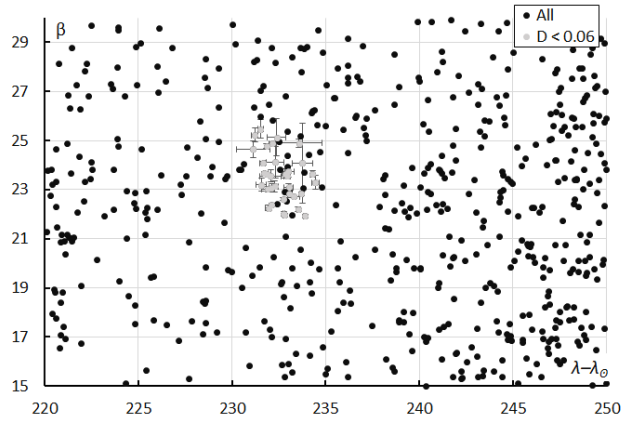

Figure 8 – The sporadic radiants during the solar-longitude interval 85° – 99° in Sun-centered geocentric ecliptic coordinates, with M2025-O1 radiants marked in grey for $D_D < 0.06$.

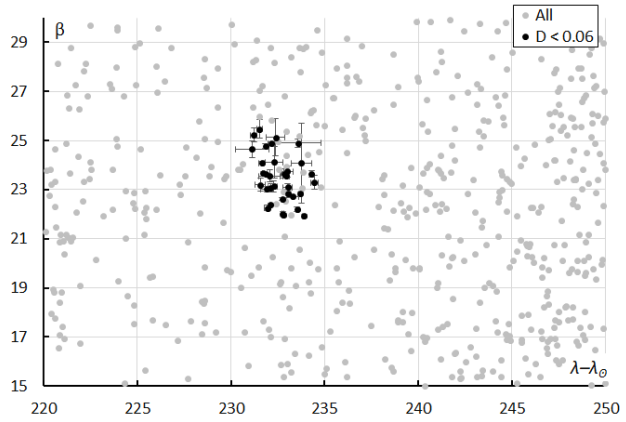

Figure 9 – The M2025-O1 radiants for $D_D < 0.06$ during the solar-longitude interval 85° – 99° in Sun-centered geocentric ecliptic coordinates, with the sporadic radiants marked in grey.

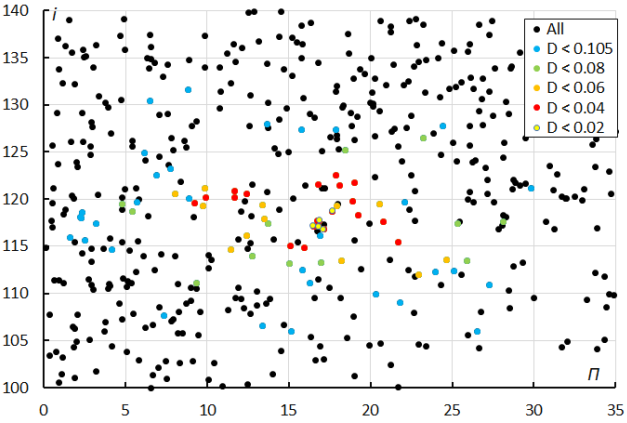

Figure 10 – The diagram of the inclination i against the longitude of perihelion Π for different classes of D criterion threshold.

4 Orbit and parent body

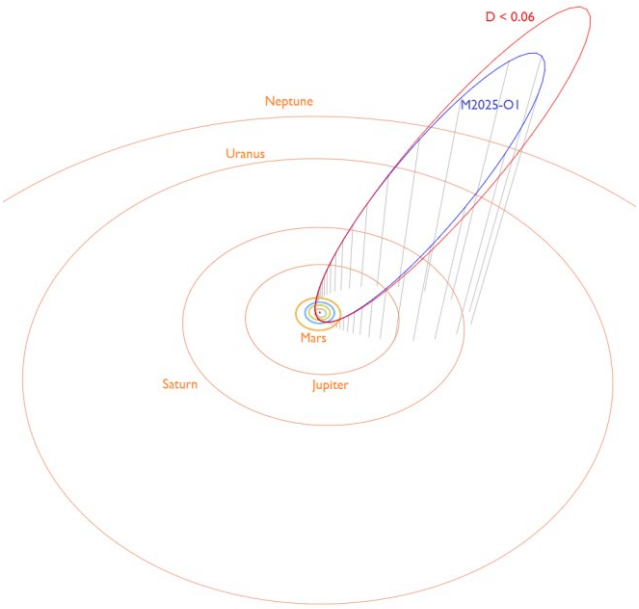

Figure 11 – Comparing the mean orbit based on the shower identification according to the two methods, blue is for M2025-O1 and red for the alternative shower search method with $D_D < 0.06$ in *Table 1*. (Plotted with the Orbit visualization app provided by Pető Zsolt).

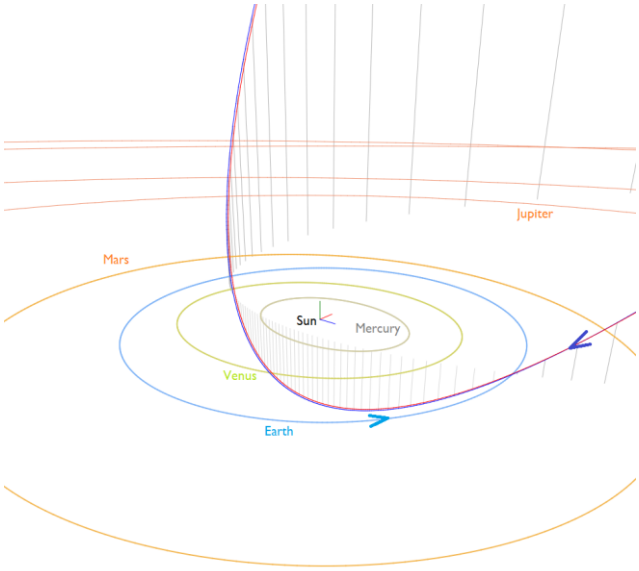

Figure 12 – Comparing the mean orbit based on the shower identification according to two methods, blue is for M2025-O1 and red for the other shower search method with $D_D < 0.06$ in *Table 1*, close-up at the inner Solar System. (Plotted with the Orbit visualization app provided by Pető Zsolt).

Table 1 – Comparing the new meteor shower, derived by two different methods, M2025-O1 lists the orbital parameters as initially derived and $D_D < 0.06$ lists the result obtained with the method described in *Section 3*.

	M2025-O1	$D_D < 0.06$
λ_O (°)	92.2	92.2
λ_{Ob} (°)	85.0	87.5
λ_{Oe} (°)	99.0	98.7
α_g (°)	319.4	318.7
δ_g (°)	9.2	8.6
$\Delta\alpha_g$ (°)	0.66	0.64
$\Delta\delta_g$ (°)	0.21	0.33
v_g (km/s)	56.9	57.2
λ_g (°)	324.95	324.35
$\lambda_g - \lambda_O$ (°)	232.75	232.37
β_g (°)	+23.72	+23.55
a (A.U.)	10.1	11.3
q (A.U.)	0.400	0.394
e	0.960	0.965
i (°)	118.4	118.3
ω (°)	283.5	284.2
Ω (°)	91.4	91.7
Π (°)	14.9	15.9
T_j	0.15	0.10
N	46	33

Figure 11 visualizes the two orbits plotted in the solar system. *Figure 12* is a close up in the inner solar system with the intersection of the meteoroid stream orbit and the Earth orbit. The M2025-O1 orbit encounters the Earth at its descending node. The Tisserand's parameter T_j identifies the orbit as of a Halley-type comet in this case with a retrograde orbit. A parent-body search top 10 includes candidates with a Southworth and Hawkings D criterion value lower than 0.4 but none of which can be associated with any certainty (*Table 2*). It would be up to meteoroid stream modelers to reconstruct the dynamic orbit evolution to see if there could be any connection.

Table 2 – Top ten search results for possible parent bodies with $D_{SH} < 0.4$.

Name	D_{SH}
C/2025 K1 (ATLAS)	0.27
C/1793 S2 (Messier)	0.30
C/1979 Y1 (Bradfield)	0.34
C/1771 A1 (Great comet)	0.35
C/1992 W1 (Ohshita)	0.35
C/1969 T1 (Tago-Sato-Kosaka)	0.35
C/2005 K2 (LINEAR)	0.39
C/2005 K2-A (LINEAR)	0.39
C/1780 U1 (Montaigne-Olbers)	0.40
C/1951 P1 (Wilson-Harrington)	0.40

This possible new meteor shower is very likely an old trail of dust, dispersed with a rather large spread in the longitude of perihelion Π and with a barely detectable weak activity. The final mean orbits obtained via the two independent meteor shower search methods are in very good agreement. The first meteor shower search includes seven orbits that failed to fit the $D_D < 0.08$ criteria in the second method, while the second method includes six orbits that were ignored by the first search method. The differences between both methods occurred mainly at the beginning of the detected activity period and concern outliers that could be sporadic contamination. In total 39 orbits were in common by both methods. All 33 orbits that fit the $D_D < 0.06$ criteria in the second method were found by the first search method too.

5 Activity in past years

A search in older GMN orbit data revealed 16 orbits that fit the $D_D < 0.06$ criterion during the interval $85° < \lambda_O < 99°$, one in 2021, two in 2022, three in 2023 and ten similar orbits in 2024. Among the 529076 orbits of SonotaCo only three similar orbits were found. Another three similar orbits were found in EDMOND data from 2015 and 2016. CAMS orbit data has not been searched. The weak activity of this meteor shower requires a high-capacity camera network to resolve the presence of these orbits within the sporadic background.

6 Conclusion

The discovery of a new meteor shower with a radiant in the constellation of Equuleus based on forty-six meteors during 2025 June 15–30 has been confirmed by using two independent meteor shower search methods. The resulting mean orbits for both search methods are in good agreement. All meteors appeared during the solar-longitude interval

85° – 99°, with most events around 23–24 June (λ_O = 92.2°). There is almost no trace of this meteor shower in past years meteor orbit datasets.

Acknowledgment

This report is based on the data of the Global Meteor Network (Vida et al., 2020a; 2020b; 2021) which is released under the CC BY 4.0 license[3]. We thank all 825 participants in the Global Meteor Network project for their contribution and perseverance. A list with the names of the volunteers who contribute to GMN has been published in the 2024 annual report (Roggemans et al., 2025).

References

Drummond J. D. (1981). "A test of comet and meteor shower associations". *Icarus*, **45**, 545–553.

Jopek T. J. (1993). "Remarks on the meteor orbital similarity D-criterion". *Icarus*, **106**, 603–607.

Jopek T. J., Rudawska R. and Pretka-Ziomek H. (2006). "Calculation of the mean orbit of a meteoroid stream". *Monthly Notices of the Royal Astronomical Society*, **371**, 1367–1372.

Moorhead A. V., Clements T. D., Vida D. (2020). "Realistic gravitational focusing of meteoroid streams". *Monthly Notices of the Royal Astronomical Society*, **494**, 2982–2994.

Roggemans P., Johannink C. and Campbell-Burns P. (2019a). "October Ursae Majorids (OCU#333)". *eMetN Meteor Journal*, **4**, 55–64.

Roggemans P., Campbell-Burns P., Kalina M., McIntyre M., Scott J. M., Šegon D., Vida D. (2025). "Global Meteor Network report 2024". *eMetN Meteor Journal*, **10**, 67–101.

Southworth R. B. and Hawkins G. S. (1963). "Statistics of meteor streams". *Smithsonian Contributions to Astrophysics*, **7**, 261–285.

Vida D., Gural P., Brown P., Campbell-Brown M., Wiegert P. (2020a). "Estimating trajectories of meteors: an observational Monte Carlo approach - I. Theory". *Monthly Notices of the Royal Astronomical Society*, **491**, 2688–2705.

Vida D., Gural P., Brown P., Campbell-Brown M., Wiegert P. (2020b). "Estimating trajectories of meteors: an observational Monte Carlo approach - II. Results". *Monthly Notices of the Royal Astronomical Society*, **491**, 3996–4011.

Vida D., Šegon D., Gural P. S., Brown P. G., McIntyre M. J. M., Dijkema T. J., Pavletić L., Kukić P., Mazur M. J., Eschman P., Roggemans P., Merlak A., Zubrović D. (2021). "The Global Meteor Network – Methodology and first results". *Monthly Notices of the Royal Astronomical Society*, **506**, 5046–5074.

[3] https://creativecommons.org/licenses/by/4.0/

New meteor shower in Indus

Denis Vida[1], **Damir Šegon**[2] **and Paul Roggemans**[3]

[1] **Department of Earth Sciences, University of Western Ontario, London, Ontario, N6A 5B7, Canada**
denis.vida@gmail.com

[2] **Astronomical Society Istra Pula, Park Monte Zaro 2, 52100 Pula, Croatia**

[3] **Pijnboomstraat 25, 2800 Mechelen, Belgium**
paul.roggemans@gmail.com

A new meteor shower on a long-period comet type orbit ($T_J = 0.85$) has been detected during June 14–21, 2025 by the Global Meteor Network. Meteors belonging to the new shower were observed between $82° < \lambda_\odot < 91°$ from a radiant at R.A. = 330.0° and Decl.= –63.8° in the constellation of Indus, with a geocentric velocity of 43.8 km/s. The new meteor shower has been listed in the Working List of Meteor Showers under the temporary name-designation: M2025-O2.

1 Introduction

The GMN radiant map for June 2025 shows a weak concentration of related radiants in the constellation of Indus. 30 meteors of this meteor shower were observed by the Global Meteor Network[4] low-light video cameras on 2025 June 13 – 24 (*Figure 1*). The shower was independently observed by cameras in two countries (Australia and New Zealand).

The shower had a median geocentric radiant with coordinates R.A. = 330.0°, Decl. = –63.8°, within a circle with a standard deviation of ±1.6° (equinox J2000.0) see *Figure 2*. The radiant drift in R.A. is +1.62 deg on the sky per degree of solar longitude and +0.23 in Dec., both referenced to $\lambda_\odot = 85.2°$ (*Figures 3 and 4*). The median Sun-centered ecliptic coordinates were $\lambda - \lambda_\odot = 219.15°$, $\beta = –47.34°$ (*Figure 5*). The geocentric velocity was 43.8 ± 0.2 km/s.

All meteors appeared during the solar-longitude interval 82° – 93°, with most events at 16–17 June (around $\lambda_\odot = 85.5°$).

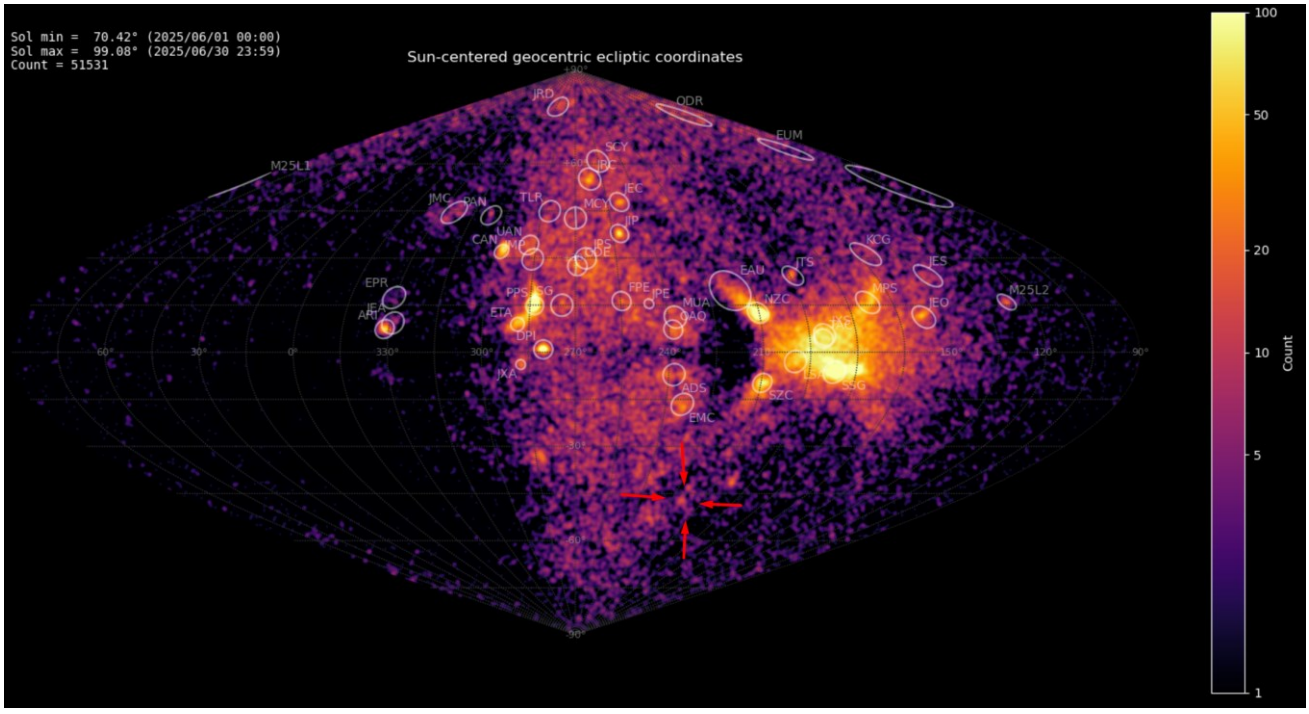

Figure 1 – Heat map with 51531 radiants obtained by the Global Meteor network in June 2025. A weak concentration is visible in Sun-centered geocentric ecliptic coordinates which was identified as a new meteor shower with the temporary identification M2025-O2.

[4] https://globalmeteornetwork.org/data/

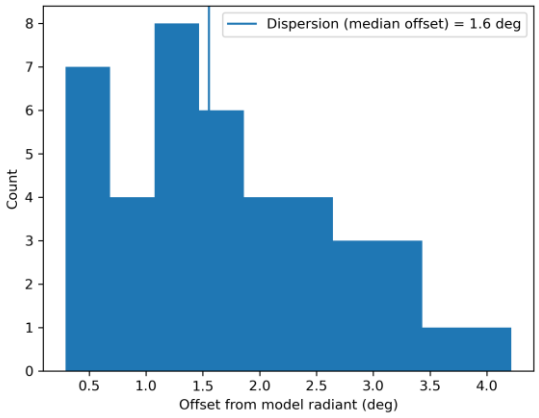

Figure 2 – Dispersion on the radiant position.

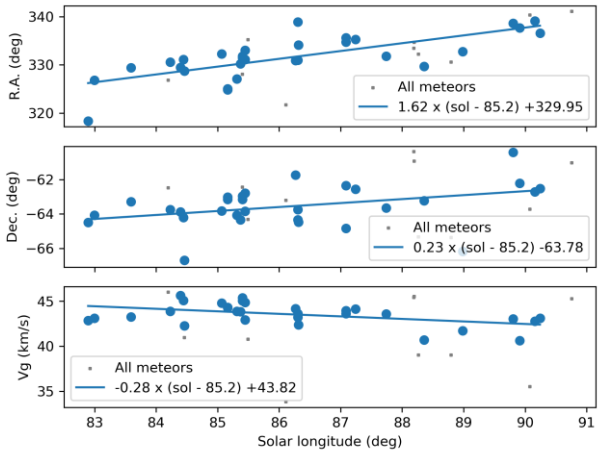

Figure 3 – The radiant drift.

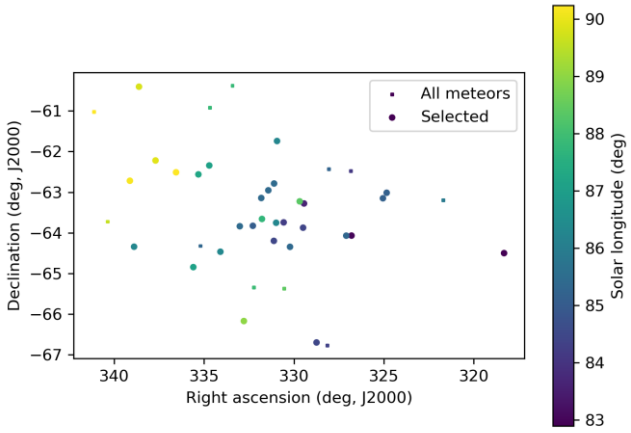

Figure 4 – The radiant distribution during the solar-longitude interval 82° – 91° in equatorial coordinates.

2 First detection

The GMN shower association criterion assumes that meteors within 1° in solar longitude, within 3° in radiant, and within 10% in geocentric velocity of a shower reference location are members of that shower. Further details about the shower association are explained in Moorhead et al. (2020). This is a rather strict criterion since meteor showers often have a larger dispersion in radiant position, velocity and activity period. Using these meteor shower selection criteria, 30 orbits have been associated with the new shower in the GMN meteor orbit database and the mean orbit has been listed in *Table 1*. This possible new meteor shower was reported to the IAU MDC and added under the temporary identification 2025-O2[5].

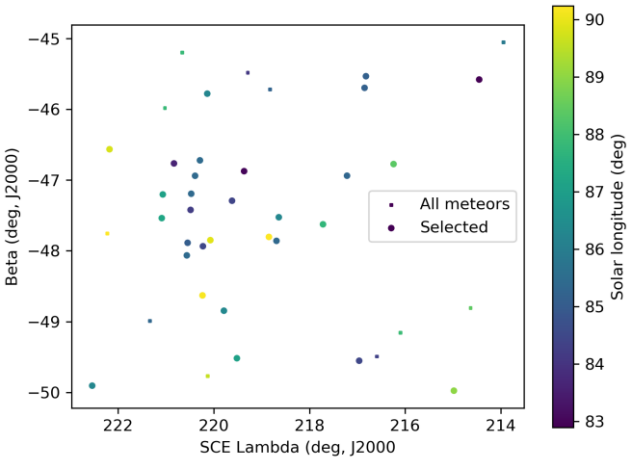

Figure 5 – The radiant distribution during the solar-longitude interval 82° – 91° in Sun centered geocentric ecliptic coordinates.

3 Another search method

Another method has been applied to check this new meteor shower discovery. The starting point here can be any visually spotted concentration of radiant points or any other indication for the occurrence of similar orbits. The method has been described before (Roggemans et al., 2019). The main difference with the method applied in *Section 2* is that three different discrimination criteria are combined in order to have only those orbits which fit different criteria thresholds. The D-criteria that we use are these of Southworth and Hawkins (1963), Drummond (1981) and Jopek (1993) combined. Instead of using a cutoff value for the threshold of the D-criteria these values are considered in different classes with different thresholds of similarity. Depending on the dispersion and the type of orbits, the most appropriate threshold of similarity is selected to locate the best fitting mean orbit as the result of an iterative procedure.

This method resulted in a mean orbit with 53 related orbits that fit within the similarity threshold with $D_{SH} < 0.20$, $D_D < 0.08$ and $D_J < 0.2$, recorded 2025 June 13 – 24. The plot of the radiant positions in equatorial coordinates, color coded for different D-criteria thresholds, shows a stretched trail in Right Ascension from about 315° to 345° due to the radiant drift (*Figure 6*), see also *Figure 3*.

Looking at the Sun-centered geocentric ecliptic coordinates the radiant drift caused by of the Earth moving on its orbit around the Sun is compensated and a more compact radiant becomes visible (*Figure 7*). The blue dots with $D_{SH} < 0.25$, $D_D < 0.105$ and $D_J < 0.25$ as well as the green dots with $D_{SH} < 0.20$, $D_D < 0.08$ and $D_J < 0.2$ display a large dispersion and may include some contamination with

[5] https://www.ta3.sk/IAUC22DB/MDC2022/Roje/pojedynczy_obiekt.php?lporz=01732&kodstrumienia=01235

sporadics. To reduce the risk of including sporadic orbits, in the second method only the 23 orbits with $D_{SH} < 0.10$, $D_D < 0.04$ and $D_J < 0.10$ are considered. *Figures 8 and 9* show that these radiants appear on top of an evenly distributed sporadic radiant background. There is another concentration of radiants visible in the upper left corner of *Figures 7, 8 and 9*. These belong to the poorly known June delta-Pavonids (JDP#835) detected by CAMS in 2014 and 2016 with only 11 orbits (Jenniskens et al., 2018). This shower seems to have displayed possible enhanced activity in 2025 and will be documented in a separate report.

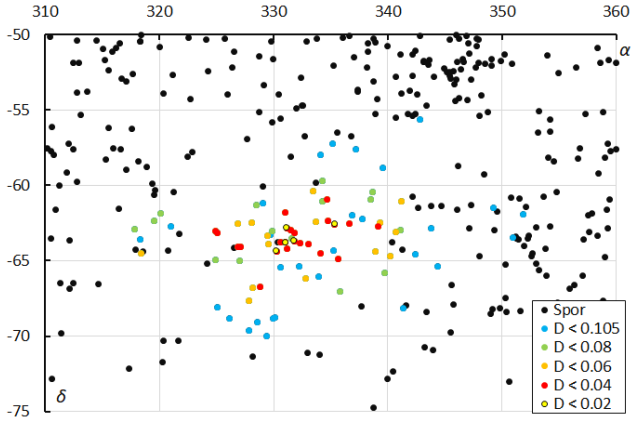

Figure 6 – The radiant distribution during the solar-longitude interval 82° – 93° in equatorial coordinates, color coded for different values of the D_D orbit similarity criterion.

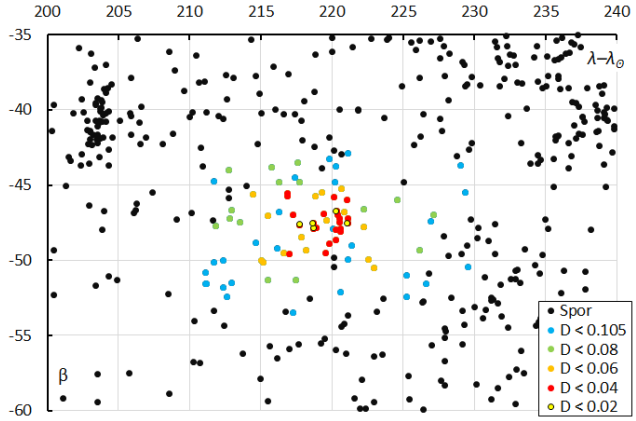

Figure 7 – The radiant distribution during the solar-longitude interval 82° – 93° in Sun-centered geocentric ecliptic coordinates, color coded for different values of the D_D orbit similarity criterion.

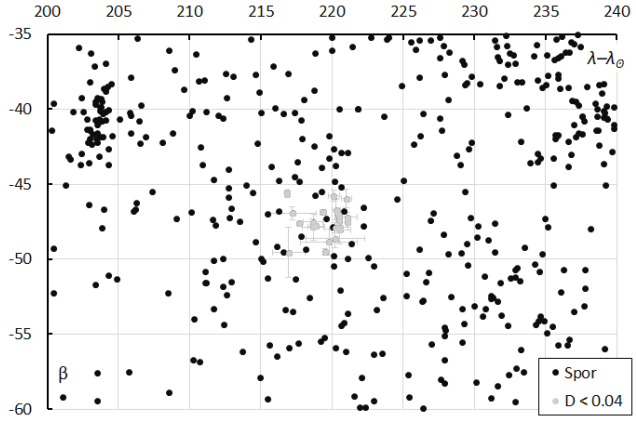

Figure 8 – The sporadic radiants during the solar-longitude interval 82° – 93° in Sun-centered geocentric ecliptic coordinates, with M2025-O2 radiants marked in grey for $D_D < 0.04$.

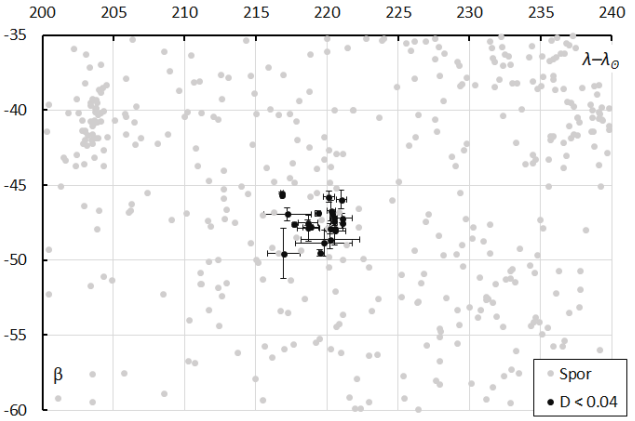

Figure 9 – The M2025-O2 radiants for $D_D < 0.04$ during the solar-longitude interval 82° – 93° in Sun-centered geocentric ecliptic coordinates, with the sporadic radiants marked in grey.

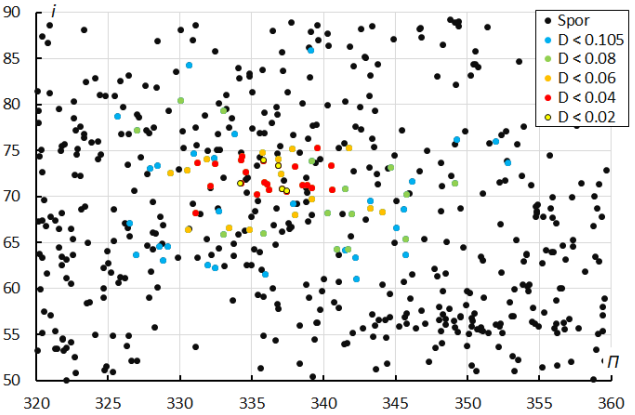

Figure 10 – The diagram of the inclination *i* against the longitude of perihelion Π color coded for different classes of D criterion threshold.

The diagram with the inclination against the longitude of perihelion (*Figure 10*) shows quite a lot dispersion on the longitude of perihelion Π.

4 Orbit and parent body

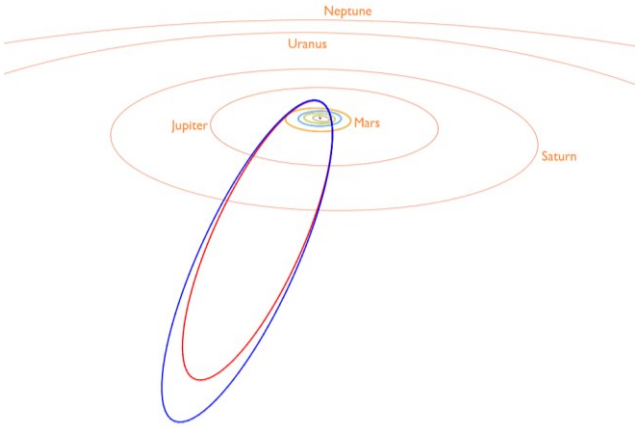

Figure 11 – Comparing the mean orbit based on the shower identification according to the two methods, red is for M2025-O2 and blue for the alternative shower search method with $D_D < 0.04$ in *Table 1*. (Plotted with the Orbit visualization app provided by Pető Zsolt).

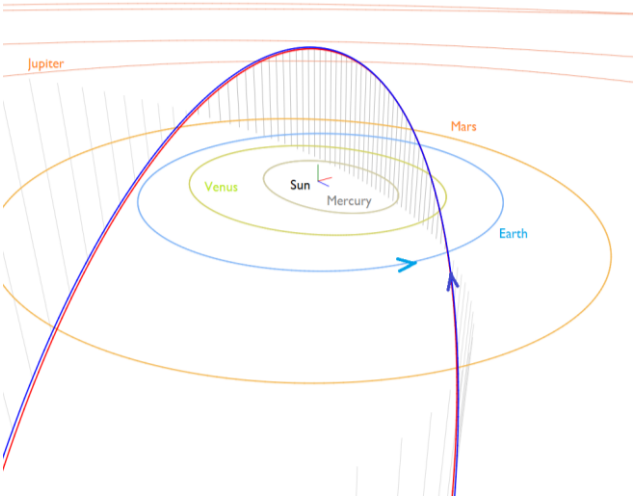

Figure 12 – Comparing the mean orbit based on the shower identification according to two methods, red is for M2025-O2 and blue for the other shower search method with $D_D < 0.04$ in *Table 1*. With an inclination of 72° the orbit is very steep on the ecliptic plane. (Plotted with the Orbit visualization app provided by Pető Zsolt).

Table 1 – Comparing the new meteor shower, derived by two different methods, M2025-O2 the orbital parameters as initially derived, $D_D < 0.04$ were derived from the method described in *Section 3*.

	M2025-O2	$D_D < 0.04$
$\lambda_\odot$ (°)	85.2	85.4
$\lambda_{\odot b}$ (°)	82.0	83.0
$\lambda_{\odot e}$ (°)	91.0	90.2
α_g (°)	330.0	331.4
δ_g (°)	–63.8	–63.7
$\Delta\alpha_g$ (°)	1.62	1.57
$\Delta\delta_g$ (°)	0.23	0.32
v_g (km/s)	43.8	43.9
λ_g (°)	304.35	305.7
$\lambda_g - \lambda_\odot$ (°)	219.15	220.1
β_g (°)	–47.34	–47.5
a (A.U.)	9.88	12.2
q (A.U.)	0.690	0.691
e	0.930	0.943
i (°)	71.6	72.1
ω (°)	70.3	69.9
Ω (°)	266.2	266.1
Π (°)	336.5	336.0
T_j	0.85	0.74
N	30	23

The Tisserand's parameter T_j identifies the orbit as of a Halley-type comet in this case with a prograde orbit. *Figure 11* visualizes the two orbits found by the two methods. *Figure 12* is a close up of the inner solar system with the steep inclined orbit of M2025-O2 and its encounter with the Earth at the ascending node. A parent-body search top 10 includes candidates with a Drummond D_D criterion value lower than 0.3 but none of which can be associated with any certainty (*Table 2*). It would be up to meteoroid stream modelers to reconstruct the dynamic orbit evolution to see if there could be any connection.

Table 2 – Top ten matches of a search for possible parent bodies with $D_D < 0.3$.

Name	D_D
C/1863 G2 (Respighi)	0.184
2012 XT134	0.213
(311044) 2004 BB103	0.231
C/1941 K1 (van Gent)	0.237
C/1376 M1	0.245
C/1883 D1 (Brooks-Swift)	0.259
C/1898 F1 (Perrine)	0.262
C/1951 C1 (Pajdusakova)	0.267
C/1912 R1 (Gale)	0.275
C/1953 G1 (Mrkos-Honda)	0.276

This possible new meteor shower is very likely an old dust trail, dispersed with a rather large spread in the longitude of perihelion Π and with a barely detectable weak activity. The final mean orbits obtained via the two independent meteor shower search methods are in very good agreement. The first meteor shower search includes three orbits that failed to fit the $D_D < 0.08$ criteria in the second method, while the second method includes eleven orbits that were ignored by the first search method. The differences between both methods occurred mainly at the end of the detected activity period and concern outliers that could be sporadic contamination. In total 27 orbits were in common by both methods. Of the 23 orbits that fit the $D_D < 0.04$ threshold in the second method, 22 were in common with the first search method.

5 Activity in past years

A search in older GMN orbit data resulted in two possible orbits with $D_D < 0.08$ in 2022, 17 in 2023 of which five with $D_D < 0.04$ and 48 orbits in 2024 of which six with $D_D < 0.04$. No other meteor orbit datasets were checked because of the lack of coverage at the southern hemisphere in the EDMOND and SonotaCo Net meteor orbit datasets.

6 Conclusion

The discovery of a new meteor shower with a radiant in the constellation of Indus based on thirty meteors during 2025 June 13–24 has been confirmed by using two independent meteor shower search methods. The resulting mean orbits for both search methods are in good agreement. All meteors appeared during the solar-longitude interval 82° – 93°, with most events around 16–17 June ($\lambda_\odot = 85.2°$). Orbits of this meteor shower were detected in 2023 and 2024, but the number of events in previous years remained below the detection threshold.

Acknowledgment

This report is based on the data of the Global Meteor Network (Vida et al., 2020a; 2020b; 2021) which is released under the CC BY 4.0 license[6]. We thank all 825 participants in the Global Meteor Network project for their contribution and perseverance. A list with the names of the volunteers who contribute to GMN has been published in the 2024 annual report (Roggemans et al., 2025).

References

Drummond J. D. (1981). "A test of comet and meteor shower associations". *Icarus*, **45**, 545–553.

Jenniskens P., Baggaley J., Crumpton I., Aldous P., Pokorny P., Janches D., Gural P. S., Samuels D., Albers J., Howell A., Johannink C., Breukers M., Odeh M., Moskovitz N., Collison J., Ganju S. (2018). "A survey of southern hemisphere meteor showers". *Planetary and Space Science*, **154**, 21–29.

Jopek T. J. (1993). "Remarks on the meteor orbital similarity D-criterion". *Icarus*, **106**, 603–607.

Jopek T. J., Rudawska R. and Pretka-Ziomek H. (2006). "Calculation of the mean orbit of a meteoroid stream". *Monthly Notices of the Royal Astronomical Society*, **371**, 1367–1372.

Moorhead A. V., Clements T. D., Vida D. (2020). "Realistic gravitational focusing of meteoroid streams". *Monthly Notices of the Royal Astronomical Society*, **494**, 2982–2994.

Roggemans P., Johannink C. and Campbell-Burns P. (2019a). "October Ursae Majorids (OCU#333)". *eMetN Meteor Journal*, **4**, 55–64.

Roggemans P., Campbell-Burns P., Kalina M., McIntyre M., Scott J. M., Šegon D., Vida D. (2025). "Global Meteor Network report 2024". *eMetN Meteor Journal*, **10**, 67–101.

Southworth R. B. and Hawkins G. S. (1963). "Statistics of meteor streams". *Smithsonian Contributions to Astrophysics*, **7**, 261–285.

Vida D., Gural P., Brown P., Campbell-Brown M., Wiegert P. (2020a). "Estimating trajectories of meteors: an observational Monte Carlo approach - I. Theory". *Monthly Notices of the Royal Astronomical Society*, **491**, 2688–2705.

Vida D., Gural P., Brown P., Campbell-Brown M., Wiegert P. (2020b). "Estimating trajectories of meteors: an observational Monte Carlo approach - II. Results". *Monthly Notices of the Royal Astronomical Society*, **491**, 3996–4011.

Vida D., Šegon D., Gural P. S., Brown P. G., McIntyre M. J. M., Dijkema T. J., Pavletić L., Kukić P., Mazur M. J., Eschman P., Roggemans P., Merlak A., Zubrović D. (2021). "The Global Meteor Network – Methodology and first results". *Monthly Notices of the Royal Astronomical Society*, **506**, 5046–5074.

[6] https://creativecommons.org/licenses/by/4.0/

June delta Pavonids (JDP#835) in 2025

Paul Roggemans[1], **Damir Šegon**[2] **and Denis Vida**[3]

[1] **Pijnboomstraat 25, 2800 Mechelen, Belgium**
paul.roggemans@gmail.com

[2] **Astronomical Society Istra Pula, Park Monte Zaro 2, 52100 Pula, Croatia**

[3] **Department of Earth Sciences, University of Western Ontario, London, Ontario, N6A 5B7, Canada**
denis.vida@gmail.com

A case study on the June delta Pavonids (JDP#835) based on Global Meteor Network orbit data identified 60 possible JDP-orbits in 2025 and 146 during the period 2021–2025. The increase in number of JDP-orbits in recent years reflects the expansion at the southern hemisphere of the Global Meteor Network and does not indicate any enhanced or unusual activity. The radiant and mean orbit are in good agreement with earlier results and provide an independent confirmation for the existence of this meteor shower, based on Global Meteor Network orbit data.

1 Introduction

The analysis of a possible new meteor shower in the constellation of Indus 16–17 June 2025 (around $\lambda_\odot = 85.5°$) revealed another concentration of radiant points with its main activity a day earlier nearby the new discovered shower which got the temporary identification M2025-O2 (Vida et al., 2025). A checkup in the IAU MDC Working List of Meteor Showers resulted in a positive identification with the June delta Pavonids (JDP#835)[7], which was reported in 2018 by Jenniskens et al. (2018) based on 11 orbits recorded by the CAMS network in 2014 and 2016. In his book 'Atlas of Earth's meteor showers' Jenniskens (2024), page 751, published newer data on the June delta Pavonids, based on 65 orbits recorded by CAMS until 2023, which hasn't been included yet in the IAU MDC Working List of Meteor Showers.

A quick search located more than 70 possible JDP members in the Global Meteor Network orbit dataset[8] for 2025 alone. Therefore, it was decided to dedicate an analysis to this so far poorly known meteor shower, to check if it displayed enhanced activity in 2025 and to provide an independent confirmation of this meteor shower for the IAU MDC Working List of Meteor Showers.

The June delta Pavonids are clearly visible on the radiant density map of the Global Meteor Network for June 2025 (*Figure 1*). In 2024 and 2023 the radiant density maps also show this radiant.

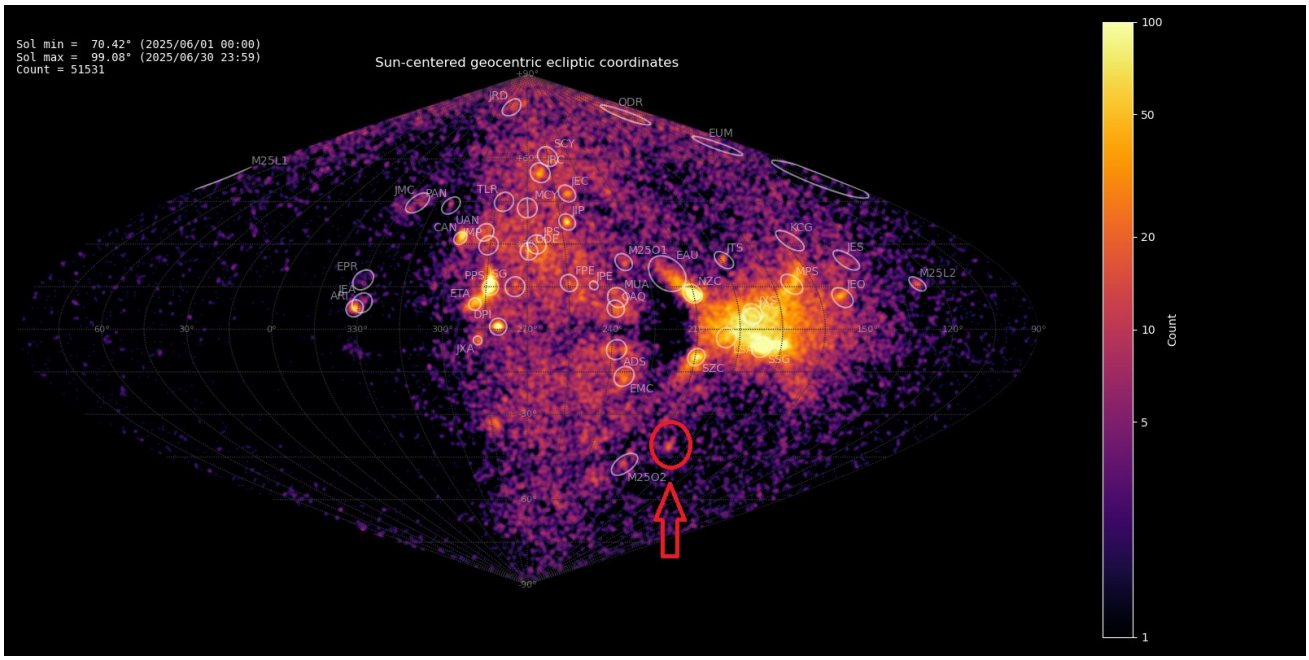

Figure 1 – Heat map with 51531 radiants obtained by the Global Meteor network in June 2025. The position of the June delta Pavonids in Sun-centered geocentric ecliptic coordinates is marked with the red arrow.

[7] https://www.ta3.sk/IAUC22DB/MDC2022/Roje/pojedynczy_obiekt.php?lporz=01419&kodstrumienia=00835

[8] https://globalmeteornetwork.org/data/

2 The search method

The visible concentration of radiant points was extracted for the time interval of $77° < \lambda_\odot < 87°$, arbitrarily limited in Sun-centered geocentric ecliptic coordinates with $195° < \lambda - \lambda_\odot < 205°$ and $-40° < \beta < -30°$. This selection includes most of the possible meteor shower members as well as the sporadic sources within this interval. This selection included 91 meteor orbits, used to compute a first mean orbit for this sample. We didn't use median values to derive a mean orbit since a vectoral solution like the method of Jopek et al. (2006) is more appropriate for orbital elements with angular values.

This first mean orbit serves as a reference orbit to start an iterative procedure to approach a mean orbit which is the most representative orbit for the similar orbits in the sample, removing outliers and sporadic orbits. This method has been described before (Roggemans et al., 2019). Three different discrimination criteria are combined in order to have only those orbits which fit the different criteria thresholds. The D-criteria that we use are these of Southworth and Hawkins (1963), Drummond (1981) and Jopek (1993) combined. The values are considered in different classes with different thresholds of similarity. We consider five different threshold levels of similarity:

- Low: $D_{SH} < 0.25$ & $D_D < 0.105$ & $D_H < 0.25$;
- Medium low: $D_{SH} < 0.2$ & $D_D < 0.08$ & $D_H < 0.2$;
- Medium high: $D_{SH} < 0.15$ & $D_D < 0.06$ & $D_H < 0.15$;
- High: $D_{SH} < 0.1$ & $D_D < 0.04$ & $D_H < 0.1$.
- Very high: $D_{SH} < 0.05$ & $D_D < 0.02$ & $D_H < 0.05$.

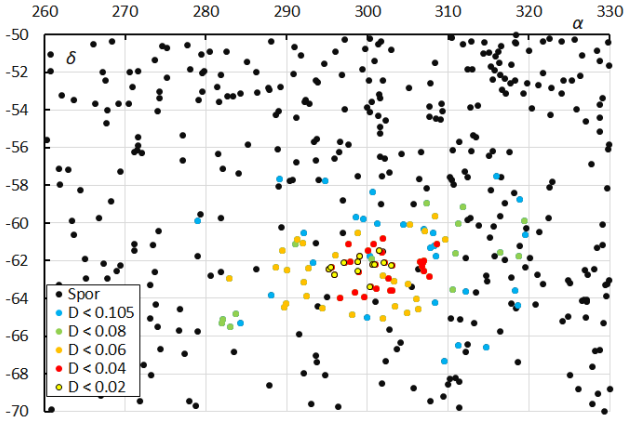

Figure 2 – The radiant distribution during the solar-longitude interval 74° – 94° in equatorial coordinates, color coded for different values of the D_D orbit similarity criterion for 2025.

Depending on the dispersion and the type of orbits, the most appropriate threshold of similarity is selected to locate the best fitting mean orbit as the result of an iterative procedure. Looking at the radiant plot in equatorial coordinates the radiant area appears stretched which is due to the movement of the Earth on its orbit around the Sun which causes the daily drift of the radiant (*Figure 2*). The radiant drift was computed to be $\Delta\alpha/\Delta\lambda_\odot = +1.43°$ and $\Delta\delta/\Delta\lambda_\odot = +0.10°$ relative to $\lambda_\odot = 84.4°$. To study meteor showers it is recommended to use the Sun-centered geocentric ecliptic coordinates since meteoroid streams are part of the solar system with the ecliptic plane as reference for the orbital elements. The movement of the Earth is compensated by subtracting the change in solar longitude. The resulting radiant plot is shown in *Figure 3*. The low threshold D criteria is obviously too tolerant and dispersed, contaminated with false positives or sporadic orbits. Considering the medium low threshold ($D_D < 0.08$) would result in 74 possible JDP-orbits. The medium high class includes 60 possible JDP-orbits which appears added to the sporadic background without affecting the random distribution of this background (*Figures 4 and 5*).

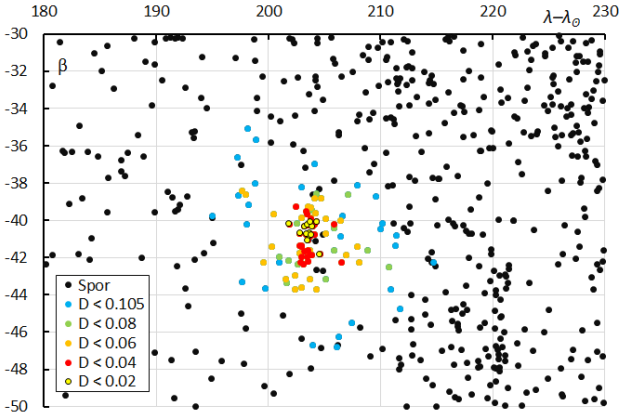

Figure 3 – The radiant distribution in Sun-centered geocentric ecliptic coordinates, color coded for different values of the D_D orbit similarity criterion for 2025.

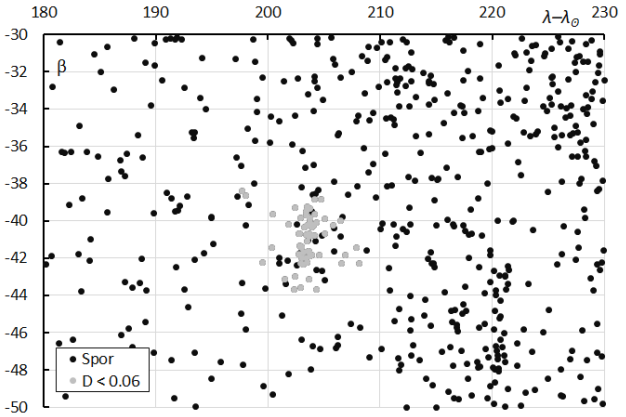

Figure 4 – The sporadic radiants in Sun-centered geocentric ecliptic coordinates, with JDP radiants marked in grey for $D_D < 0.06$ for 2025.

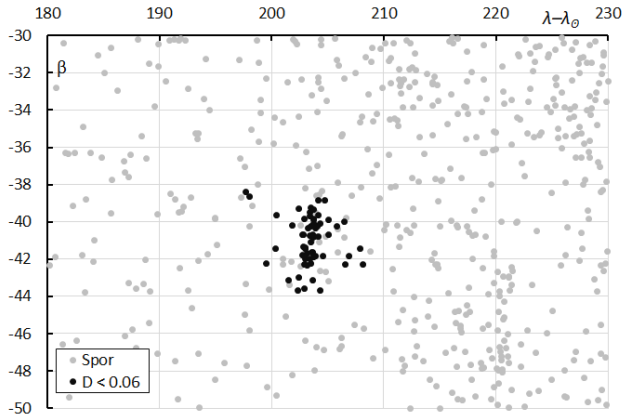

Figure 5 – The JDP radiants for $D_D < 0.06$ in Sun-centered geocentric ecliptic coordinates, with the sporadic radiants marked in grey for 2025.

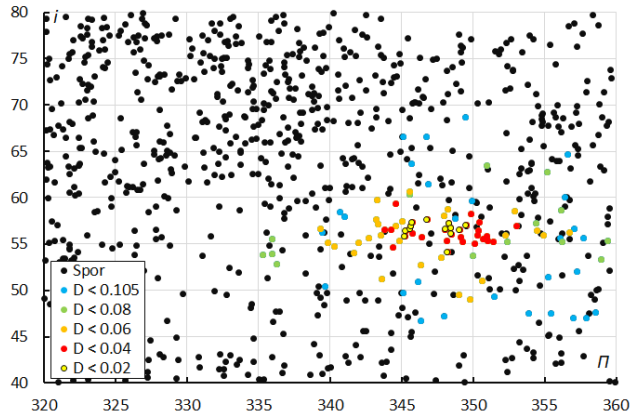

Figure 6 – Diagram of inclination i against the longitude of perihelion Π, color coded for different values of the D_D orbit similarity criterion for 2025.

The distribution of the inclination against the longitude of perihelion (*Figure 6*) shows a large spread in the longitude of perihelion, indicating that this is a rather dispersed old meteoroid stream.

The June delta Pavonids are an annual shower and appears each year in GMN orbit data since 2021. The number of orbits identified per year reflects the expansion of the GMN camera network at the southern hemisphere; one orbit in 2021, none in 2022, 28 in 2023, 41 in 2024 and 60 in 2025, or 130 orbits in total that fulfil the discrimination criteria with $D_{SH} < 0.15$ & $D_D < 0.06$ & $D_H < 0.15$. Most orbits were obtained by New Zealand and Australian GMN station, some by Brazilian and South African stations. These 130 radiants are plotted in *Figure 7*, the sporadic background was left away as the data wasn't extracted for these five years (too many meteors).

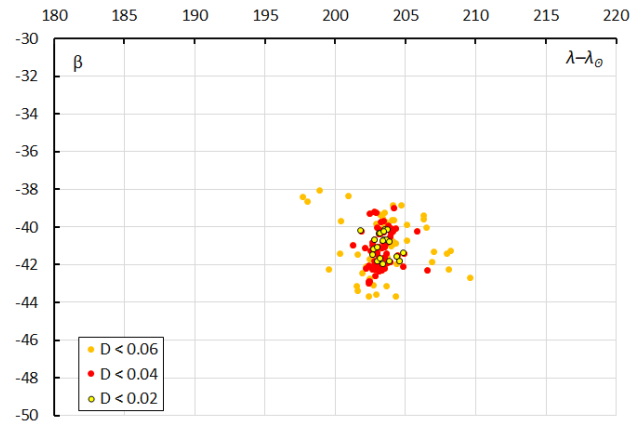

Figure 7 – The radiant distribution in Sun-centered geocentric ecliptic coordinates, color coded for different values of the D_D orbit similarity criterion for the 130 JDP-orbits obtained during 2021-2025.

Figure 8 shows the radiant distribution in Sun-centered geocentric ecliptic coordinates color code for the variation in geocentric velocity for the period 2021–2025. The drift in Sun-centered geocentric ecliptic coordinates $\Delta(\lambda-\lambda_\odot)/\Delta\lambda_\odot$ and $\Delta\beta/\Delta\lambda_\odot$ is very small, almost negligible as well as the drift in geocentric velocity $\Delta v_g/\Delta\lambda_\odot$.

Figure 9 shows the distribution of the inclination against the longitude of perihelion for the 130 orbits obtained during the past five years and displays the same large dispersion in the longitude of perihelion as the result for 2025 in *Figure 6*.

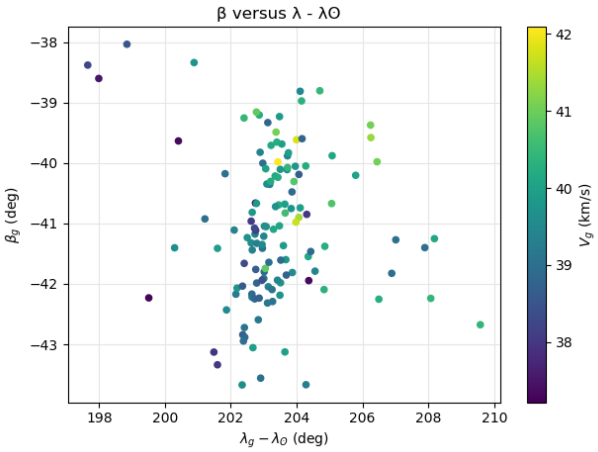

Figure 8 – The radiant distribution in Sun-centered geocentric ecliptic coordinates, color coded for the variation in geocentric velocity.

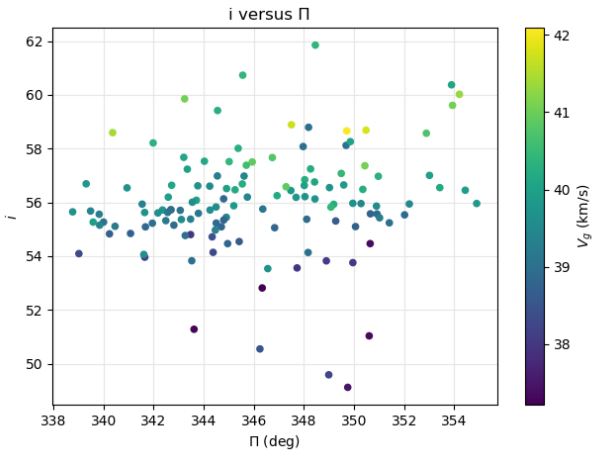

Figure 9 – Diagram of inclination i against the longitude of perihelion Π, color coded for the variation in geocentric velocity for the period 2021–2025.

3 GMN shower association method

The GMN shower association criterion assumes that meteors within 1° in solar longitude, within 3° in radiant, and within 10% in geocentric velocity of a shower reference location are members of that shower. Further details about the shower association are explained in Moorhead et al. (2020). This is a rather strict criterion since meteor showers often have a larger dispersion in radiant position, velocity and activity period. Using these meteor shower selection criteria, 146 orbits have been associated with the June delta Pavonids in the GMN meteor orbit database and the resulting mean orbit has been listed in *Table 1*.

This method classifies more meteors as June delta Pavonids than the method based on the threshold of the D-criteria. The shower had a median geocentric radiant with coordinates R.A. = 298.1°, Decl. = –62.9°, within a circle with a standard deviation of ±1.1° (equinox J2000.0) see

Figure 10. This is in perfect agreement with the results based on the D-criteria method. The radiant drift is also in good agreement for both methods.

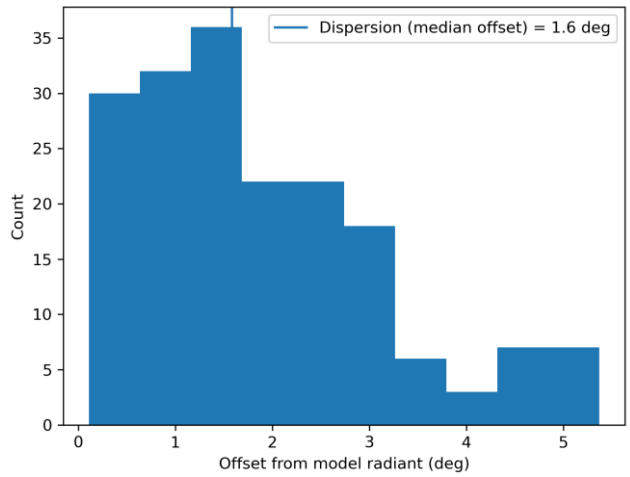

Figure 10 – Dispersion on the radiant position.

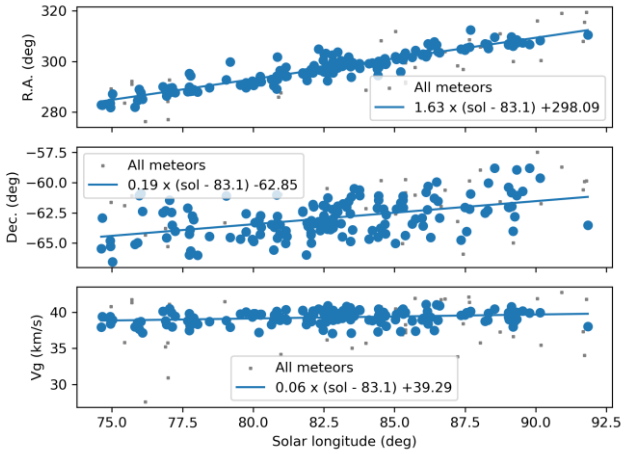

Figure 11 – The radiant drift.

4 The JDP-orbit

With 60 JDP orbits available for 2025, 130 for the past five years based on D-criteria and 146 based on the GMN radiant classification, GMN has twice as much data for this meteor shower than the most recent published results for CAMS (Jenniskens, 2024). This is a lot more than the eleven orbits that were used for the first and only entry about this meteoroid stream listed on the IAU MDC working list. In *Table 1* we compare the orbital parameters obtained by CAMS with the results of GMN for 2025 and 2021–2025 based on two different methods. The results are in very good agreement except for the longitude of perihelion *Π*.

Jenniskens (2024) mentions that the JDP meteoroids penetrate deep, the median begin height is a few kilometers deeper for GMN compared to CAMS. It is not clear if this is due to a difference in camera equipment. *Figure 12* visualizes the four different orbits in the solar system, most of it below the ecliptic plane. The orbits differ mainly in semi major axis *a* and eccentricity *e*, which both are very sensitive to the slightest uncertainty in the measured velocity. The aphelion for the GMN 21–25 orbit is about 60 AU, as comparison the distance of planet Neptune from the Sun is about 30 AU. *Figure 13* shows the orbit in the inner solar system with the intersection at the orbit of the Earth at the ascending node where the JDP orbit crosses from south of the ecliptic to north of it. The meteor shower search routine found some orbits fitting the D-criterion threshold at the descending node but too few to be relevant.

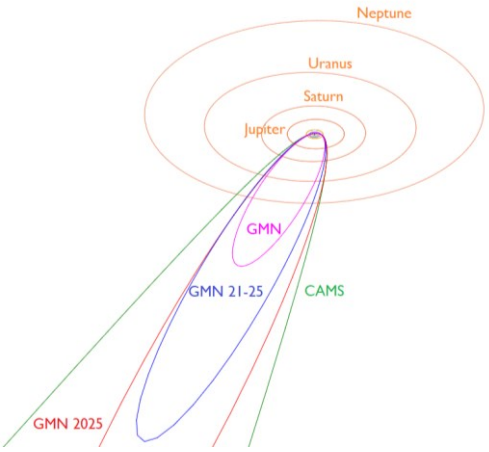

Figure 12 – Comparing the mean orbit obtained by CAMS (green) and by GMN in 2025 (red) and during 2021–2025 (blue for 130 orbits based on D-criteria with $D_D < 0.06$, purple for the 146 based on the GMN classification method) in *Table 1*. (Plotted with the Orbit visualization app provided by Pető Zsolt).

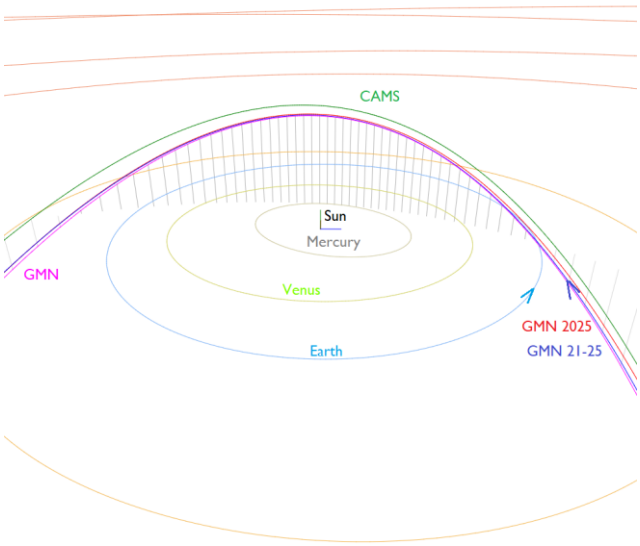

Figure 13 – Comparing the mean orbit obtained by CAMS (green) and by GMN in 2025 (red) and during 2021–2025 (blue for 130 orbits based on D-criteria with $D_D < 0.06$, purple for the 146 based on the GMN classification method) in *Table 1*. (Plotted with the Orbit visualization app provided by Pető Zsolt).

The plotted CAMS orbit shows a slight shift away from the GMN solutions which may be the result of working with median values of the orbital elements instead of computing a mean orbit like for GMN. The three solutions for GMN are in perfect agreement. Note that plotting a 3D view of a meteoroid stream orbit relative to the orbits of the planets has some perspective effect depending on the point of view.

Table 1 – Comparing the orbital parameters obtained by CAMS (Jenniskens, 2024) and the mean orbit obtained by GMN for 2025 and for the period 2021-2025, both based on orbits that fulfill $D_D < 0.06$.

	CAMS	GMN 25	GMN 21–25	GMN
$\lambda_\odot$ (°)	83.1	84.4	83.0	82.8
$\lambda_{\odot b}$ (°)	72	74	74	74.6
$\lambda_{\odot e}$ (°)	90	91	92	91.8
α_g (°)	298.1	300.7	298.1	298.1
δ_g (°)	–63.4	–62.3	–62.9	–62.9
$\Delta\alpha_g$ (°)	+1.74	+1.43	+1.62	+1.63
$\Delta\delta_g$ (°)	+0.22	+0.10	+0.13	+0.19
v_g (km/s)	39.7	39.6	39.6	39.3
λ_g (°)	–	288.1	286.5	203
λ_g–$\lambda_\odot$ (°)	203.0	203.5	203.2	203.5
β_g (°)	–41.4	–40.7	–41.1	–41.1
H_b (km)	106.2	102.6	102.9	–
H_{max} (km)	91.4	93.1	93.0	–
H_e (km)	86.8	88.5	87.7	–
a (A.U.)	625	38.7	30.3	18.5
q (A.U.)	0.584	0.570	0.574	0.573
e	0.999	0.985	0.981	0.969
i (°)	56.0	56.5	56.0	55.9
ω (°)	81.1	83.3	82.8	83.1
Ω (°)	263.0	263.9	263.3	262.7
Π (°)	344.2	347.2	346.1	345.8
T_j	0.60	0.65	0.69	0.80
N	65	60	130	146

The Tisserand's parameter T_j identifies the orbit as of a long-period comet type. A parent-body search top 10 includes candidates with a threshold for the Drummond D_D criterion value lower than 0.30 but none of which can be associated with any certainty (*Table 2*).

Table 2 – Top ten matches of a search for possible parent bodies with $D_D < 0.30$.

Name	D_D
2020 KC7	0.209
2017 DQ36	0.241
C/1978 C1 (Bradfield)	0.241
2012 XT134	0.245
C/1376 M1	0.246
2015 WG9	0.25
(311044) 2004 BB103	0.251
2008 AK33	0.254
2015 YD18	0.258
2016 XK2	0.264

5 Conclusion

This case study confirms the existence of the June delta Pavonids (JDP#835) listed in the IAU MDC Working List of Meteor Showers based on 11 orbits obtained by CAMS in 2014 and 2016 (Jenniskens et al., 2018). GMN obtained 60 orbits that fulfil the discrimination criterion threshold with $D_{SH} < 0.15$ & $D_D < 0.06$ & $D_H < 0.15$. Checking older GMN data, 130 candidate orbits were found. The usual GMN method for shower classification identified 146 JDP meteors. The resulting mean orbit for all three GMN solutions is in good agreement with the result by CAMS published by Jenniskens (2024) which were not yet included in the IAU MDC Working List of Meteor Showers. We propose to consider this meteor shower to be added to the established showers.

Acknowledgment

This report is based on the data of the Global Meteor Network (Vida et al., 2020a; 2020b; 2021) which is released under the CC BY 4.0 license[9]. We thank all 825 participants in the Global Meteor Network project for their contribution and perseverance. A list with the names of the volunteers who contribute to GMN has been published in the 2024 annual report (Roggemans et al., 2025).

References

Drummond J. D. (1981). "A test of comet and meteor shower associations". *Icarus*, **45**, 545–553.

Jenniskens P., Baggaley J., Crumpton I., Aldous P., Pokorny P., Janches D., Gural P. S., Samuels D., Albers J., Howell A., Johannink C., Breukers M., Odeh M., Moskovitz N., Collison J., Ganju S. (2018). "A survey of southern hemisphere meteor showers". *Planetary and Space Science*, **154**, 21–29.

Jenniskens P. (2024). Atlas of Earth's meteor showers. Elsevier, Cambridge, United states. ISBN 978-0-443-23577-1.

Jopek T. J. (1993). "Remarks on the meteor orbital similarity D-criterion". *Icarus*, **106**, 603–607.

Jopek T. J., Rudawska R. and Pretka-Ziomek H. (2006). "Calculation of the mean orbit of a meteoroid stream". *Monthly Notices of the Royal Astronomical Society*, **371**, 1367–1372.

Moorhead A. V., Clements T. D., Vida D. (2020). "Realistic gravitational focusing of meteoroid streams". *Monthly Notices of the Royal Astronomical Society*, **494**, 2982–2994.

Roggemans P., Johannink C. and Campbell-Burns P. (2019a). "October Ursae Majorids (OCU#333)". *eMetN Meteor Journal*, **4**, 55–64.

[9] https://creativecommons.org/licenses/by/4.0/

Roggemans P., Campbell-Burns P., Kalina M., McIntyre M., Scott J. M., Šegon D., Vida D. (2025). “Global Meteor Network report 2024”. *eMetN Meteor Journal*, **10**, 67–101.

Southworth R. B. and Hawkins G. S. (1963). “Statistics of meteor streams”. *Smithsonian Contributions to Astrophysics*, **7**, 261–285.

Vida D., Gural P., Brown P., Campbell-Brown M., Wiegert P. (2020a). “Estimating trajectories of meteors: an observational Monte Carlo approach - I. Theory”. *Monthly Notices of the Royal Astronomical Society*, **491**, 2688–2705.

Vida D., Gural P., Brown P., Campbell-Brown M., Wiegert P. (2020b). “Estimating trajectories of meteors: an observational Monte Carlo approach - II. Results”. *Monthly Notices of the Royal Astronomical Society*, **491**, 3996–4011.

Vida D., Šegon D., Gural P. S., Brown P. G., McIntyre M. J. M., Dijkema T. J., Pavletić L., Kukić P., Mazur M. J., Eschman P., Roggemans P., Merlak A., Zubrović D. (2021). “The Global Meteor Network – Methodology and first results”. *Monthly Notices of the Royal Astronomical Society*, **506**, 5046–5074.

Vida D., Šegon D., Roggemans P. (2025). “New meteor shower in Indus”. *eMetN Meteor Journal*, **10**, 264–268.

Two meteor shower outbursts with potential connection to comet 73P/Schwassmann-Wachmann

Denis Vida[1], **Damir Šegon**[2] **and Paul Roggemans**[3]

[1] **Department of Earth Sciences, University of Western Ontario, London, Ontario, N6A 5B7, Canada**
denis.vida@gmail.com

[2] **Astronomical Society Istra Pula, Park Monte Zaro 2, 52100 Pula, Croatia**

[3] **Pijnboomstraat 25, 2800 Mechelen, Belgium**
paul.roggemans@gmail.com

Two new meteor showers with a Jupiter Family Comet type orbit ($2.00 < T_J < 3.00$) were detected during 2025 May 30–June 3 by the Global Meteor Network. Meteors belonging to these new showers were observed from two radiants at R.A. = 197°, Decl.= +52° and R.A. = 203°, Decl.= +7°, both likely dynamical related to comet 73P/Schwassmann-Wachmann fragments. The new meteor showers have been listed in the Working List of Meteor Showers under the temporary name-designation: M2025-L1 and M2025-L2.

1 Introduction

The first outburst occurred during 2025 May 30–June 1. Thirty-three meteors were recorded using the Global Meteor Network low-light video cameras[10]. The shower was detected by stations in 14 countries; Belgium, the Czech Republic, Germany, France, Croatia, Hungary, Italy, South Korea, The Netherlands, New Zealand, Russia, Slovenia, the United Kingdom, and the United States. The shower had a median geocentric radiant with coordinates R.A. = 196.4°, Decl. = +51.0° (equinox J2000.0), within a circle with a standard deviation of ±1.8°. The geocentric velocity was 12.1 ± 0.1 km/s (*Figure 1*).

The second outburst began roughly simultaneously with the first one but lasted longer, until June 3. Forty-one meteors were recorded using the Global Meteor Network low-light video cameras. The shower was detected by stations in 16 countries; Australia, Belgium, Brazil, Canada, Germany, Greece, Croatia, Hungary, Italy, South Korea, The Netherlands, New Zealand, Slovenia, South Africa, the United Kingdom, and the United States. The radiants of the second outburst were significantly offset from the first, by around 44 degrees in equatorial coordinates. The second shower had a median geocentric radiant with coordinates R.A. = 203.0°, Decl. = +7.6° (equinox J2000.0), within a circle with a standard deviation of ±0.9°. The geocentric velocity was 11.7 ± 0.1 km/s (*Figure 2*).

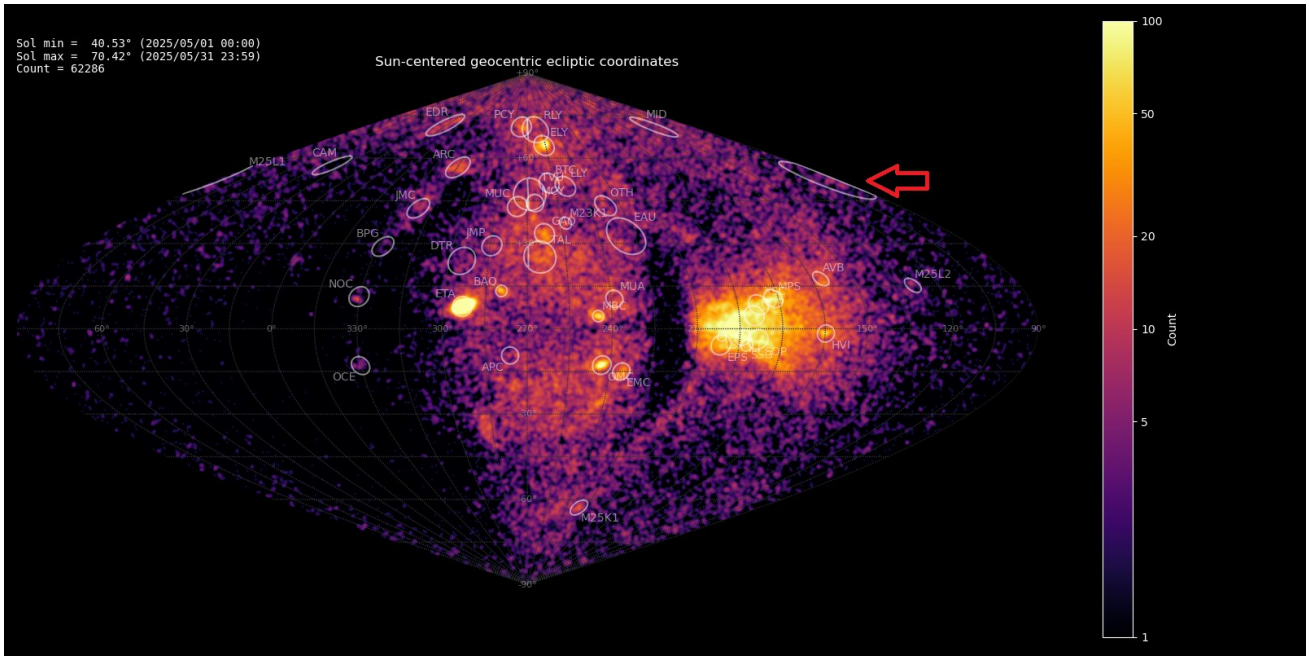

Figure 1 – Heat map with 62286 radiants obtained by the Global Meteor network in May 2025 in Sun-centered geocentric ecliptic coordinates. The radiant of the first outburst is marked with a red arrow (M2025-L1).

[10] https://globalmeteornetwork.org/data/

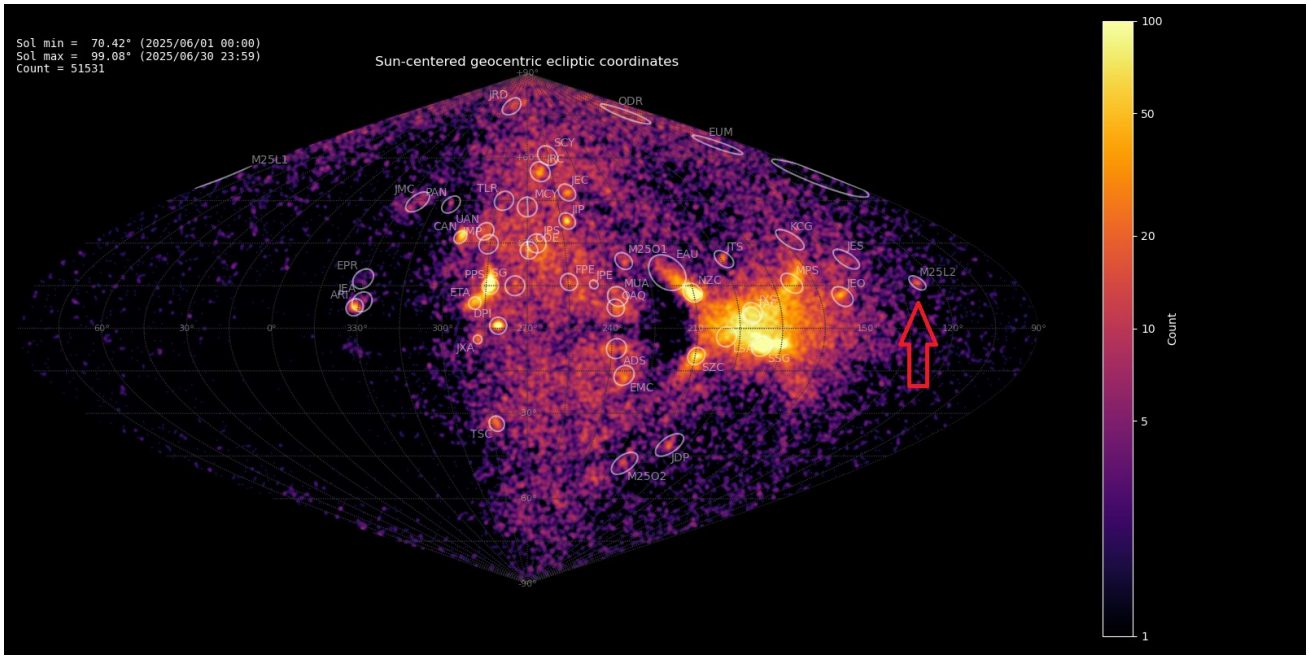

Figure 2 – Heat map with 51531 radiants obtained by the Global Meteor network in June 2025 in Sun-centered geocentric ecliptic coordinates. The radiant of the second outburst is marked with a red arrow (M2025-L2).

2 The first analysis

The GMN shower association criterion assumes that meteors within 1° in solar longitude, within 3° in radiant, and within 10% in geocentric velocity of a shower reference location are members of that shower. Further details about the shower association are explained in Moorhead et al. (2020). This is a rather strict criterion since meteor showers often have a larger dispersion in radiant position, velocity and activity period. Using this method, 33 orbits were identified with the first outburst and 41 with the second outburst.

The radiant drift in R.A. was +1.68° on the sky per degree of solar longitude and –0.44° in Decl., both referenced to solar longitude 69.5° for the first outburst (*Figure 5*).

The radiant drift in R.A. was –0.07° on the sky per degree of solar longitude and +0.46° in Decl., both referenced to solar longitude 71.5° for the second outburst (*Figure 6*).

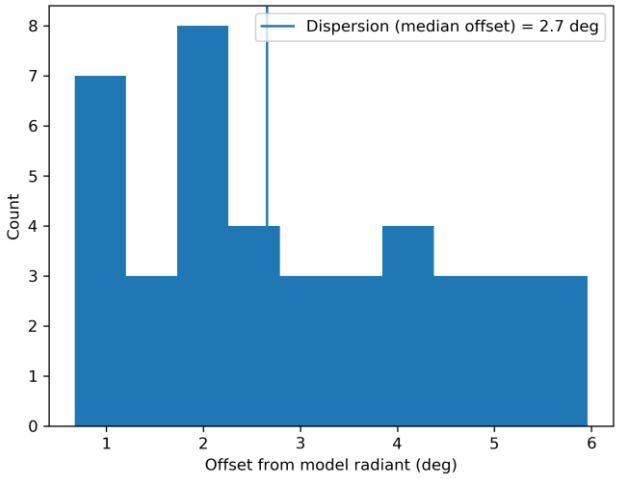

Figure 3 – Dispersion on the radiant position for the first outburst (M2025-L1).

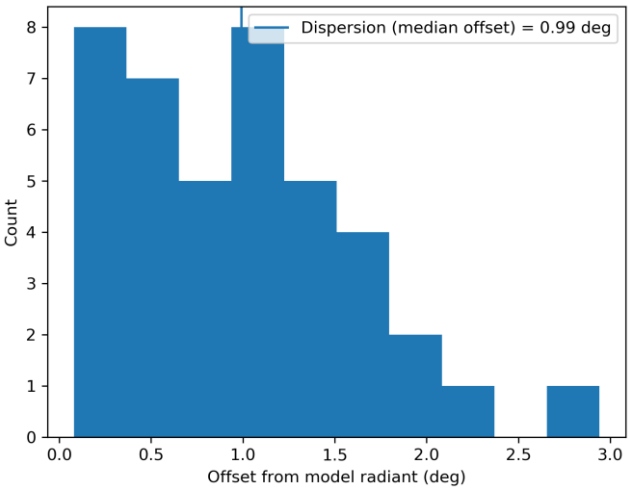

Figure 4 – Dispersion on the radiant position for the second outburst (M2025-L2).

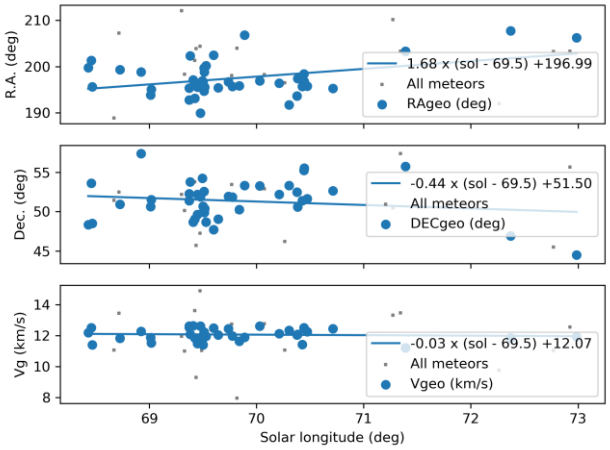

Figure 5 – The radiant drift for the first outburst.

For the first outburst, the geocentric, Sun-centered ecliptic longitude (λ–$\lambda_\odot$) was 96.87°, and the geocentric ecliptic latitude was +52.23° (*Figure 9*). The activity period

spanned solar longitudes 68°–73°, with a clear peak at 69.5° with a zenith hourly rate (ZHR) of about 0.2 meteors/hr. This peak of activity matches the tau Herculid meteor shower, although the radiant location is over 10 degrees away from the 2022 tau Herculid outburst.

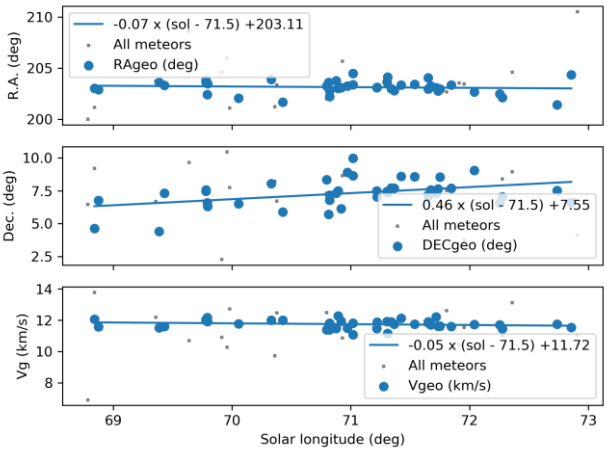

Figure 6 – The radiant drift for the second outburst.

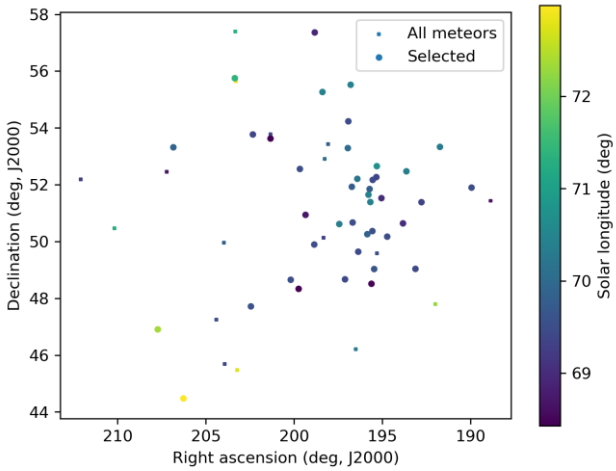

Figure 7 – The radiant distribution during the solar-longitude interval 68° – 73° in equatorial coordinates for the first outburst.

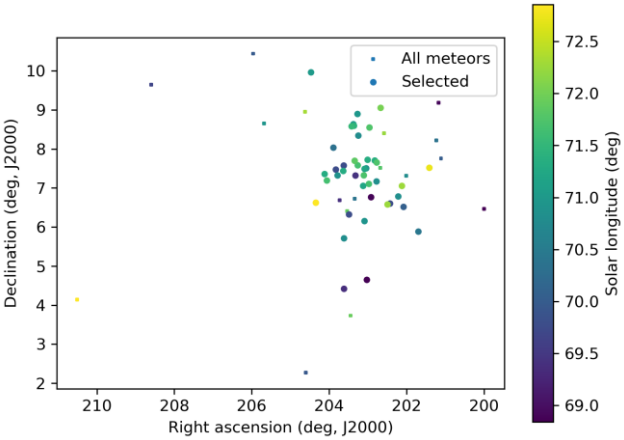

Figure 8 – The radiant distribution during the solar-longitude interval 68° – 73° in equatorial coordinates for the second outburst.

For the second outburst, the geocentric, Sun-centered ecliptic longitude (λ–$\lambda_\odot$) was 126.99°, and the geocentric ecliptic latitude was +15.9.°. The activity period spanned solar longitudes 68°–73°, with a broad peak around 71.5°.

Both outbursts were reported to the IAU-MDC working list of meteor showers and added as M2025-L1 for the first outburst and M2025-L2 for the second outburst.

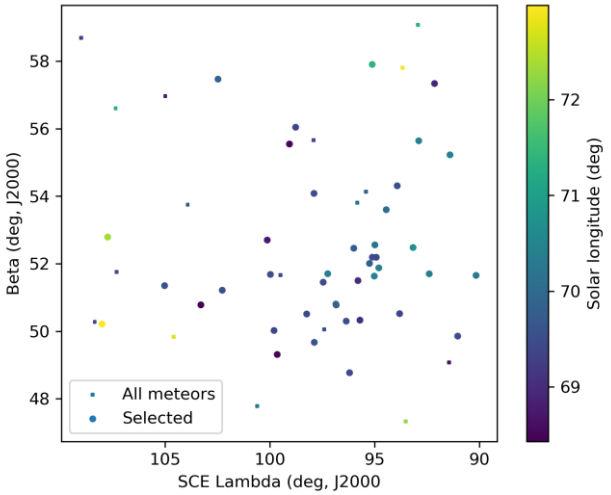

Figure 9 – The radiant distribution during the solar-longitude interval 68° – 73° in Sun centered geocentric ecliptic coordinates for the first outburst.

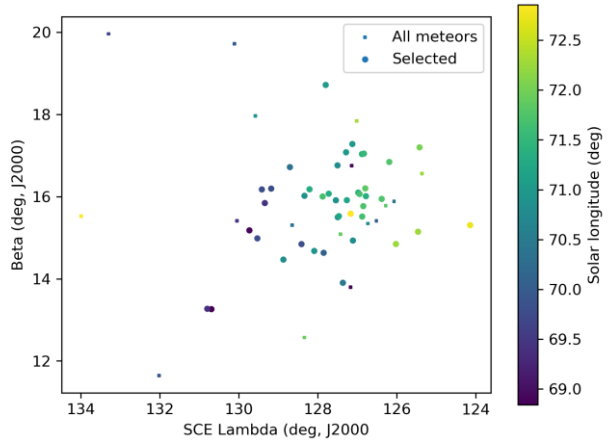

Figure 10 – The radiant distribution during the solar-longitude interval 68° – 73° in Sun centered geocentric ecliptic coordinates for the second outburst.

3 Another search method

Another method has been applied to check this new meteor shower discovery. The starting point here can be any visually spotted concentration of radiant points or any other indication for the occurrence of similar orbits. The method has been described before (Roggemans et al., 2019). The main difference with the method applied in *Section 2* is that three different discrimination criteria are combined in order to have only those orbits which fit different criteria thresholds. The D-criteria that we use are these of Southworth and Hawkins (1963), Drummond (1981) and Jopek (1993) combined. Instead of using a cutoff value for the D-criteria these values are considered in different classes with different thresholds of similarity. Depending on the dispersion and the type of orbits, the most appropriate threshold of similarity is selected to locate the best fitting mean orbit as the result of an iterative procedure. We consider five different threshold levels of similarity:

- Low: $D_{SH} < 0.25$ & $D_D < 0.105$ & $D_H < 0.25$;

- Medium low: $D_{SH} < 0.2$ & $D_D < 0.08$ & $D_H < 0.2$;
- Medium high: $D_{SH} < 0.15$ & $D_D < 0.06$ & $D_H < 0.15$;
- High: $D_{SH} < 0.1$ & $D_D < 0.04$ & $D_H < 0.1$.
- Very high: $D_{SH} < 0.05$ & $D_D < 0.02$ & $D_H < 0.05$.

For the first outburst the procedure converged after a few iterations at a mean orbit for all orbits that fitted the high threshold class. The radiant points for the lower threshold classes appear very scattered but with a clear concentration of radiants (*Figure 11*). The second outburst took many more iteration steps and converged at an optimal mean orbit for the very high threshold class for which the radiants show a very distinct concentration (*Figure 12*).

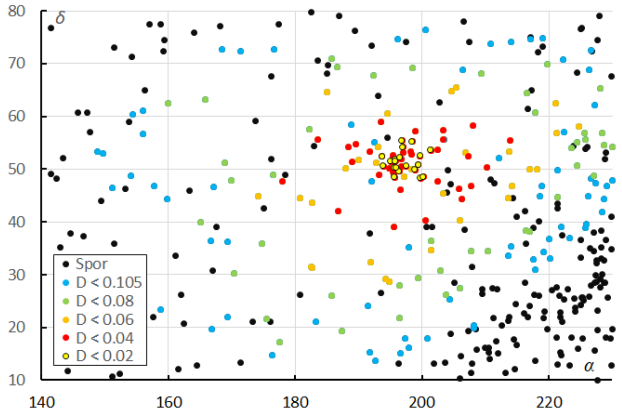

Figure 11 – The radiant distribution during the solar-longitude interval 68° – 73° in equatorial coordinates for the first outburst, color coded for different thresholds of the D_D orbit similarity criteria.

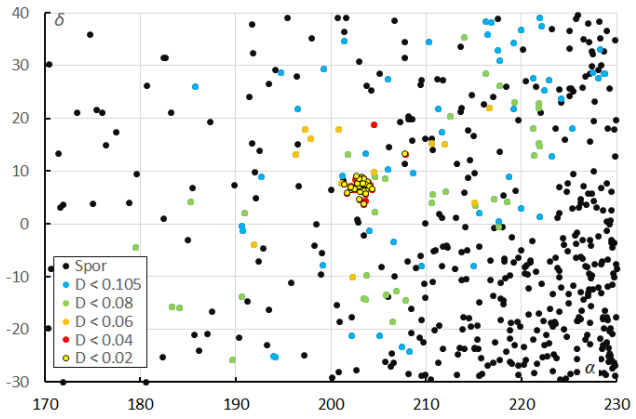

Figure 12 – The radiant distribution during the solar-longitude interval 68° – 73° in equatorial coordinates for the second outburst, color coded for different thresholds of the D_D orbit similarity criteria.

Looking at the plot with the radiants in Sun-centered geocentric ecliptic coordinates for the first outburst (*Figure 13*), the radiant drift has been compensated but the radiant of the first outburst still appears rather diffuse compared to the concentration at the bottom right in the plot which is the radiant for the second outburst. *Figure 14* shows the radiants in Sun-centered geocentric ecliptic coordinates centered on the second outburst.

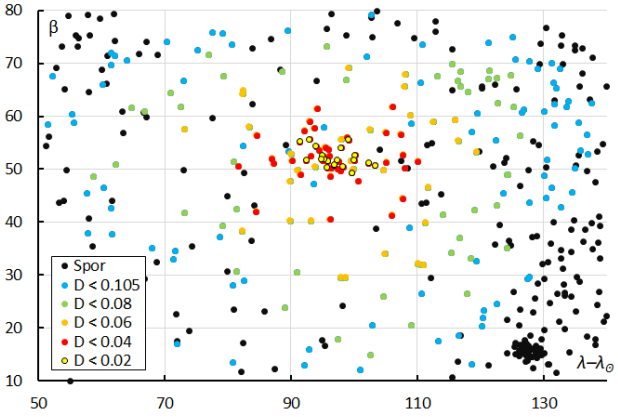

Figure 13 – The radiant distribution in Sun-centered geocentric ecliptic coordinates for the first outburst, color coded for different thresholds of the D_D orbit similarity criteria.

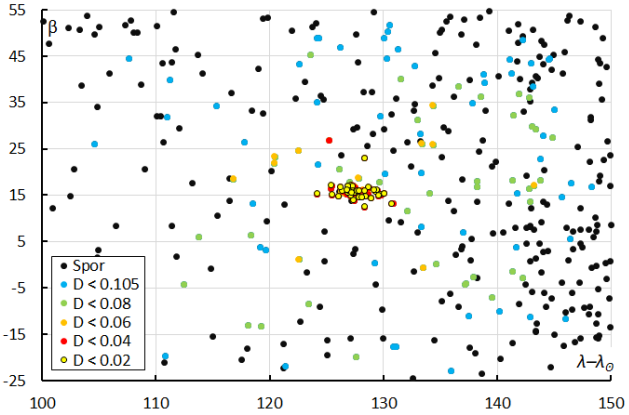

Figure 14 – The radiant distribution in Sun-centered geocentric ecliptic coordinates for the second outburst, color coded for different thresholds of the D_D orbit similarity criteria.

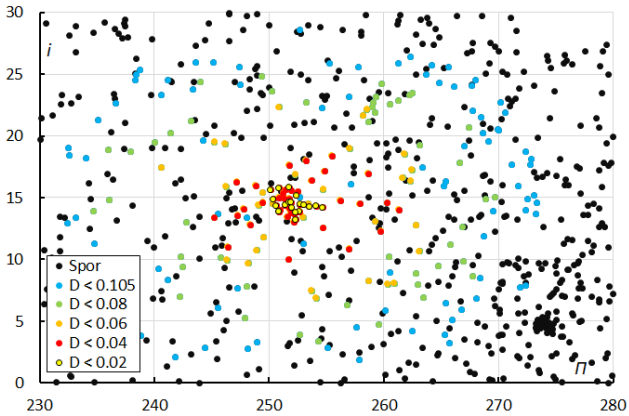

Figure 15 – Diagram of inclination i against the longitude of perihelion Π for the first outburst, color coded for different thresholds of the D_D orbit similarity criteria.

The concentration of similar orbits becomes even more obvious in the diagram of the inclination i against the longitude of perihelion Π. The concentration is more distinc in this diagram than in the radiant plots, for the orbits of the first outburst in *Figure 15* and the second outburst in *Figure 16*. Orbits that fit the more tolerant discrimination thresholds are most likely sporadics that fullfil these criteria by chance but some orbits may be more dispersed shower members. Similarity criteria do not provide any certainty in these specific cases.

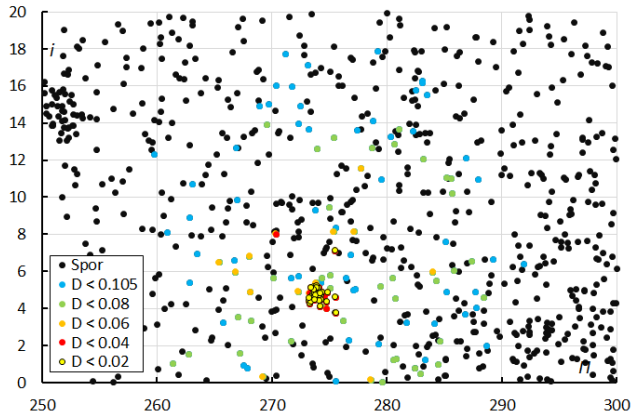

Figure 16 – Diagram of inclination i against the longitude of perihelion Π for the second outburst, color coded for different thresholds of the D_D orbit similarity criteria.

When all data were collected the GMN shower association criterion identified 52 orbits for the first outburst, eight of which fail in the discrimination threshold with $D_{SH} < 0.1$ & $D_D < 0.04$ & $D_H < 0.1$. 46 orbits were identified for the second outburst according to the GMN shower association criterion for which only two fail to fit the above thresholds of the similarity criteria.

The method based on D-criteria identified 56 orbits for the first outburst that fulfil the discrimination threshold with $D_{SH} < 0.1$ & $D_D < 0.04$ & $D_H < 0.1$ of which 12 were not detected by the GMN shower association criterion. For the second outburst this method identified 47 orbits of which only three were not detected by the GMN shower association criterion.

4 The orbits of both outbursts

The discovery of the two outbursts was announced as soon as the data for these nights were processed (Vida et al., 2025). The data has also been added to the IAU MDC Working List of Meteor Showers as M2025-L1[11] and M2025-L2[12]. Meanwhile more meteors were associated with both orbits and identified as M25L1 and M25L2 in the GMN meteor orbit dataset. The mean orbits for the different datasets and methods are in very good agreement apart from the difference in radiant drift for the first outburst which is due to the rather scattered radiant and short time span to derive the radiant drift. The different solutions are listed in *Table 1* for the first outburst and in *Table 2* for the second outburst. The column MDC lists the initial values as included in the IAU MDC Working List of Meteor Showers, M25-L1 and M25-L2 are the parameters for all orbits with this identification in the GMN orbit dataset. The columns $D_D < 0.04$ and $D_D < 0.02$ are the solutions obtained with the shower identification method based on D-criteria for these D-criteria thresholds. The different datasets and both different methods result in almost identical orbital parameters.

Table 1 – Comparing the orbits for the first outburst, derived by the two methods, MDC lists the orbital parameters as initially derived and reported to the IAU-MDC, M25-L1 with all data processed, $D_D < 0.04$ and $D_D < 0.02$ are the mean orbits according to the method described in *Section 3*.

	MDC	M25-L1	$D_D < 0.04$	$D_D < 0.02$
$\lambda_\odot$ (°)	69.5	69.6	69.7	69.5
$\lambda_{\odot b}$ (°)	68.0	68.4	68.4	68.4
$\lambda_{\odot e}$ (°)	73.0	73.0	73.0	73.0
α_g (°)	197.0	196.6	196.6	196.6
δ_g (°)	+51.5	+51.6	+51.6	+51.2
$\Delta\alpha_g$ (°)	+1.68	+1.82	+1.43	–
$\Delta\delta_g$ (°)	–0.44	–0.31	+0.33	–
v_g (km/s)	12.1	12.0	12.0	12.0
λ_g (°)	166.37	165.88	165.9	166.5
λ_g–$\lambda_\odot$ (°)	96.87	95.91	96.1	96.8
β_g (°)	+52.23	+51.69	+51.7	+51.7
a (A.U.)	2.83	2.80	2.80	2.81
q (A.U.)	1.013	1.013	1.013	1.013
e	0.642	0.638	0.639	0.640
i (°)	14.6	14.5	14.5	14.5
ω (°)	182.4	182.2	182.4	182.4
Ω (°)	69.8	70.0	70.0	69.6
Π (°)	252.2	252.1	252.3	252.0
T_j	2.93	2.95	2.95	2.94
N	33	52	56	20

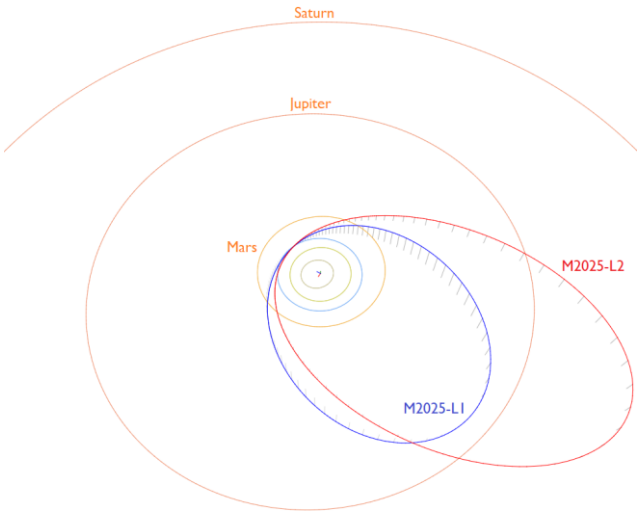

Figure 17 – The mean orbits for both outbursts, blue is for L2025-L1 and red for L2025-2. (Plotted with the Orbit visualization app provided by Pető Zsolt).

[11] https://www.ta3.sk/IAUC22DB/MDC2022/Roje/pojedynczy_obiekt.php?lporz=01730&kodstrumienia=01232

[12] https://www.ta3.sk/IAUC22DB/MDC2022/Roje/pojedynczy_obiekt.php?lporz=01731&kodstrumienia=01233

Table 2 – Comparing the orbits for the second outburst, derived by the two methods, MDC lists the orbital parameters as initially derived and reported to the IAU-MDC, M25-L2 with all data processed, $D_D < 0.04$ and $D_D < 0.02$ are the mean orbits according to the method described in *Section 3*.

	MDC	M25-L2	$D_D < 0.04$	$D_D < 0.02$
$\lambda_\odot$ (°)	71.5	71.0	71.0	71.2
$\lambda_{\odot b}$ (°)	68.0	68.8	68.8	68.8
$\lambda_{\odot e}$ (°)	73.0	72.9	72.9	72.9
α_g (°)	203.1	203.1	203.2	203.2
δ_g (°)	+7.5	+7.3	+7.3	+7.3
$\Delta\alpha_g$ (°)	–0.07	–0.06	+0.02	+0.09
$\Delta\delta_g$ (°)	+0.46	+0.45	+0.23	+0.46
v_g (km/s)	11.7	11.8	11.8	11.8
λ_g (°)	198.49	198.46	198.5	198.6
λ_g–$\lambda_\odot$ (°)	126.99	127.32	127.5	127.4
β_g (°)	+15.93	+15.81	+15.9	+15.9
a (A.U.)	3.921	4.03	3.96	3.96
q (A.U.)	0.980	0.979	0.979	0.979
e	0.750	0.757	0.753	0.753
i (°)	4.8	4.8	4.8	4.8
ω (°)	202.9	202.9	202.8	202.9
Ω (°)	71.1	71.0	71.1	71.1
Π (°)	274.0	273.9	273.9	274.0
T_j	2.47	2.44	2.46	2.46
N	41	46	47	38

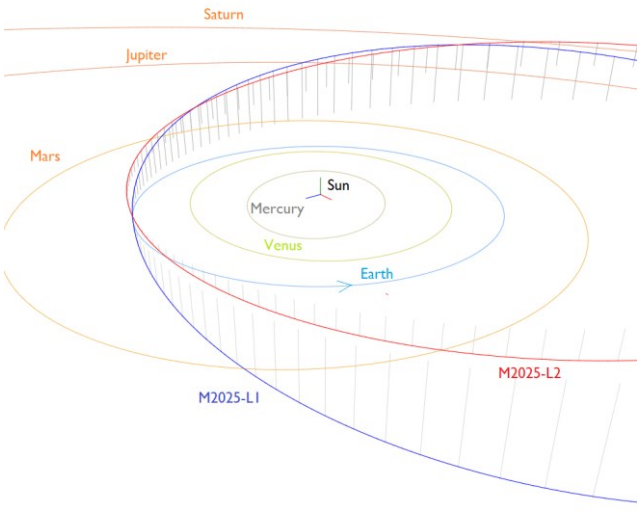

Figure 18 – The mean orbits for both outbursts, blue is for L2025-L1 and red for L2025-2, close-up in the inner Solar System. (Plotted with the Orbit visualization app provided by Pető Zsolt).

Figure 17 shows both orbits relative to the planets. M2025-L1 has its aphelion (4.6 AU) within the orbit of Jupiter and M2025-L2 has its aphelion (7 AU) between the orbits of Jupiter and Saturn. *Figure 18* shows a close-up in the inner solar system with both dust trails catching up with the Earth from the rear, meaning that the radiants are located at the evening sky with meteors that hit the Earth with a very slow geocentric velocity.

5 Parent body search

The Tisserand's parameter T_j identifies the orbits of both outbursts as of a Jupiter Family Comet type, hence a comet is the most likely candidate as parent body.

A search for a parent body using the Drummond D-criterion returned several matches on minor planets with $D_D < 0.07$, but only one comet: 73P/Schwassmann-Wachmann ($D_D = 0.06$), the parent body of the tau Herculids, suggests a tentative dynamical relationship for the first outburst (*Table 3*).

Table 3 – Top ten search results for possible parent bodies for the first outburst M2025-L1with $D_D < 0.07$.

Name	D_D
2014 JL25	0.039
2010 JN71	0.053
2014 ER49	0.055
2021 GR7	0.056
2018 JZ1	0.059
2019 KZ3	0.061
2006 HQ30	0.062
73P/Schwassmann-Wachmann 3-S	0.062
2025 KH2	0.062
2007 KE4	0.065

For the second outburst the top-ten closest objects during a parent-body search using the Drummond D-criterion were all fragments of comet 73P, all with $D_D < 0.062$; the best matching fragment was component Y, with $D_D = 0.054$ (*Table 4*).

Table 4 – Top ten search results for possible parent bodies for the second outburst M2025-L2 with $D_D = 0.062$.

Name	D_D
73P/Schwassmann-Wachmann 3-Y	0.054
73P/Schwassmann-Wachmann 3-BW	0.056
73P/Schwassmann-Wachmann 3-AP	0.059
73P/Schwassmann-Wachmann 3-AS	0.059
73P/Schwassmann-Wachmann 3-BC	0.06
73P/Schwassmann-Wachmann 3-AL	0.06
73P/Schwassmann-Wachmann 3-BV	0.06
73P/Schwassmann-Wachmann 3-Q	0.06
73P/Schwassmann-Wachmann 3-BS	0.06
73P/Schwassmann-Wachmann 3-W	0.06

The Canadian Meteor Orbit Radar (CMOR) did not detect any members of either outburst, suggesting that the events were dominated by larger particles, in contrast to the 2022 tau Herculid outburst, which was rich in smaller meteoroids

and well observed by CMOR (Egal et al., 2023). The two temporally adjacent but dynamically distinct 2025 outbursts indicate the presence of separate dust filaments from comet 73P intersecting the Earth's orbit within a few days of each other (M2025-L1 represented best by 73P fragment S). Although similar in timing to the 2022 tau Herculid outburst, both 2025 radiants are spatially offset, implying distinct release epochs or differing trail evolution.

Notably, the 2022 tau Herculid radiant at R.A. = 209.17°, Decl. = +28.21°, lies almost equidistant between the 2025 outburst radiants (about 20° from each one), further supporting the interpretation of multiple discrete filaments originating from comet 73P. The complicating factor in dynamical modelling of the meteoroid complex is the high uncertainty of the comet's orbit prior to 1930. Further modelling work is required to investigate whether the observed showers are caused by older trails, ejecta from the fragments after the break-up (observed for some of them shortly after 1995), or by material released in 1995 but with different ejection velocities.

6 Conclusion

Two meteor outbursts detected and covered by the Global Meteor Network during 2025 May 30–June 3 have been analyzed by two different methods and were reported to the IAU MDC as two possible new meteor showers. The orbits proved to be Jupiter Family comet type meteor orbits and a parent body search resulted in a most likely dynamical relationship with comet 73P/Schwassmann-Wachmann fragments related with the tau Herculids which displayed strong activity in 2022. No other optical or radar observations for these 2025 outbursts were know at the time this report was written.

Acknowledgment

This report is based on the data of the Global Meteor Network (Vida et al., 2020a; 2020b; 2021) which is released under the CC BY 4.0 license[13]. We thank all 825 participants in the Global Meteor Network project for their contribution and perseverance. A list with the names of the volunteers who contribute to GMN has been published in the 2024 annual report (Roggemans et al., 2025).

References

Drummond J. D. (1981). "A test of comet and meteor shower associations". *Icarus*, **45**, 545–553.

Egal A., Wiegert P.A., Brown P.G., Vida D. (2023). "Modelling the 2022-Herculid outburst". *The Astrophysical Journal*, **949**, Issue 2, id.96, 18 pages.

Jopek T. J. (1993). "Remarks on the meteor orbital similarity D-criterion". *Icarus*, **106**, 603–607.

Jopek T. J., Rudawska R. and Pretka-Ziomek H. (2006). "Calculation of the mean orbit of a meteoroid stream". *Monthly Notices of the Royal Astronomical Society*, **371**, 1367–1372.

Moorhead A. V., Clements T. D., Vida D. (2020). "Realistic gravitational focusing of meteoroid streams". *Monthly Notices of the Royal Astronomical Society*, **494**, 2982–2994.

Roggemans P., Johannink C. and Campbell-Burns P. (2019a). "October Ursae Majorids (OCU#333)". *eMetN Meteor Journal*, **4**, 55–64.

Roggemans P., Campbell-Burns P., Kalina M., McIntyre M., Scott J. M., Šegon D., Vida D. (2025). "Global Meteor Network report 2024". *eMetN Meteor Journal*, **10**, 67–101.

Southworth R. B. and Hawkins G. S. (1963). "Statistics of meteor streams". *Smithsonian Contributions to Astrophysics*, **7**, 261–285.

Vida D., Gural P., Brown P., Campbell-Brown M., Wiegert P. (2020a). "Estimating trajectories of meteors: an observational Monte Carlo approach - I. Theory". *Monthly Notices of the Royal Astronomical Society*, **491**, 2688–2705.

Vida D., Gural P., Brown P., Campbell-Brown M., Wiegert P. (2020b). "Estimating trajectories of meteors: an observational Monte Carlo approach - II. Results". *Monthly Notices of the Royal Astronomical Society*, **491**, 3996–4011.

Vida D., Šegon D., Gural P. S., Brown P. G., McIntyre M. J. M., Dijkema T. J., Pavletić L., Kukić P., Mazur M. J., Eschman P., Roggemans P., Merlak A., Zubrović D. (2021). "The Global Meteor Network – Methodology and first results". *Monthly Notices of the Royal Astronomical Society*, **506**, 5046–5074.

Vida D., Brown P., Egal A. (2025). "Two meteor shower outbursts with potential connection to comet 73P". CBET 5561, D.W.E. Green, editor.

[13] https://creativecommons.org/licenses/by/4.0/

New meteor shower in Eridanus

Damir Šegon[1], **Denis Vida**[2] **and Paul Roggemans**[3]

[1] **Astronomical Society Istra Pula, Park Monte Zaro 2, 52100 Pula, Croatia**

[2] **Department of Earth Sciences, University of Western Ontario, London, Ontario, N6A 5B7, Canada**
denis.vida@gmail.com

[3] **Pijnboomstraat 25, 2800 Mechelen, Belgium**
paul.roggemans@gmail.com

A new meteor shower on a Long-period comet type orbit ($T_J = -0.22$) has been detected during July 25 – August 3, 2025 by the Global Meteor Network. Meteors belonging to the new shower were observed between $122° < \lambda_\odot < 131°$ from a radiant at R.A. = 29.5° and Decl.= –21.1° in the constellation of Eridanus, with a geocentric velocity of 61.4 km/s. The new meteor shower has been listed in the Working List of Meteor Showers under the temporary name-designation: M2025-P1.

1 Introduction

The GMN radiant map for July 28–29, 2025 shows a weak concentration of related radiants in the constellation of Eridanus not far from the established shower, eta Eridanids (ERI#191). 32 meteors of this meteor shower were observed by the Global Meteor Network[14] low-light video cameras on 2025 July 25 – August 3 with most events on July 28–29 (*Figure 1*). The shower was independently observed by cameras in six countries (Australia, Brazil, Greece, South Korea, New Zealand and the United States).

The shower had a median geocentric radiant with coordinates R.A. = 29.5°, Decl. = –21.1°, within a circle with a standard deviation of ±1.1° (equinox J2000.0) see *Figure 2*. The radiant drift in R.A. is +0.79 deg on the sky per degree of solar longitude and +0.56 in Dec., both referenced to $\lambda_\odot = 125.6°$ (*Figures 3 and 4*). The median Sun-centered ecliptic coordinates were $\lambda - \lambda_\odot = 253.3°$, $\beta = -30.9°$ (*Figure 5*). The geocentric velocity was 61.4 ± 0.2 km/s.

This possible new meteor shower was reported to the IAU MDC and added under the temporary identification 2025-P1[15].

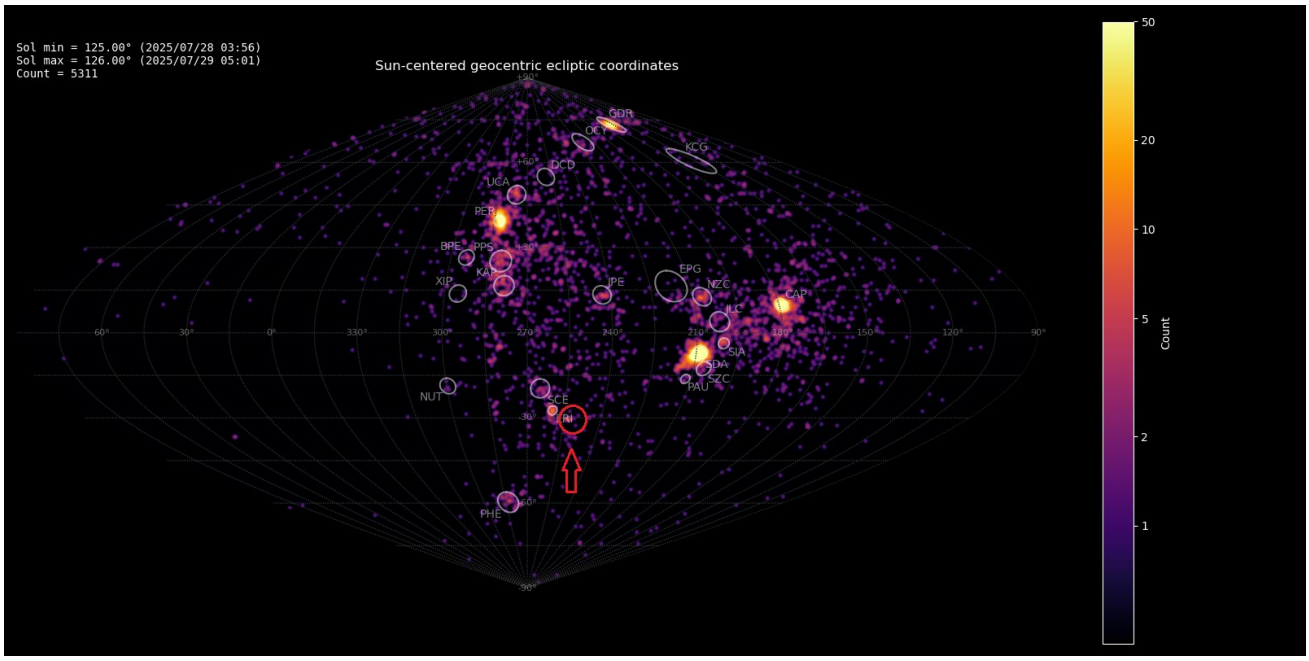

Figure 1 – Heat map with 5311 radiants obtained by the Global Meteor network on July 28–29 2025. A weak concentration is visible in Sun-centered geocentric ecliptic coordinates which was identified as a new meteor shower with the temporary identification M2025-P1.

[14] https://globalmeteornetwork.org/data/

[15] https://www.ta3.sk/IAUC22DB/MDC2022/Roje/pojedynczy_obiekt.php?lporz=01734&kodstrumienia=01236

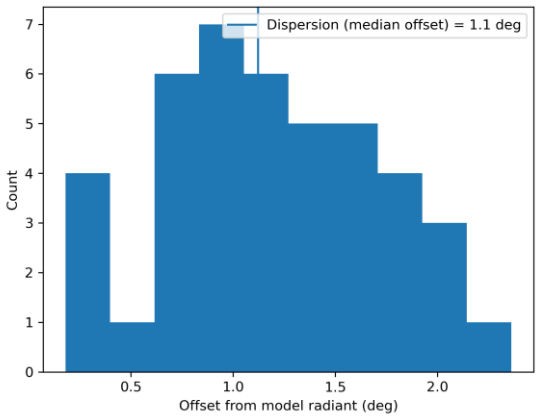

Figure 2 – Dispersion on the radiant position.

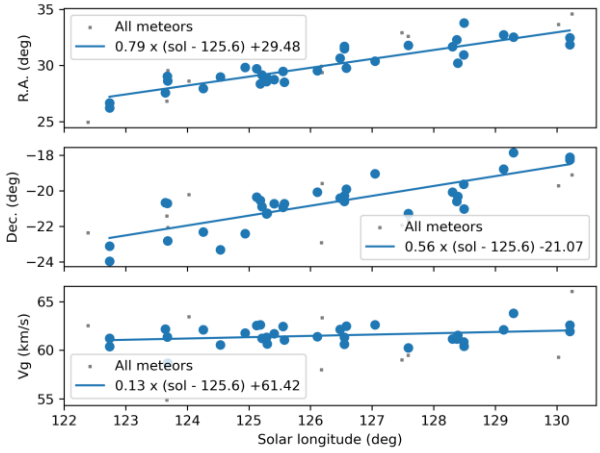

Figure 3 – The radiant drift.

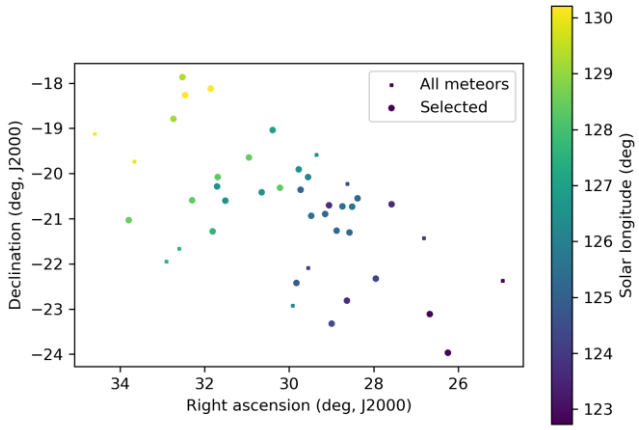

Figure 4 – The radiant distribution during the solar-longitude interval 122° – 131° in equatorial coordinates.

2 First detection

The GMN shower association criterion assumes that meteors within 1° in solar longitude, within 3° in radiant, and within 10% in geocentric velocity of a shower reference location are members of that shower. Further details about the shower association are explained in Moorhead et al. (2020). This is a rather strict criterion since meteor showers often have a larger dispersion in radiant position, velocity and activity period. Using these meteor shower selection criteria, 32 orbits have been associated with the new shower in the GMN meteor orbit database and the mean orbit has been listed in *Table 1*.

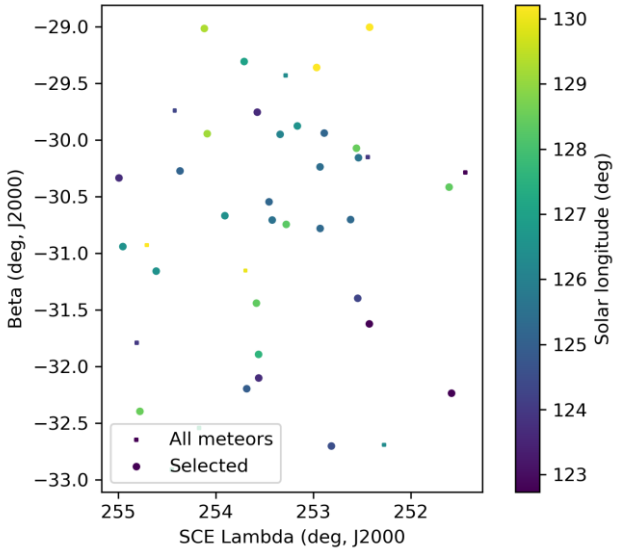

Figure 5 – The radiant distribution during the solar-longitude interval 122° – 131° in Sun centered geocentric ecliptic coordinates.

3 Another search method

Another method has been applied to check this new meteor shower discovery. The starting point here can be any visually spotted concentration of radiant points or any other indication for the occurrence of similar orbits. The method has been described before (Roggemans et al., 2019). The main difference with the method applied in *Section 2* is that three different discrimination criteria are combined in order to have only those orbits which fit different criteria. The D-criteria that we use are these of Southworth and Hawkins (1963), Drummond (1981) and Jopek (1993) combined. Instead of using a cutoff value for the threshold of the D-criteria these values are considered in different classes with different thresholds of similarity. Depending on the dispersion and the type of orbits, the most appropriate threshold of similarity is selected to locate the best fitting mean orbit as the result of an iterative procedure.

This method resulted in a mean orbit with 89 related orbits that fit within the similarity threshold with $D_{SH} < 0.20$, $D_D < 0.08$ and $D_J < 0.20$, recorded 2025 July 25 – August 3. The plot of the radiant positions in equatorial coordinates, color coded for different D-criteria thresholds, shows a stretched trail in Right Ascension from about 25° to 35° due to the radiant drift (*Figure 6*), see also *Figure 3*.

Looking at the Sun-centered geocentric ecliptic coordinates the radiant drift caused by of the Earth moving on its orbit around the Sun is compensated and a more compact radiant becomes visible (*Figure 7*). The blue dots with $D_{SH} < 0.25$, $D_D < 0.105$ and $D_J < 0.25$ as well as the green dots with $D_{SH} < 0.20$, $D_D < 0.08$ and $D_J < 0.20$ display a large dispersion and may include some contamination with sporadics and outliers belonging to the nearby eta Eridanids (ERI#191). To reduce the risk of including these orbits, in

the second method only the 27 orbits that fit the threshold with $D_{SH} < 0.10$, $D_D < 0.05$ and $D_J < 0.10$ are considered.

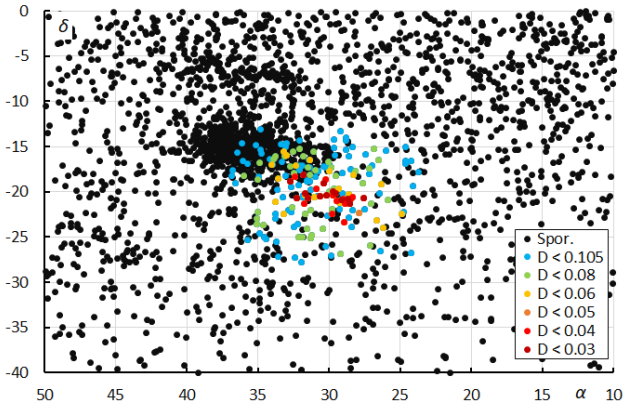

Figure 6 – The radiant distribution during the solar-longitude interval 122° – 131° in equatorial coordinates, color coded for different values of the D_D orbit similarity criterion.

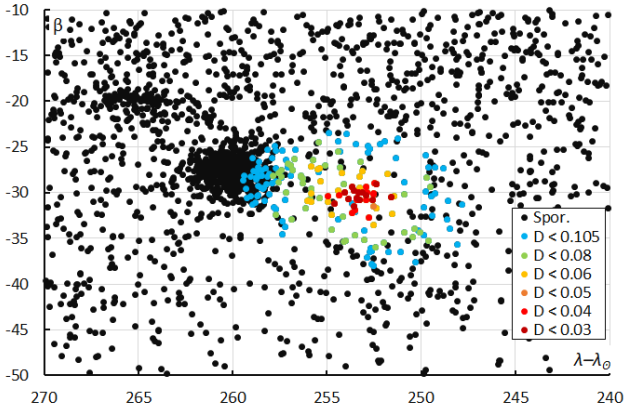

Figure 7 – The radiant distribution during the solar-longitude interval 122° – 131° in Sun-centered geocentric ecliptic coordinates, color coded for different values of the D_D orbit similarity criterion.

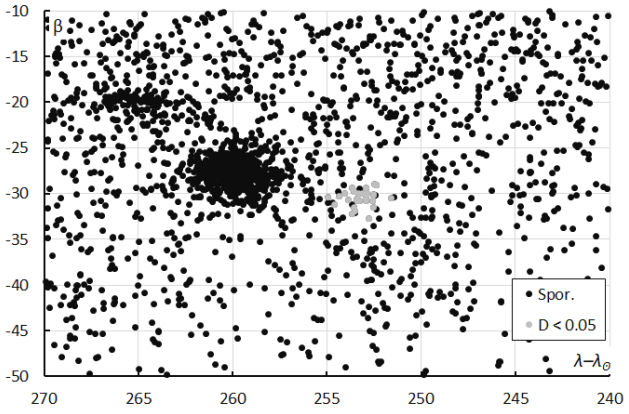

Figure 8 – The sporadic radiants during the solar-longitude interval 122° – 131° in Sun-centered geocentric ecliptic coordinates, with M2025-P1 radiants marked in grey for $D_D < 0.05$.

Figures 8 and 9 show that these radiants appear on top of an evenly distributed sporadic radiant background. The other concentration of radiants visible left of M2025-P1 in *Figures 7, 8 and 9* belong to the eta Eridanids (ERI#191). Left above the eta Eridanids another concentration is visible, which are radiants of the 77-Cetids (SCE#1070) which looks like a duplicate of the rho Eridanids (RER#738), both reported by Jenniskens (2024). The presence of these other sources nearby M2025-P1 is a likely explanation why M2025-P1 remained unnoticed so far.

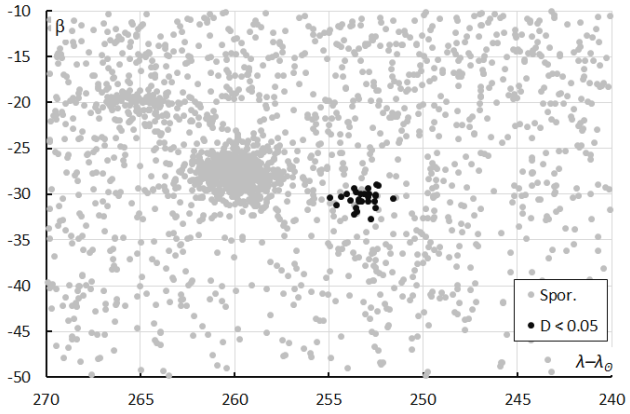

Figure 9 – The M2025-P1 radiants for $D_D < 0.05$ during the solar-longitude interval 122° – 131° in Sun-centered geocentric ecliptic coordinates, with the sporadic radiants marked in grey.

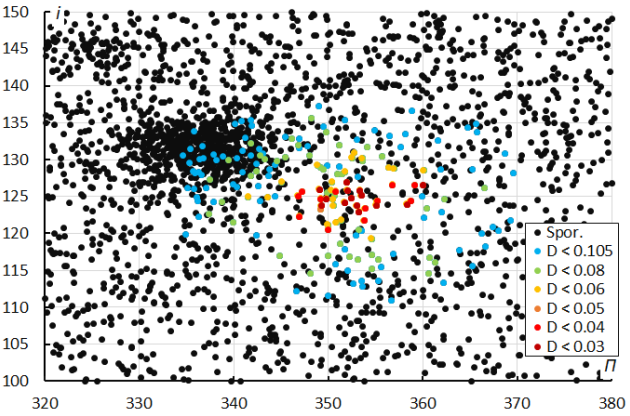

Figure 10 – The diagram of the inclination *i* against the longitude of perihelion *Π* color coded for different classes of D criterion threshold.

The diagram with the inclination against the longitude of perihelion (*Figure 10*) shows quite a lot dispersion on the longitude of perihelion *Π*.

4 Orbit and parent body

The final mean orbits obtained by the two methods are almost identical (*Figure 11*, *Table 1*). The orbit of the eta Eridanids has been included to show that this is a very different orbit than M2025-P1. *Figure 12* shows the orbits in the inner solar system. The dust of M2025-P1 crosses the Earth orbit at its ascending node, hitting the Earth almost head-on from below the ecliptic plane.

Only one orbit of the 32 meteors identified as M2025-P1 by the first shower identification fails to fit the $D_{SH} < 0.20$, $D_D < 0.08$ and $D_J < 0.2$ threshold. Six meteors identified by the first method were not used in the second method because they fail to fit the $D_{SH} < 0.10$, $D_D < 0.05$ and $D_J < 0.10$ threshold. Only one orbit (20250731142527_hG3bc) identified by the second method was ignored by the first method.

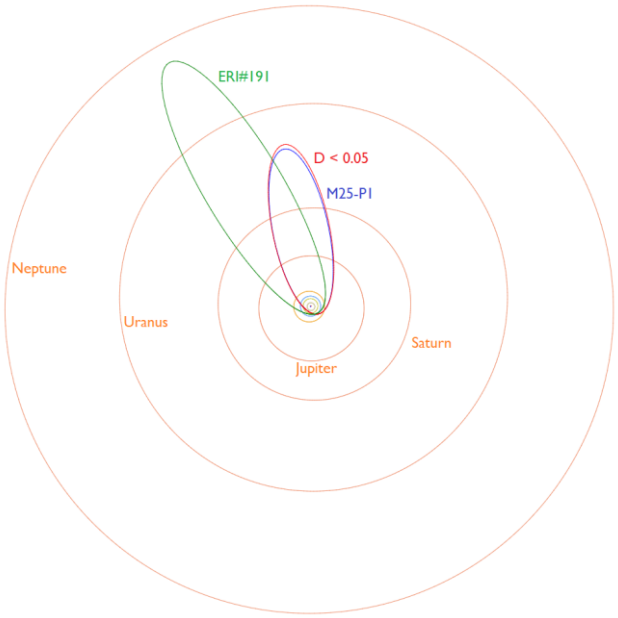

Figure 11 – Comparing the mean orbit based on the shower identification according to the two methods, blue is for M2025-P1 and red for the alternative shower search method with $D_D < 0.05$ in *Table 1*. (Plotted with the Orbit visualization app provided by Pető Zsolt).

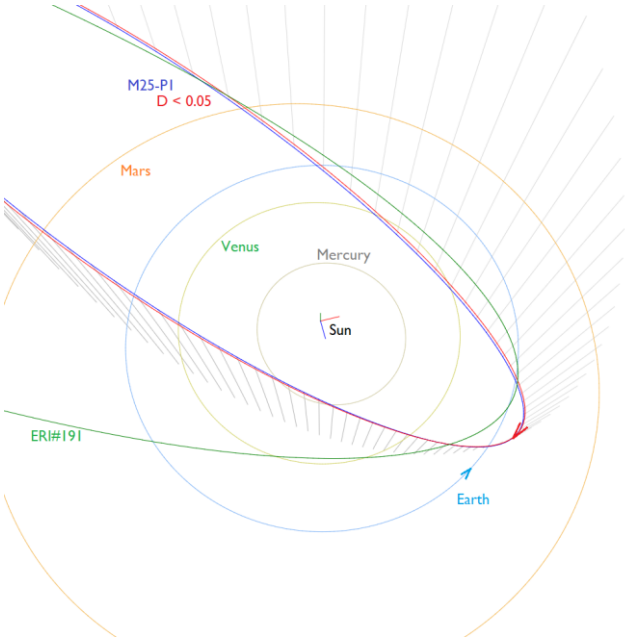

Figure 12 – Comparing the mean orbits in the inner solar system, blue is for M2025-P1 and red for the other shower search method with $D_D < 0.05$ in *Table 1*. (Plotted with the Orbit visualization app provided by Pető Zsolt).

The Tisserand's parameter T_j identifies the orbit as of a long-period comet type in this case with a retrograde orbit. A parent-body search top 10 includes candidates with a threshold for the Drummond D_D criterion value lower than 0.25 but none of which can be associated with any certainty (*Table 2*). Comet C/1852 K_1 (Chacornac) is considered as a likely source for the eta Eridanids (ERI#191) (Jenniskens, 2024, page 445). It would be up to meteoroid stream modelers to reconstruct the dynamic orbit evolution to see if there could be any connection between this comet and the different meteor showers that could be related.

Table 1 – Comparing the new meteor shower, derived by two different methods, M2025-P1 the orbital parameters as initially derived, the parameters under $D_D < 0.05$ were derived from the method described in *Section 3*.

	M2025-P1	$D_D < 0.05$
$\lambda_\odot$ (°)	125.8	126.1
$\lambda_{\odot b}$ (°)	122.7	123.6
$\lambda_{\odot e}$ (°)	130.2	130.2
α_g (°)	29.8	29.8
δ_g (°)	–20.6	–20.6
$\Delta\alpha_g$ (°)	+0.79	+0.67
$\Delta\delta_g$ (°)	+0.56	+0.48
v_g (km/s)	61.4	61.5
λ_g (°)	19.5	19.5
$\lambda_g - \lambda_\odot$ (°)	253.4	253.3
β_g (°)	–30.6	–30.3
a (A.U.)	12.5	13.5
q (A.U.)	0.8654	0.8638
e	0.9308	0.9362
i (°)	124.2	124.6
ω (°)	45.76	46.01
Ω (°)	306.27	306.47
Π (°)	352.04	352.48
T_j	–0.22	–0.26
N	32	27

Table 2 – Top ten matches of a search for possible parent bodies with $D_D < 0.25$.

Name	D_D
C/1877 G_1 (Winnecke)	0.111
C/1852 K_1 (Chacornac)	0.121
C/1886 J_1 (Brooks)	0.165
C/2020 H_2 (Pruyne)	0.172
273P/Pons-Gambart	0.208
C/2020 A_2 (Iwamoto)	0.215
C/2013 UQ_4 (Catalina)	0.234
C/1994 G_1-A (Takamizawa-Levy)	0.247
C/1994 G_1-B (Takamizawa-Levy)	0.25
C/1925 G_1 (Orkisz)	0.25

5 Activity in past years

A search in older GMN orbit data resulted in one possible orbit with $D_D < 0.06$ in 2020, one in 2021, 16 in 2022, 17 in 2023 and 33 orbits in 2024. SonotaCo Net has 18 orbits with $D_D < 0.06$ in different years from 2007 onwards. EDMOND had only seven orbits with $D_D < 0.06$ between 2008 and 2015 but this network had rather poor coverage of the Southern hemisphere. No other meteor orbit datasets were checked. The activity in the past years indicates that M2025-P1 is an annual shower.

6 Conclusion

The discovery of a new meteor shower with a radiant in the constellation of Eridanus based on thirty-two meteors during 2025 July 25 – August 3 has been confirmed by using two independent meteor shower search methods. The resulting mean orbits for both search methods are in good agreement. All meteors appeared during the solar-longitude interval 122° – 131°, with most events around 28–29 July ($\lambda_{\odot}$ = 125.6°). Orbits of this meteor shower were detected in previous years, but the presence of the nearby eta Eridanids as a much stronger source is a likely explanation why M2025-P1 hasn't been detected earlier.

Acknowledgment

This report is based on the data of the Global Meteor Network (Vida et al., 2020a; 2020b; 2021) which is released under the CC BY 4.0 license[16]. We thank all 825 participants in the Global Meteor Network project for their contribution and perseverance. A list with the names of the volunteers who contribute to GMN has been published in the 2024 annual report (Roggemans et al., 2025).

References

Drummond J. D. (1981). "A test of comet and meteor shower associations". *Icarus*, **45**, 545–553.

Jenniskens P. (2024). Atlas of Earth's meteor showers. Elsevier, Cambridge, United states. ISBN 978-0-443-23577-1.

Jopek T. J. (1993). "Remarks on the meteor orbital similarity D-criterion". *Icarus*, **106**, 603–607.

Jopek T. J., Rudawska R. and Pretka-Ziomek H. (2006). "Calculation of the mean orbit of a meteoroid stream". *Monthly Notices of the Royal Astronomical Society*, **371**, 1367–1372.

Moorhead A. V., Clements T. D., Vida D. (2020). "Realistic gravitational focusing of meteoroid streams". *Monthly Notices of the Royal Astronomical Society*, **494**, 2982–2994.

Roggemans P., Johannink C. and Campbell-Burns P. (2019a). "October Ursae Majorids (OCU#333)". *eMetN Meteor Journal*, **4**, 55–64.

Roggemans P., Campbell-Burns P., Kalina M., McIntyre M., Scott J. M., Šegon D., Vida D. (2025). "Global Meteor Network report 2024". *eMetN Meteor Journal*, **10**, 67–101.

Southworth R. B. and Hawkins G. S. (1963). "Statistics of meteor streams". *Smithsonian Contributions to Astrophysics*, **7**, 261–285.

Vida D., Gural P., Brown P., Campbell-Brown M., Wiegert P. (2020a). "Estimating trajectories of meteors: an observational Monte Carlo approach - I. Theory". *Monthly Notices of the Royal Astronomical Society*, **491**, 2688–2705.

Vida D., Gural P., Brown P., Campbell-Brown M., Wiegert P. (2020b). "Estimating trajectories of meteors: an observational Monte Carlo approach - II. Results". *Monthly Notices of the Royal Astronomical Society*, **491**, 3996–4011.

Vida D., Šegon D., Gural P. S., Brown P. G., McIntyre M. J. M., Dijkema T. J., Pavletić L., Kukić P., Mazur M. J., Eschman P., Roggemans P., Merlak A., Zubrović D. (2021). "The Global Meteor Network – Methodology and first results". *Monthly Notices of the Royal Astronomical Society*, **506**, 5046–5074.

[16] https://creativecommons.org/licenses/by/4.0/

Outburst of a new meteor shower in Aries

Damir Šegon[1], **Denis Vida**[2] **and Paul Roggemans**[3]

[1] **Astronomical Society Istra Pula, Park Monte Zaro 2, 52100 Pula, Croatia**

[2] **Department of Earth Sciences, University of Western Ontario, London, Ontario, N6A 5B7, Canada**
denis.vida@gmail.com

[3] **Pijnboomstraat 25, 2800 Mechelen, Belgium**
paul.roggemans@gmail.com

A new meteor shower on a retrograde Halley-type comet orbit ($T_J = –0.69$) has been detected by the Global Meteor Network during an outburst that lasted about 3.5 hours on August 26–27, 2025 ($153.61° < \lambda_\odot < 153.75°$). Meteors belonging to the new shower were observed between $145° < \lambda_\odot < 155°$ from a radiant at R.A. = 47.6° and Decl.= +11.4° in the constellation of Aries, with a geocentric velocity of 68.5 km/s. The new meteor shower has been listed in the Working List of Meteor Showers under the temporary name-designation: M2025-Q1.

1 Introduction

The GMN radiant map for August 26–27, 2025 shows a clear concentration of related radiants in the constellation of Aries. 33 meteors of this meteor shower were observed by the Global Meteor Network[17] low-light video cameras on 2025 August 26 – 27 in about 30 hours with an outburst of a so far dormant unknown meteor shower that lasted 3.5 hours (*Figure 1*). The shower was independently observed by cameras in 19 countries (Belgium, Bulgaria, Czechia, Germany, France, Greece, Croatia, Hungary, Italy, South Korea, Luxembourg, the Netherlands, New Zealand, Romania, Russia, Slovenia, Slovakia, United Kingdom and the United States).

The shower had a median geocentric radiant with coordinates R.A. = 47.5°, Decl. = +11.5°, within a circle with a standard deviation of ±0.4° (equinox J2000.0) see *Figure 2*. The radiant drift in R.A. is +0.34 deg on the sky per degree of solar longitude and +0.06 in Dec., both referenced to $\lambda_\odot = 153.5°$ (*Figures 3 and 4*). The median Sun-centered ecliptic coordinates were $\lambda - \lambda_\odot = 254.8°$, $\beta = –6.0°$ (*Figure 5*). The geocentric velocity was 68.3 ± 0.2 km/s.

This possible new meteor shower was reported to the IAU MDC and added under the temporary identification 2025-Q1[18].

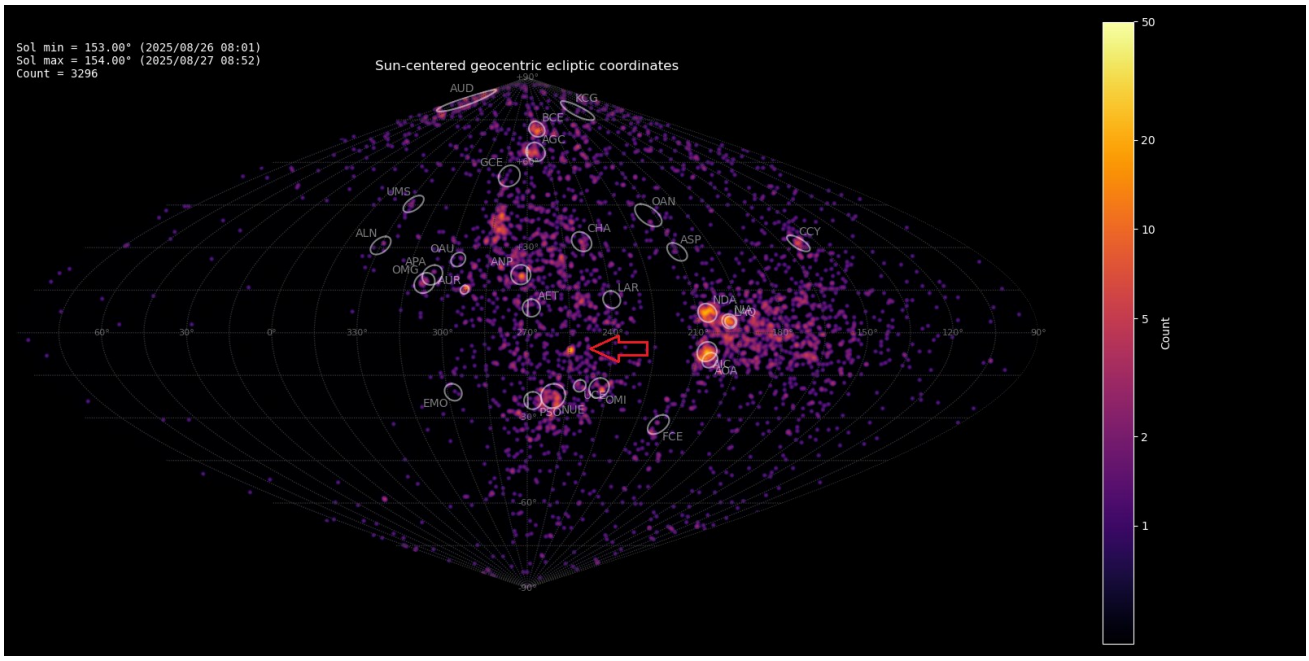

Figure 1 – Heat map with 3296 radiants obtained by the Global Meteor network on August 26–27, 2025. A distinct concentration is visible in Sun-centered geocentric ecliptic coordinates which was identified as a new meteor shower with the temporary identification M2025-Q1.

[17] https://globalmeteornetwork.org/data/

[18] https://www.ta3.sk/IAUC22DB/MDC2022/Roje/pojedynczy_obiekt.php?lporz=02184&kodstrumienia=01237

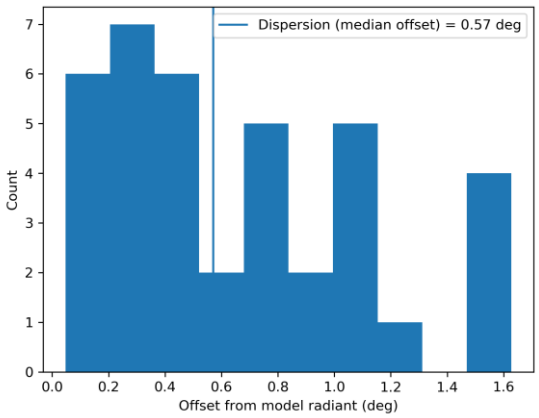

Figure 2 – Dispersion on the radiant position.

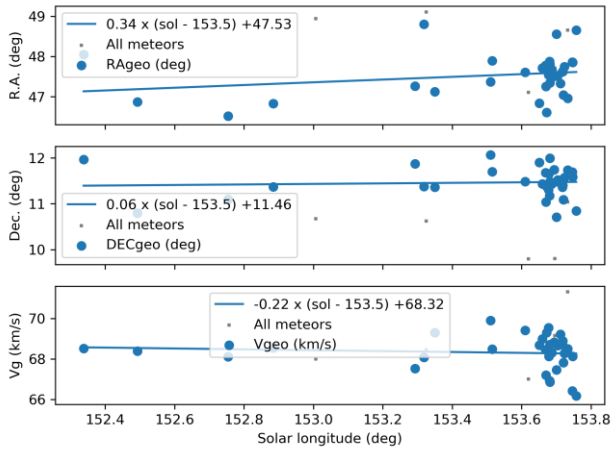

Figure 3 – The radiant drift.

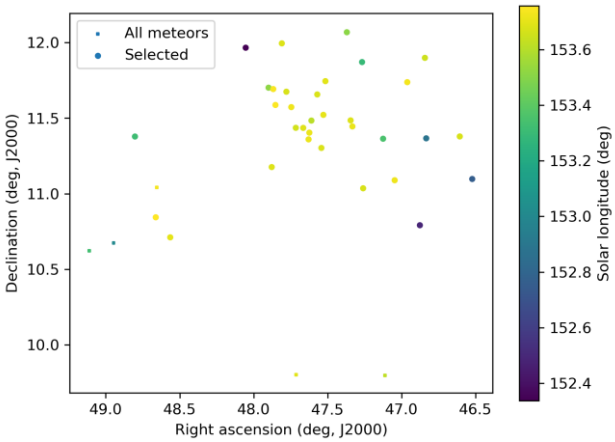

Figure 4 – The radiant distribution during the solar-longitude interval 152.3° – 153.8° in equatorial coordinates.

2 First detection

The GMN shower association criterion assumes that meteors within 1° in solar longitude, within 3° in radiant, and within 10% in geocentric velocity of a shower reference location are members of that shower. Further details about the shower association are explained in Moorhead et al. (2020). This is a rather strict criterion since meteor showers often have a larger dispersion in radiant position, velocity and activity period. Using these meteor shower selection criteria, 33 orbits have been associated with the new shower in the GMN meteor orbit database and the mean orbit has been listed in *Table 1*.

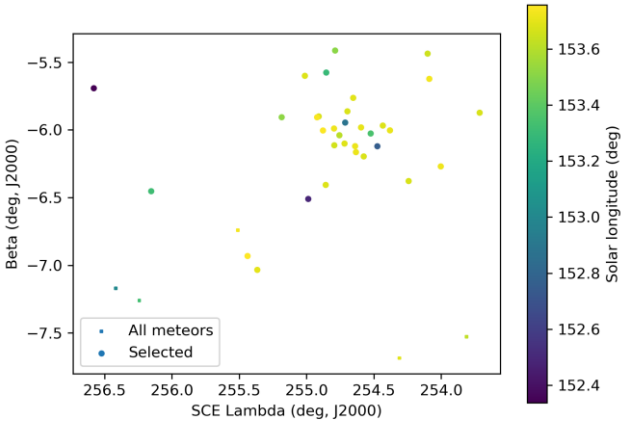

Figure 5 – The radiant distribution during the solar-longitude interval 152.3° – 153.8° in Sun centered geocentric ecliptic coordinates.

3 Another search method

Another method has been applied to check this new meteor shower discovery. The starting point here can be any visually spotted concentration of radiant points or any other indication for the occurrence of similar orbits. The method has been described before (Roggemans et al., 2019). The main difference with the method applied in *Section 2* is that three different discrimination criteria are combined in order to have only those orbits which fit different thresholds of these criteria. The D-criteria that we use are these of Southworth and Hawkins (1963), Drummond (1981) and Jopek (1993) combined. Instead of using a cutoff value for the threshold of the D-criteria these values are considered in different classes with different thresholds of similarity. Depending on the dispersion and the type of orbits, the most appropriate threshold of similarity is selected to locate the best fitting mean orbit as the result of an iterative procedure.

The outburst occurred during the solar-longitude interval 152.3° – 153.8° and only this time interval has been considered for the first detection. To check for the presence of meteor shower members outside this interval a sample of the orbit database from $\lambda_O = 140°$ until $\lambda_O = 155.3°$, the latest data available at the time of this analysis, has been used for the shower search.

To generate an initial reference orbit to approach the most likely representative orbit for this new meteor shower, all orbits with $253° < \lambda_g - \lambda_O < 263°$, $-9° < \beta < -3°$ and 64 km/s $< v_g <$ 72 km/s were selected. This sample counted 165 orbits which included the concentration caused by the new shower outburst. The mean orbit for this selection was used as a reference orbit to start an iterative procedure to approach the most likely mean orbit for the new meteor shower in this sample. The iteration was started with $D_{SH} < 0.20$, $D_D < 0.08$ and $D_J < 0.20$ as thresholds to filter out sporadic contamination. The procedure converged at a mean orbit valid for $D_{SH} < 0.05$, $D_D < 0.02$ and $D_J < 0.05$ as threshold values.

This method resulted in a mean orbit with 41 related orbits that fit within the similarity threshold with $D_{SH} < 0.125$, $D_D < 0.05$ and $D_J < 0.125$, recorded 2025 August 18–28. 21 of these orbits were recorded during the short time interval $152.3° < \lambda_\odot < 153.8°$. The plot of the radiant positions in equatorial coordinates, color coded for different D-criteria thresholds, shows a large dispersion for the threshold values larger than $D_D < 0.05$ (*Figure 6*) with a dense concentration of radiants that fit $D_{SH} < 0.125$, $D_D < 0.05$ and $D_J < 0.125$ or better.

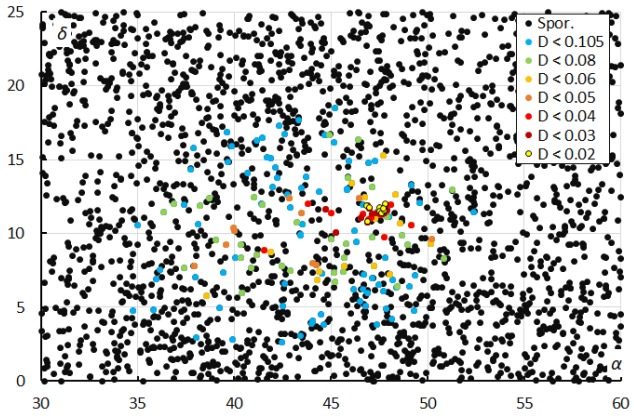

Figure 6 – The radiant distribution during the solar-longitude interval 140° – 155° in equatorial coordinates, color coded for different values of the D_D orbit similarity criterion.

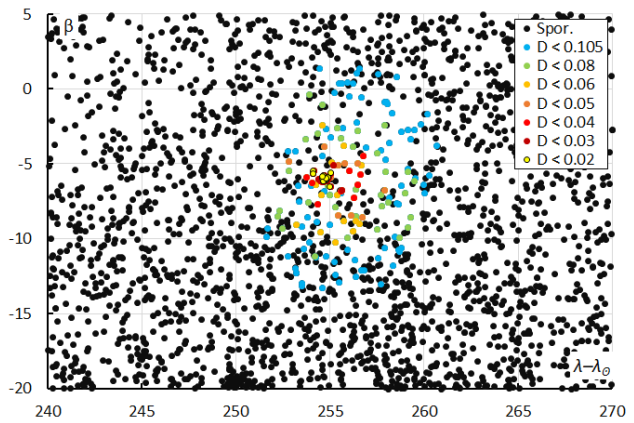

Figure 7 – The radiant distribution during the solar-longitude interval 140° – 155° in Sun-centered geocentric ecliptic coordinates, color coded for different values of the D_D orbit similarity criterion.

Looking at the Sun-centered geocentric ecliptic coordinates the radiant drift caused by of the Earth moving on its orbit around the Sun is compensated and a more compact radiant becomes visible (*Figure 7*). The sky is densely covered with sporadic radiants in this region, so there is a lot of risk for contamination with sporadics when identifying meteor showers. There is another strong concentration visible at $\lambda_g - \lambda_\odot = 250°$ and $\beta = -20°$ identified as the nu Eridanids (NUE#337) which have their main activity one week later.

Figures 8 and 9 show that the selected meteors, identified as members of the new meteor shower do not affect the evenly distribution of the sporadic radiant background.

The diagram with the inclination against the longitude of perihelion (*Figure 10*) shows a strong concentration for the selected orbits with a lot dispersion for the orbits that fit the more tolerant threshold values for the D-criteria.

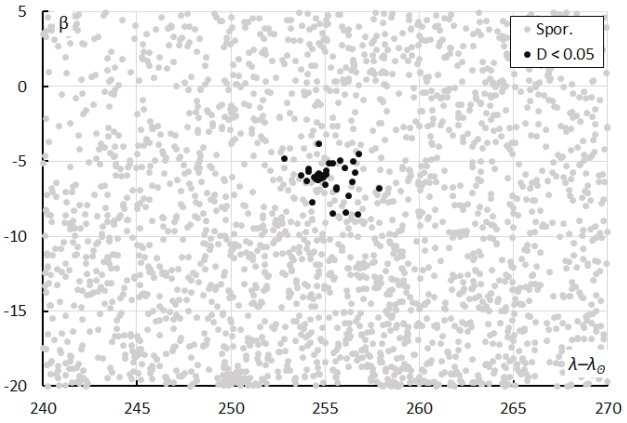

Figure 8 – The M2025-Q1 radiants for $D_D < 0.05$ during the solar-longitude interval 140° – 155° in Sun-centered geocentric ecliptic coordinates, with the sporadic radiants marked in grey.

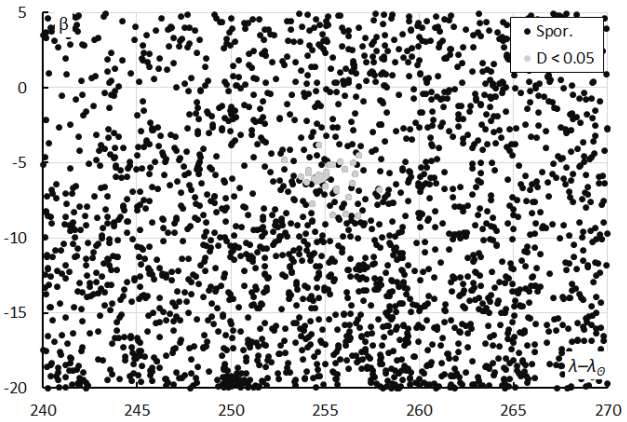

Figure 9 – The sporadic radiants during the solar-longitude interval 140° – 155° in Sun-centered geocentric ecliptic coordinates, with M2025-Q1 radiants marked in grey for $D_D < 0.05$.

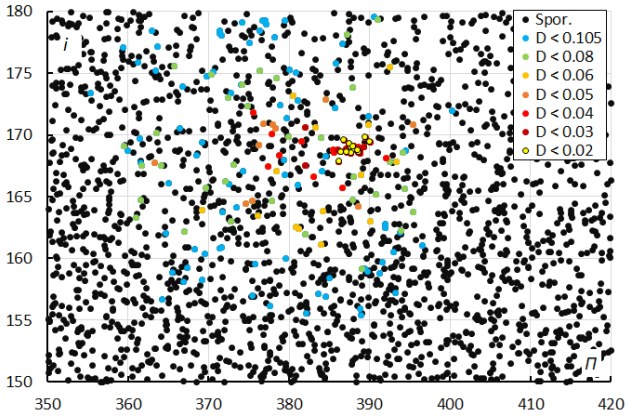

Figure 10 – The diagram of the inclination *i* against the longitude of perihelion *Π* color coded for different classes of D criterion threshold.

The concentration of radiants is outstanding when we limit the orbit sample plotted in *Figures 7 and 10* to the time interval $153° < \lambda_\odot < 154°$ (*Figures 11 and 12*), the very high threshold points remain. The orange dots with $0.06 < D_D < 0.04$ in *Figures 7 and 10* are most probably related to this outburst but occurred before and after the outburst and appear more dispersed.

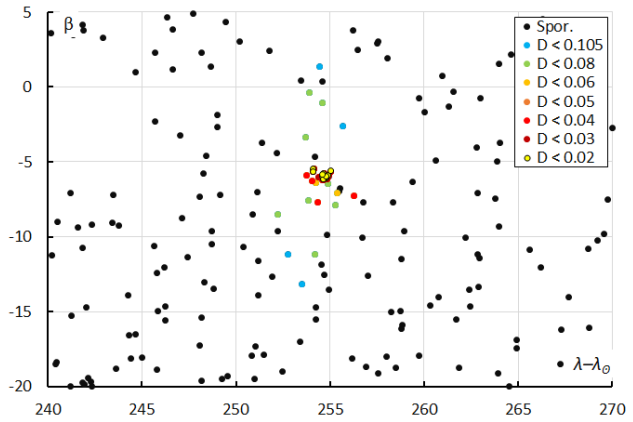

Figure 11 – The radiant distribution during the solar-longitude interval 153° – 154° in Sun-centered geocentric ecliptic coordinates, color coded for different values of the D_D orbit similarity criterion.

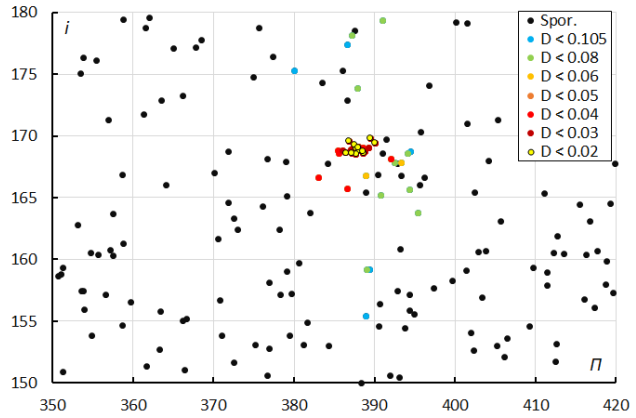

Figure 12 – The diagram of the inclination i against the longitude of perihelion Π color coded for different classes of D criterion thresholds during the solar-longitude interval 153° – 154°.

4 Orbit and parent body

The final mean orbits obtained by the two methods are listed in *Table 1*. There are five orbits from previous years among the 33 orbits used to define 2025-Q1. Five of these 33 orbits fail to fit the D criteria thresholds with $D_{SH} < 0.125$, $D_D < 0.05$ and $D_J < 0.125$ for their own mean orbit. The alternative shower identification method using the D-criteria thresholds found 41 orbits, 19 of which occurred before or after the interval $153° < \lambda_\odot < 154°$. 21 identical meteors were classified as new shower members by both methods. Six meteors used by the first method were not detected by the second method. The second method identified three orbits as shower members that were not detected by the first method apart from the 17 meteors recorded before or after the outburst. Despite the differences in the composition of the orbit selections, the resulting mean orbits are in good agreement, mainly defined by the 21 orbits in common. *Figure 13* shows the two orbits plotted in the solar system with 2025-Q1 as reported to the IAU MDC, while $D_D < 0.05$ includes 17 outliers recorded before and after the outburst and three meteors during the outburst that were not included in the M2025-Q1 selection. The apparent large difference in aphelia is due to the slightly higher average velocity and therefore larger value for the eccentricity e.

Table 1 – Comparing the new meteor shower, derived by two different methods, M2025-Q1 the orbital parameters as initially derived, the parameters under $D_D < 0.05$ were derived from the method described in *Section 3*, (*) is the solution for the outburst interval 153°–154° in solar longitude.

	M2025-Q1	$D_D < 0.05$	$D_D < 0.05$(*)
$\lambda_\odot$ (°)	153.5	153.7	153.7
$\lambda_{\odot b}$ (°)	152.3	145.0	153.0
$\lambda_{\odot e}$ (°)	153.9	155.0	154.0
α_g (°)	47.5	47.0	47.6
δ_g (°)	+11.5	+11.4	+11.5
$\Delta\alpha_g$ (°)	+0.34	+0.78	+1.00
$\Delta\delta_g$ (°)	+0.06	+0.22	+0.35
v_g (km/s)	68.3	68.7	68.7
λ_g (°)	48.3	47.8	48.4
$\lambda_g - \lambda_\odot$ (°)	254.8	254.8	254.6
β_g (°)	–6.0	–6.0	–6.0
a (A.U.)	12.7	20.0	26.6
q (A.U.)	0.804	0.816	0.806
e	0.937	0.959	0.970
i (°)	168.7	168.8	168.7
ω (°)	54.7	52.5	53.9
Ω (°)	333.5	331..5	333.7
Π (°)	28.2	27.8	27.6
T_j	–0.69	–0.82	–0.89
N	33	41	22

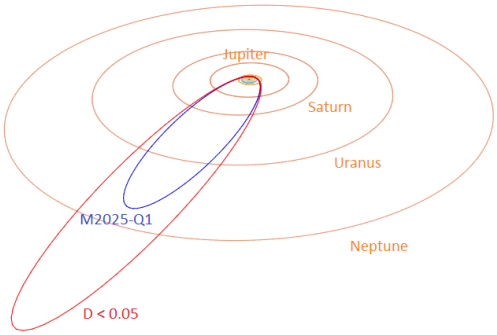

Figure 13 – Comparing the mean orbit based on the shower identification according to the two methods, blue is for M2025-Q1 and red for the alternative shower search method with $D_D < 0.05$ in *Table 1*. (Plotted with the Orbit visualization app provided by Pető Zsolt).

Figure 14 shows the orbits in the inner solar system. The dust of M2025-Q1 crosses the Earth orbit at its ascending node, hitting the Earth almost head-on from below the ecliptic plane.

The Tisserand's parameter T_j identifies the orbit as of a Halley comet type in this case with a retrograde orbit. A parent-body search top 10 includes candidates with a threshold for the Drummond D_D criterion value lower than

0.25 but none of which can be associated with any certainty (*Table 2*).

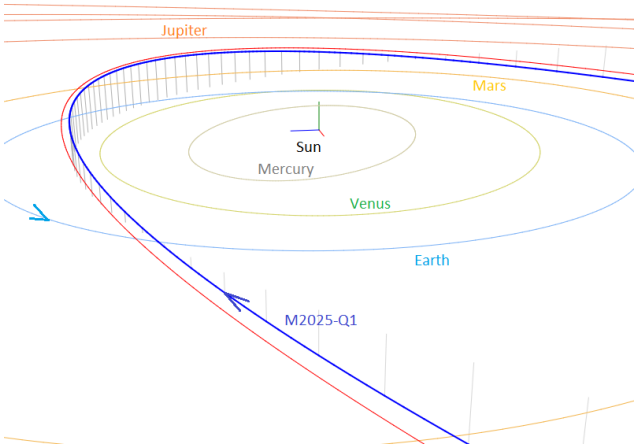

Figure 14 – Comparing the mean orbits in the inner solar system, blue is for M2025-Q1 and red for the other shower search method with $D_D < 0.05$ in *Table 1*. (Plotted with the Orbit visualization app provided by Pető Zsolt).

Table 2 – Top ten matches of a search for possible parent bodies with $D_D < 0.25$.

Name	D_D
C/1698 R1	0.111
C/2020 R4 (ATLAS)	0.129
C/1946 K1 (Pajdusakova-Rotbart-Weber)	0.13
C/1893 N1 (Rordame-Quenisset)	0.133
C/1862 N1 (Schmidt)	0.162
C/1864 N1 (Tempel)	0.178
C/1917 H1 (Schaumasse)	0.184
C/1999 S4 (LINEAR)	0.211
C/1947 S1 (Bester)	0.219
C/2002 T7 (LINEAR)	0.222

5 Activity in past years

A search in older GMN orbit data resulted in 93 possible orbits with $D_D < 0.06$, most of them at solar longitudes before or after the 2025 outburst. Six in 2020, 15 in 2021, 18 in 2022 with one during the outburst interval, 26 in 2023 with two during the outburst interval and 28 orbits in 2024 with 7 during the outburst interval. No other meteor orbit datasets were checked. The activity in the past years indicates that M2025-Q1 may display weak annual activity between solar longitudes 140° and 165°.

6 Conclusion

The discovery of a new meteor shower with a radiant in the constellation of Aries based on thirty-two meteors during August 26–27, 2025 has been confirmed by using two independent meteor shower search methods. The resulting mean orbits for both search methods are in good agreement. All meteors appeared during the solar-longitude interval 145° – 155°, with most events in less than 3.5 hours during an outburst on 26–27 August ($\lambda_\odot$ = 153.61°–153.75°). Orbits of this meteor shower were detected in previous years. Meanwhile this new meteor shower was independently reported by the meteor camera network in Belarus and Ukraine using UFOOrbit with four paired meteors between solar longitude 153.67° and 153.73° (Harachka and Aitov, 2025).

Acknowledgment

This report is based on the data of the Global Meteor Network (Vida et al., 2020a; 2020b; 2021) which is released under the CC BY 4.0 license[19]. We thank all 825 participants in the Global Meteor Network project for their contribution and perseverance. A list with the names of the volunteers who contribute to GMN has been published in the 2024 annual report (Roggemans et al., 2025).

References

Drummond J. D. (1981). "A test of comet and meteor shower associations". *Icarus*, **45**, 545–553.

Harachka Y., Aitov A. (2025). "Possible new meteor shower at the border between the constellations Aries and Cetus". *eMetN Meteor Journal*, **10**, 293–294.

Jopek T. J. (1993). "Remarks on the meteor orbital similarity D-criterion". *Icarus*, **106**, 603–607.

Jopek T. J., Rudawska R. and Pretka-Ziomek H. (2006). "Calculation of the mean orbit of a meteoroid stream". *Monthly Notices of the Royal Astronomical Society*, **371**, 1367–1372.

Moorhead A. V., Clements T. D., Vida D. (2020). "Realistic gravitational focusing of meteoroid streams". *Monthly Notices of the Royal Astronomical Society*, **494**, 2982–2994.

Roggemans P., Johannink C. and Campbell-Burns P. (2019a). "October Ursae Majorids (OCU#333)". *eMetN Meteor Journal*, **4**, 55–64.

Roggemans P., Campbell-Burns P., Kalina M., McIntyre M., Scott J. M., Šegon D., Vida D. (2025). "Global Meteor Network report 2024". *eMetN Meteor Journal*, **10**, 67–101.

Southworth R. B. and Hawkins G. S. (1963). "Statistics of meteor streams". *Smithsonian Contributions to Astrophysics*, **7**, 261–285.

Vida D., Gural P., Brown P., Campbell-Brown M., Wiegert P. (2020a). "Estimating trajectories of meteors: an observational Monte Carlo approach - I. Theory".

[19] https://creativecommons.org/licenses/by/4.0/

Monthly Notices of the Royal Astronomical Society, **491**, 2688–2705.

Vida D., Gural P., Brown P., Campbell-Brown M., Wiegert P. (2020b). “Estimating trajectories of meteors: an observational Monte Carlo approach - II. Results”. *Monthly Notices of the Royal Astronomical Society*, **491**, 3996–4011.

Vida D., Šegon D., Gural P. S., Brown P. G., McIntyre M. J. M., Dijkema T. J., Pavletić L., Kukić P., Mazur M. J., Eschman P., Roggemans P., Merlak A., Zubrović D. (2021). “The Global Meteor Network – Methodology and first results”. *Monthly Notices of the Royal Astronomical Society*, **506**, 5046–5074.

Vida D., Šegon D. (2025). “New meteor shower in Aries”. CBET. Submitted.

Possible new meteor shower at the border between the constellations Aries and Cetus

Yury Harachka, Alexander Aitov

Minsk, Belarus
astronominsk@gmail.com

A possible new meteor shower has been discovered on August 27, 2025 (at $\lambda_\odot = 153.7°$) by Belarusian and Ukrainian video meteor networks. The radiant at $\alpha = 47.9°$ and $\delta = +11.8°$ is situated at the border between the constellations Aries and Cetus, with a geocentric velocity v_g of 64.3 ± 3.2 km/s.

1 Observations

During the night of 26 – 27 August, 2025, the Belarusian and the Ukrainian meteor networks recorded activity from an unidentified radiant at the border between the constellations Aries and Cetus. Four multi-station meteors with very close radiants were captured. *Figure 1* shows images of all 4 meteors, which had a fast angular velocity and absolute magnitudes in the range –2.1m to 0.0m. All meteors were registered within the interval in solar longitude of 153.67° to 153.73° and during a short period lasting 1 hour and 20 minutes.

Figure 2 shows the projection of recorded meteors onto the Earth's surface.

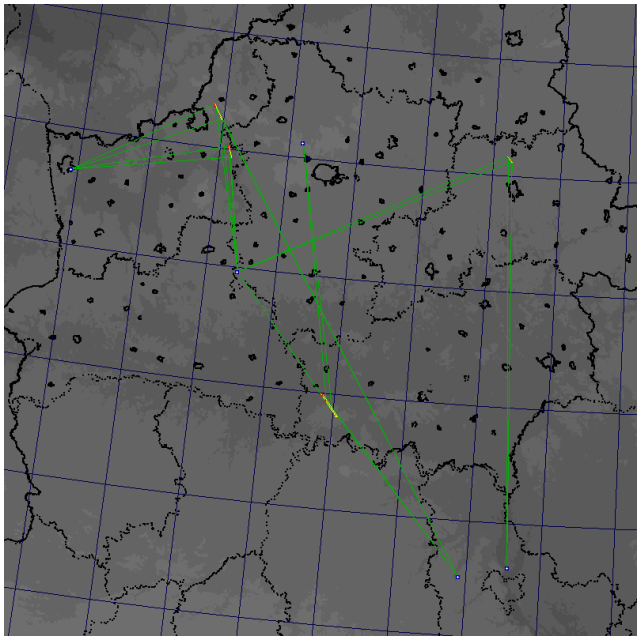

Figure 2 – Meteor trajectories from this unknown radiant in projected on the Earth's surface.

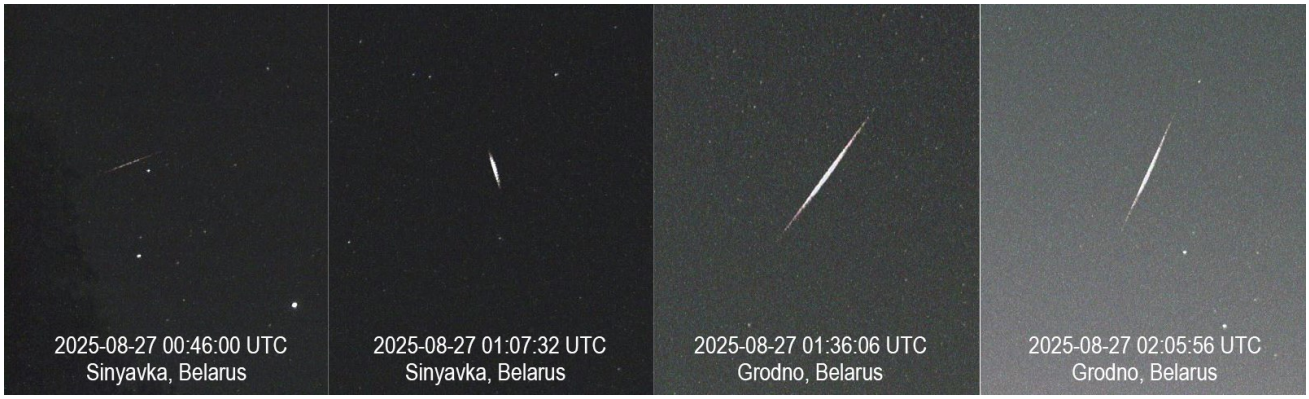

Figure 1 – Four meteors from the possible new meteor shower recorded during the night of 26–27 August 2025.

2 Results

The data were processed in UFOOrbit (SonotaCo)[20]. *Table 1* shows the calculated individual parameters for each meteor on August 27, 2024.

Table 1 – The orbital parameters of the four meteors recorded from the possible new meteor shower on 2025 August 27.

	$0^h46^m00^s$	$1^h07^m32^s$	$1^h36^m05^s$	$2^h05^m56^s$
$\lambda_\odot$ (°)	153.67	153.69	153.71	153.73
Mag_{abs}	0	–0.9	–2.1	–1.8
α_g (°)	48.58	47.45	48.02	47.54
δ_g (°)	11.84	11.87	11.78	11.68
λ_g (°)	49.38	48.32	48.39	48.02
β_g (°)	–5.95	–5.62	–6.23	–6.06
v_g (km/s)	63.28	67.06	66.68	60.22
a (A.U.)	1.9	5.21	4.27	1.36
q (A.U.)	0.74	0.783	0.789	0.626
e	0.611	0.85	0.815	0.538
ω (°)	72.92	59.288	59.144	94.948
Ω (°)	333.673	333.688	333.707	333.727
i (°)	168.24	169.33	168.86	167.79

Figure 3 shows the distribution of the radiants at the celestial sphere at the border between the constellations Aries and Cetus.

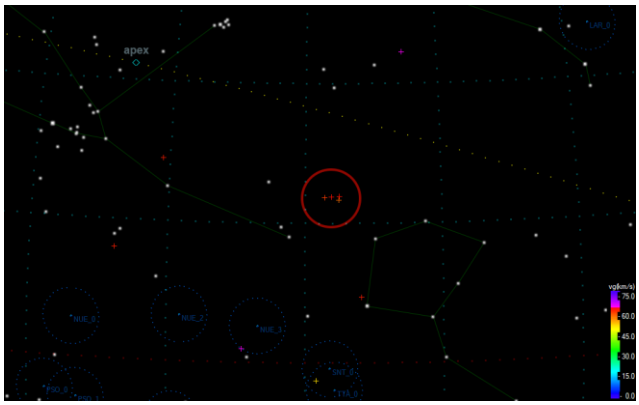

Figure 3 – Distribution of the radiants at the celestial sphere. The red circle indicates the radiant area of the possible new meteor shower.

It should be noted that the radiant of the zeta Arietids (ZAR, #00193)[21] is located 2 degrees northeast of the unidentified activity. However, this meteor shower was removed from the IAU MDC list of active showers. In addition, the peak activity of the zeta Arietids shower is indicated as $\lambda_\odot = 146.7°$, which is approximately 7 days earlier. This makes the relation between the unidentified activity and the zeta Arietids unlikely.

The radiant parameters and orbital elements averaged for the four meteors are as follows:

- $\lambda_\odot = 153.6996° \pm 0.0233°$
- $\alpha_g = 47.90° \pm 0.52°$
- $\delta_g = 11.79° \pm 0.09°$
- $v_g = 64.3 \pm 3.2$ km/s
- $a = 3.18 \pm 1.85$ AU
- $q = 0.735 \pm 0.076$ AU
- $e = 0.703 \pm 0.152$
- $\omega = 71.575° \pm 16.868°$
- $\Omega = 333.699° \pm 0.023°$
- $i = 168.56° \pm 0.68°$

Acknowledgment

The author would like to thank all operators and people involved in the Belarusian and Ukrainian meteor networks. We would especially like to thank our Ukrainian colleagues who continue to be involved in meteor astronomy during this difficult time for Ukraine. The author would also like to thank Paul Roggemans for his help in writing this report.

[20] SonotaCo, www.sonotaco.com

[21] IAU MDC, https://www.ta3.sk/IAUC22DB/MDC2022/Roje/roje_lista.php?corobic_roje=0&sort_roje=0

Meteoroids 2025 Conference, a report

Jeff Wood

PO Box 162 Willetton, Western Australia Australia 6955
rvball1@hotmail.com

A summary report is presented about the 12th Meteoroids Conference which took place from 7th July until 11th July 2025 at Curtin University Bentley, Perth Western Australia 6102.

1 Introduction

Meteoroids 2025 in Perth Western Australia was the 12th conference on meteor astronomy since the first Meteoroids conference was organized in Smolenice, Slovakia in July 1992. With the Covid epidemic the 2022 conference was conducted online meaning 2025 was the first time in 6 years that delegates could meet in person.

The 2025 conference was organized by Curtin University. 78 participants registered to attend in person with another 7 registering to participate online. The program with links to the abstracts in PDF can be found online[22]. A conference is more than just a series of oral and poster presentations. Much of the time was spent on formal and informal sessions, discussions and social outings.

In this report we will give a short overview of the different sessions.

Figure 1 – The Meteoroids 2025 logo.

2 Monday 7th July

The conference commenced with a registration session at 8h30m am on Monday 7 July. The conference was opened with a welcome from Ellie Sanson (LOC Chair), Gretchen Benedix (Curtin Associate Deputy Vice Chancellor – Research) and Pavel Koten (SOC Chair) who also presented the first lecture of the conference on meteor clusters and tracing meteoroid fragmentation in near Earth Space.

Figure 2 – Gretchen Bennedix officially opens the conference.

The day was divided into a series of short lectures with three main themes. Within each theme there were a range of speakers who presented their topics in short twelve minutes timeslots followed by a three-minute question time. The keynote speakers were given double this timeframe.

The themes for the day were:

- *Composition and Physical Properties* - featuring clustering, fragmentation, the physical characteristics of shower meteoroids inferred through dynamic nested sampling, comparing mechanical strengths of real and simulated meteoroids, the AMOS global meteor network presented by Juraj Toth, ongoing investigations with the Lowell Observatory Meteor Camera Network, comparative analysis of meteor spectra observed simultaneously from multiple locations, modeling of faint meteors and bolides using AMOS all sky data and a novel approach for revealing dynamic disintegration of irregular shaped meteoroids using a particle sintered model.
- *Future Methods and Techniques* – featuring machine learning in meteor science, presented by Simon Anghel, 10 years of the digital Desert Fireball Network from meteorites to space debris, the use of events-based cameras, a real time all sky fireball camera array

[22] https://meteoroids2025.gfo.rocks/

prototype DFN initial results, Investigation of the possibilities of simultaneous meteor observations from Russia and Tajikistan, classical histogram analysis of radar and optical meteor data and enhancing meteoroid research through the NASA Science Explorer.

- *Career sessions* – opportunities for career paths in space research.

There were three breaks during the day for morning tea, lunch and afternoon tea. These featured delicious canapes of food and a range of drinks all of which were enjoyed by each and every participant.

At the conclusion of the day's presentations a welcome function had been planned to be held at the Perth Observatory located at Bickley some 35 km east of the Perth CBD. However, inclement weather saw this event cancelled and replaced by an informal meal and gathering at Curtin University. This finished at around 9^h30^m pm.

Figure 3 – Perth Observatory.

3 Tuesday 8th July

The Fourth Session "*Meteor Physics and Chemistry*" focused on the physics of a meteoroid flight in the atmosphere. The presentations covered a variety of topics including meteor spectroscopy advances presented by Adriana Pisarčíková, spectroscopic observations of mm sized meteors, the annual variation of sodium in the Geminid spectra over 6 years, proposal of a new long-life mechanism of persistent meteor trails and the lateral spreading of meteoroid fragments.

The fifth session "*Entry Acoustics*" consisted of four talks concerning meteoroid entry and sounds. First the Perth Array results were presented followed by infrasound analysis of HTV Missions and rocket launches from Tanegashima Space Centre Japan. Then infrasound observations for three SRC re-entries. The last talk was by Jana Clemente and covered the interesting topic of seismo-acoustic entry signals of fireballs.

In the afternoon the sixth session covered *meteorite recoveries* in Oman, New Zealand, the UK and Australia. A wide range of approaches were revealed by the speakers including the use of drones to recover meteorites in remote places such as the Nullarbor Plain in Australia.

Figure 4 – Hadrien Devilleboix hunting meteorites on the Nullarbor Plain Australia using drones.

Figure 5 – Luke Burgin describes the first New Zealand camera assisted meteorite recovery.

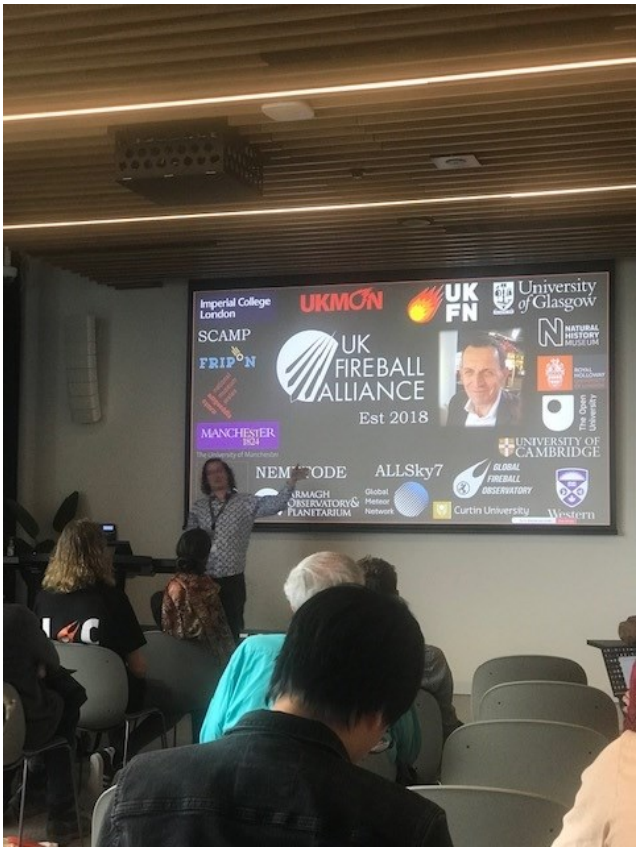

Figure 6 – Luke Daly and the UK Fireball Alliance.

Luke Daly conducted a very entertaining talk on the UKFAll rising – the expansion of the UK Fireball Alliance. Luke demonstrated how the partnership between professional researchers, amateur astronomers and the general public could all work together to successfully recover meteorites.

The seventh session concerned *the influx of Interplanetary and Interstellar meteoroids*. Margaret Campbell-Brown commenced this session with an interesting talk connecting meteor radar observing biases with simultaneous optical observations. This was followed by a novel approach by Gregg Cole to predict how interstellar material from Alpha Centauri could be delivered to the solar system and fall upon the Earth. Further talks were about debiasing meteor flux estimates using the DFN Clear Sky Survey, understanding the impact risk and preparing future instrumentation. Other talks were about using Antarctic/Greenland dust deposits with meteoroid models and using the lunar impact records to decipher the flux of kilometric asteroids on Earth. This session concluded with a vigorous, but respectful panel discussion concerning interstellar meteoroids. This caused much interest given the recent entry of Comet C2025 N1/ATLAS into the Solar System.

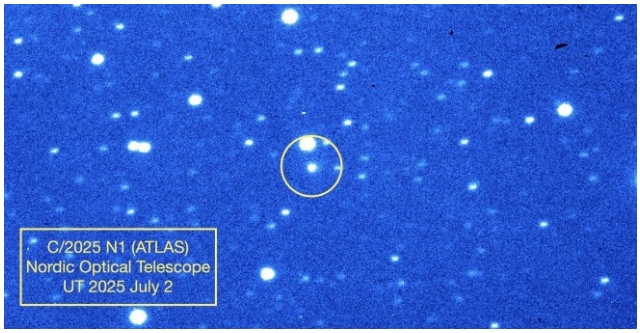

Figure 7 – Comet C2025 N1/ATLAS position on 2 July 2025 circled[23].

Figure 8 – Group discussion.

4 Wednesday 9th July

The eighth session covered talks on *Meteoroids in Space*. The first talk was by Eloy Peña Asensio on the topic of the ESA's LUMIO mission applying meteor characterization through far side lunar impact flash observations.

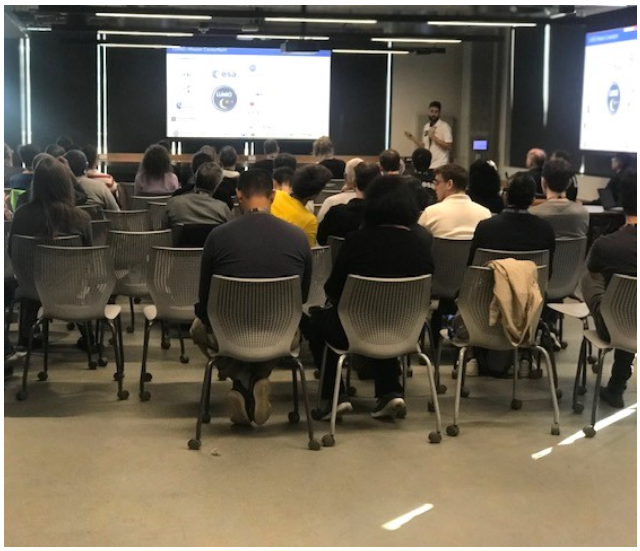

Figure 9 – Eloy Peña Asensio and the ESA's LUMIO mission.

Jack Lopez presented a talk on the effects of meteoroids as illumination of lunar surface on water-ice stability. Mark Millinger was the final speaker with the topic mitigating meteoroid impact risk and preparing future instrumentation.

The ninth session was an information poster session. There were 24 interesting posters on display. Conference participants spent just over an hour viewing and in discussion among one another and with those displaying the posters. These discussions continued over yet another delicious lunch.

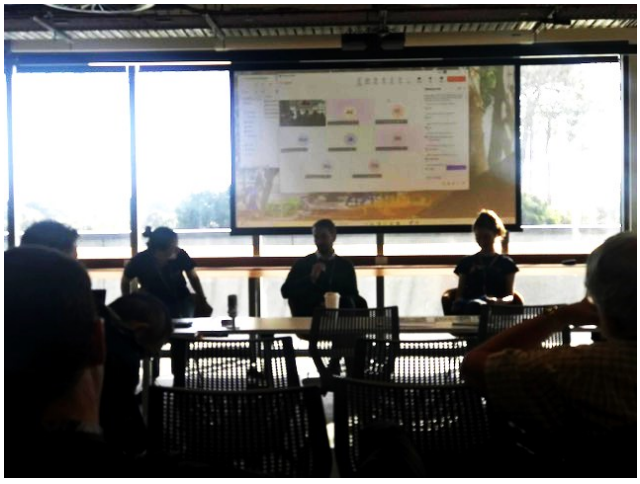

Figure 10 – Poster session with brunch.

[23] https://www.universetoday.com/article_images/C2025N1_NOT_20250711_151807.jpg

Figure 11 – Swan River[24].

After lunch it was time for excursions. Some participants spent the afternoon sailing on the Swan River whereas others paid visits to some of the laboratories and other places of interest around the Curtin University Campus.

5 Thursday 12th July

The 10th Session of the conference was concerned with *Planetary defense before impact and upon impact*. There were 9 talks on this topic. Speakers included David Coward, Peter Brown and Elizabeth Silber The talks were Planetary Defence Activities of the ESA, the Pan Starrs search from Near Earth Objects including potentially hazardous comets, the Southern Hemisphere Asteroid Research Consortium SHARC, hypervelocity cratering and disruption of Hydrous CM Chondrite and CI Simulant, the search for hydroacoustic signals from bolides, dynamical and physical properties of Decameter size Earth impactors, the 20 May 2023 bolide over NE Australia, Ground to space observations and finding fireballs in lightning using GOES weather satellite data.

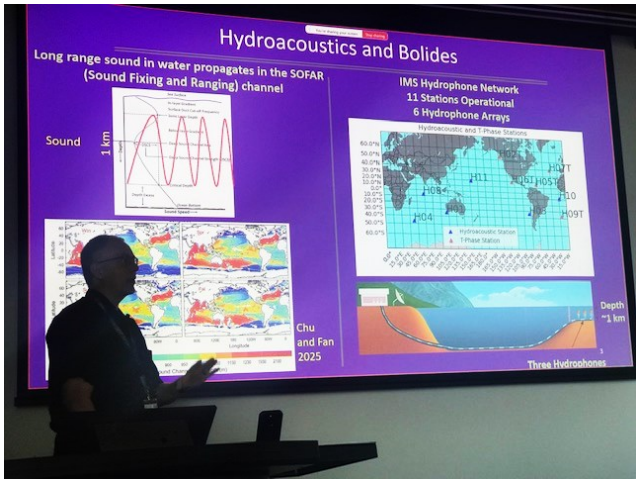

Figure 12 – Peter Brown speaking on searching for hydroacoustic signals from Bolides.

A panel discussion concerning imminent impactors followed. Many questions were raised about the 2029 Apophis flyby. Fortunately, Apophis will miss the Earth.

Figure 13 – Panel discussion with at left Nicholas Moskovitz and Ellie Sansom, Peter Brown seated at right.

After lunch the 11th Session was concerned with *Dynamical evolution of meteoroids*. Talks covered Missing Pieces: The atmospheric filter and the curious case of carbonaceous chondrites, a near Earth object model calibrated to Earth impactors, forecasting the 2025 Draconids, the dynamical history of the kappa Cygnid and August Draconid Meteoroids followed by preliminary results concerning the origin of the Geminid Meteor Stream.

The 12th session for the day was about *Space debris* both natural and human produced. Benjamin Hartig spoke about space debris re-entries over Australia and included a survey of events, environmental risk and correlation with Earth Observation imagery. Belia Hatty spoke about the Desert Fireball Network capturing images of a Russian Soyuz re-entry over Australia.

Figure 14 – Maria Hajdukova presenting her talk.

[24] https://www.westernaustralia.com/en/attraction/swan-river/56b267542880253d74c4f9eb

The 13th and final session for the day was the *IAU Meteor Commission 22 business meeting*. The first item concerned the official meteor shower list. Maria Hajdukova described the steps that have been taken to remove duplicate showers. Also, a new way to standardize the nomenclature of meteor showers using a number designation rather than the traditional method. A passionate, robust but very respectful debate followed. The meeting attendees were divided into two camps: those who wanted to implement the new nomenclature and those who preferred to keep the traditional names. In the end after each side presented their views time ran out before a clear consensus if any could be reached.

The second item was to announce the organizing committee members for 2024–2028.

Figure 15 – Announcing the Organizing Committee Members for 2024 to 2028 for Commission 22.

The third and last item of the Business meeting was to decide where the 13th Meteoroids Conference was to be held. It was decided to accept the bid by the European Space Agency Facility (ESAC) located in Villafranca del Castillo, about 30 km West/Northwest of Madrid pending capacity.

Thursday evening saw participants travel to the Western Australian Boola Bardip Museum for the conference dinner. Participants and guests were seated at a long table and served a wonderful four course meal featuring, fine Western Australian wines and food. A good time was enjoyed by one and all. After the dinner some of the younger participants continued celebrating in a couple of the bars in the Northbridge District of Perth.

Figure 16 – Conference Dinner held in the WA Museum.

6 Friday 11th July

The final session of the Conference concerned *Meteoroid sources*. The topics covered were the origin of our meteorites in the asteroid belt, searching for tidal disruption signatures amongst NEA's and impact data, Analysis of FRIPON Meteoroid Orbits and their association with known NEA's, which meteoroids are from asteroids and which are from comets? Meteor showers as a tool to investigate evolutionary history of the parent comets, reassessing 1200 meteor showers and their links to the near-Earth environment. Observations of the outburst of the tau Herculid Meteor Shower in 2022 and the Investigation of the delta Cancrid Asteroid Meteoroid Complex. Highlights of this session were the presentations by Peter Jenniskens, Tom Do and Junichi Watanabe.

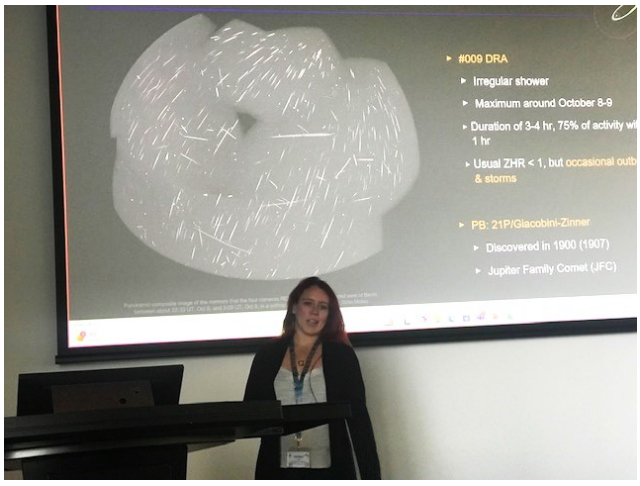

Figure 17 – Auriane Egal with her talk about forecasting the 2025 Draconids.

Figure 18 – The discussion panel from left to right; Peter Jenniskens, Jeremie Vauballion, Junichi Watanabe, Margaret Campbell-Brown, Patrick Shober and Hadrien Devillepoix (standing).

When the formal talks on Meteoroid Sources concluded, Hadrien Devillepoix hosted a panel discussion concerning outstanding questions in linking meteoroids and their parent bodies.

After the panel session it was a matter of thanking the organizing committees who did an amazing job with ensuring the Conference ran so smoothly. Well done for making this event one to remember.

Visual meteor observations winter 2025

Koen Miskotte

Dutch Meteor Society
k.miskotte@upcmail.nl

A summary is presented of the author's visual meteor observations during the winter months of 2025.

1 Looking back at 2024

After the very successful year 2023, a somewhat less successful year followed. Of course, the moon cooperated less in 2024 than the previous year. A first quarter moon during the Perseids is of course not too bad, but a lot of moonlight during the Geminids makes a huge difference. In total, 84.17 hours could be observed during 31 different sessions. This yielded 1631 meteors, which means that this year ends a little below average. The Perseids could be observed well. First a week from the Netherlands (4 clear nights), then a week from Saint-Trinit in the south of France (6 nights). The second week I was able to observe together with Selma Koelers, Carl Johannink, Peter van Leuteren and Sietse Dijkstra. And this was a very successful week!

In total for the period 1980–2024, observations have been made in 1330 different nights (3791.98 hours effective) and that yielded 95570 meteors.

2 The 2025 meteor observations

2025 January 2–3

The first major shower of the year is of course the Quadrantids meteor shower. With a maximum on 3 January around 16^h UT, the emphasis was mainly on the morning of the 3rd and evening of the 3th of January. Clearings were expected for the night of 2–3 January. The evening session of 3 January could unfortunately not take place: too much cloud cover.

That evening and night, Sat24 and the rain radar were consulted regularly. Sometimes it cleared up nicely, but it quickly became overcast again. This was also the case around 1^h UT when it was still largely cloudy. But the Sat24 images did show a larger area of clearing that should arrive around 2^h UT. Indeed, the area of clearing became visible in the north. I quickly installed myself on the roof. Indeed, it was possible to make observations between 01^h54^m and 02^h58^m UT. Sometimes I stopped briefly to let clouds pass. In total, 13 Quadrantids, 1 Antihelion and 2 sporadic meteors were seen in these 0.931 effective hours with a limiting magnitude of 6.3 (*Table 1*). The most beautiful meteor was a –1 Quadrantid in Boötes. Also worth mentioning is a slow magnitude 0 sporadic meteor that seemed to rise from the horizon low in the north.

After this, the clouds came in for a while. However, between 04^h35^m and 04^h59^m UT it was mostly clear again. In these 0.40 effective hours, another 6 Quadrantids and 1 sporadic meteor were seen. One of those Quadrantids was a –3 meteor. Too bad the weather did not cooperate better.

Figure 1 – Bright Quadrantid captured with all sky station EN908 Ermelo in the evening of January 3, 2025 during a short clearing.

Table 1 – Meteor counts during the night of Januari 2–3, 2025.

Date	Period UT		$T_{eff.}$ hr.	*Lm*	*K*	Meteor showers				
Start	Start	End				QUA	COM	ANT	SPO	Total
03/01/2025	01:53	02:58	0.993	6.30	1.06	13	0	1	2	16
03/01/2025	04:35	04:59	0.400	6.30	1.07	6	0	0	1	7

Table 2 – Meteor counts during the night January 31–February 1, 2025.

Date	Period UT		$T_{eff.}$ hr.	*Lm*	*K*	Meteor showers			
Start	Start	End				COM	ANT	SPO	Total
01/02/2025	00:13	01:14	1.000	6.21	1.02	1	1	4	6
01/02/2025	01:14	02:15	1.000	6.25	1.02	0	1	4	5

January 31–February 1, 2025

During this somewhat hazy night observations were carried out between 00^h13^m and 02^h15^m UT: 2 hours effective yielded 11 meteors of which 2 Antihelion and 1 late #020 Coma Berenicid. As expected, the hourly frequencies were low. The most beautiful meteor appeared around 01^h02^m UT: a medium fast –2 orange colored meteor moved from Ursa Major to Gemini.

February 1–2, 2025

Thanks to the weekend I could observe a bit longer, now between 02^h05^m and 05^h08^m UT, 3 hours effectively. It was a nice clear and transparent sky with the limiting magnitude rising to 6.3. That usually produces a bit more meteors as can be seen in *Table 3*. Of the 23 observed meteors there were 4 meteors from the Antihelion region and another late # 020 Coma Berenicid. Also, two nice meteors: at 03^h19^m UT a –1 sporadic meteor moved from the Corona Borealis to Boötes, and around 4^h22^m UT a sporadic meteor with mv 0 was seen in Lyra.

Table 3 – Meteor counts during the night February 1–2, 2025.

Date	Period UT		$T_{eff.}$ hr.	*Lm*	*K*	Meteor showers			
Start	Start	End				COM	ANT	SPO	Total
02/02/2025	02:05	03:06	1.000	6.30	1.02	0	2	6	8
02/02/2025	03:06	04:07	1.000	6.30	1.02	0	2	5	7
02/02/2025	04:07	05:08	1.000	6.27	1.02	1	0	7	8

Table 4 – Meteor counts during the night February 2–3, 2025.

Date	Period UT		$T_{eff.}$ hr.	*Lm*	*K*	Meteor showers			
Start	Start	End				COM	ANT	SPO	Total
03/02/2025	02:18	03:19	1.000	6.19	1.02	0	1	3	4
03/02/2025	03:19	04:20	1.000	6.22	1.02	0	1	5	6
03/02/2025	04:20	05:21	1.000	6.15	1.02	0	0	4	4

February 2–3, 2025

During this night, a three-hour session took place. However, the sky had become a bit hazier, there was some fog and now and then with a passing tuft of cirrus. A limiting magnitude of 6.2 and with a somewhat larger decay towards the horizon (*Table 4*). This almost always has an effect on the number of meteors seen. I counted just 14 meteors, of which 2 from the Antihelion region. This time also no really bright meteors were seen, so it became a somewhat boring session… After this night there were still a number of clear skies (evenings) but no more observations were made in February. The wet and gray weather also returned. Fortunately, March would be a much better month for meteor observations. So, at the beginning of March, it was again possible to observe for three nights.

March 2–3, 2025

Due to the forecast of fog, it was decided to start observing early in the evening. However, it turned out that it remained clear until dawn. As expected very low activity, especially the first hour was boring (*Table 5*). A short +1 sporadic meteor was most noteworthy. The next night it was also clear but very foggy. No observations during that night.

March 4–5, 2025

This was a rather hazy and misty night with temperatures down to –3 Celsius. Despite that I still counted 13 meteors during 2 hours (*Table 6*). A beautiful –1 sporadic meteor moved from Corona Borealis to Hercules.

March 5–6, 2025

Good transparency yielded 18 meteors in 3 hours (*Table 7*). The best meteor this time was a beautiful blue-white +1 Antihelion with a long wake. These were the last winter observations of the 2024–2025 season. During Full Moon later in the month there were many clear nights, so let's hope the many clear nights of March will become a trend this year.

Table 5 – Meteor counts during the night March 2–3, 2025.

Date	Period UT		$T_{eff.}$ hr.	*Lm*	*K*	Meteor showers		
Start	Start	End				ANT	SPO	Total
02/03/2025	21:22	22:23	1.000	6.20	1.02	2	1	3
02/03/2025	22:23	23:24	1.000	6.23	1.02	1	4	5
02/03/2025	23:24	00:26	1.000	6.28	1.02	2	3	5

Table 6 – Meteor counts during the night March 4–5, 2025.

Date	Period UT		$T_{eff.}$ hr.	*Lm*	*K*	Meteor showers		
Start	Start	End				Start	Start	End
05/03/2025	00:45	01:52	1.100	6.13	1.02	1	4	5
05/03/2025	01:52	02:55	1.033	6.17	1.02	1	7	8

Table 7 – Meteor counts during the night March 5–6, 2025.

Date	Period UT		$T_{eff.}$ *hr.*	*Lm*	*K*	Meteor showers		
Start	Start	End				Start	Start	End
06/03/2025	01:35	02:36	1.000	6.22	1.02	1	2	3
06/03/2025	02:36	03:39	1.033	6.22	1.02	2	7	9
06/03/2025	03:39	04:40	1.000	6.12	1.02	0	6	6

Figure 2 – Three hours before starting the visual meteor observations, a bright fireball was captured with my all sky camera EN908 Ermelo. March 30, 2025 at $22^h30^m05^s$ UT. The fireball was also captured by other EN stations. The image is a bit unsharp because of dew inside the plastic dome.

Meteor observations and fireballs Spring 2025

Koen Miskotte

Dutch Meteor Society
k.miskotte@upcmail.nl

A summary of the author's visual and all-sky meteor observations is presented.

1 Introduction

In the last visual report (Miskotte, 2025) I wrote as the last sentence: "Let's hope that the many clear nights will become a trend this year". Well, the months after that spring was full of clear nights and dry conditions. But there are some reservations: why doesn't this happen in the fall instead of during the low meteor activity in the spring? Murphy's Law in full swing!

In the spring, the Moon always quickly interferes after the New Moon phase. This has to do with the steep angle that the ecliptic makes with the horizon in the spring from the Northern hemisphere. Already during the first quarter phase, the Moon interferes all night long. Advantage: after the Full Moon (this year on March 14), the Moon quickly disappears from the astronomical scene.

2 The night reports

March 17–18, 2025

This session started with very low expectations, after all we are in the nadir of meteor activity in the northern hemisphere. And then also observing in the evening. Observations were carried out between 19^h25^m and 21^h27^m UT. Two hours and only 7 meteors of which 3 Antihelion (ANT) and no bright meteors were seen. The SQM measurements clearly show how much light comes from the houses and gardens, SQM measurements remained around 19.00… Fortunately, the public street lighting is dimmed at night and is well shielded.

March 18–19, 2025

Another evening session because of the Moon. The session started a bit later. The sky was just as clear as the previous one, but it was remarkable that the SQM of maximum 20.12 was already a lot better: most people turn off their garden lights after 21^h UT. Two hours effectively yield 11 meteors, of which 4 ANT. A +1 SPO is the highlight of this session.

March 19–20, 2025

This time a three-hour session because Thursday was also a day off for me. Signed in between 21^h55^m and 00^h58^m UT. During the last hour some clouds suddenly appeared out of nowhere and moved north. The session ended when cirrus came in from the west. During 3 hours effectively 21 meteors were counted among which 5 Antihelion meteors are seen, the nicest a +1 right through Cepheus. Another striking appearance was a nice slow +1 sporadic (SPO) meteor moving from the Ursa Major to Boötes.

Table 1 – Meteor counts March 17, 18, 19–20 and 28, April 1, 3 and 4, 2025.

Date	Period UT		$T_{eff.}$ hr.	*Lm*	*K*	Meteor shower		
Start	Start	End				ANT	SPO	Total
17/03/2025	19:25	20:26	1.000	6.06	1.03	1	2	3
17/03/2025	20:26	21:27	1.000	6.16	1.03	2	2	4
18/03/2025	20:58	21:59	1.000	6.10	1.03	1	3	4
18/03/2025	21:59	23:00	1.000	6.25	1.03	3	4	7
19/03/2025	21:55	22:56	1.000	6.06	1.00	2	3	5
19/03/2025	22:56	23:57	1.000	6.19	1.00	1	7	8
20/03/2025	23:57	00:58	1.000	6.27	1.03	2	6	8
28/03/2025	00:43	01:44	1.000	6.22	1.03	1	6	7
28/03/2025	01:44	02:45	1.000	6.18	1.03	2	4	6
01/04/2025	00:18	11:40	1.367	6.20	1.03	5	5	10
03/04/2025	00:15	01:16	1.000	6.19	1.00	2	5	7
03/04/2025	01:16	02:17	1.000	6.15	1.00	0	5	5
03/04/2025	02:17	03:18	1.000	6.06	1.00	1	3	4
04/04/2025	00:41	02:11	1.500	6.25	1.03	3	9	12

After the Full Moon came the Lyrid period, always a beautiful period in the (meteor-quiet) spring. Unfortunately, the weather did not cooperate, the period between April 21 and 25 was almost cloudy.

April 18–19, 2025

So far, this was the clearest night from Ermelo in 2025. An enormous transparency (and darkness with SQM measurements above 20.40, almost a record from my home), also at low altitude resulted in relatively many meteors. The Milky Way was visible from Cassiopeia to below Scutum! That happens so rarely. More than two hours of observing yielded 30 meteors, of which 6 Lyrids (LYR) and 5 Antihelion meteors. The most beautiful meteor was a slow +1 ANT in the Big Dipper.

April 19–20, 2025

Clear again, but it was less transparent than the previous night. Between 23^h40^m and 01^h30^m UT 16 meteors were counted, of which 2 ANT and 2 LYR. No really bright meteors.

April 25, 2025: Knight in the Order of Orange Nassau!

No observations but I was making orange pastries that night because of King's Day on April 27, a national day off. However, in the morning I was lured to the town hall of Ermelo. There I was surprised with a medal and can call myself Knight in the Order of Oranje-Nassau (*Figure 1*). This was organized by a number of members of the Dutch Meteor Society. I got this honor because of the observations, the interest in meteors, the processing of observations, articles, editor of the magazine *eRadiant* (2005–2018) and many participations in the expeditions. A big thank you to my fellow DMS friends. As I said at the spring DMS meeting: this is also the result of a positive interaction between me and a number of DMS members.

Figure 1 – The author together with the Mayor of Ermelo Hans van Daalen (© Dyane Ribbink).

April 26–27, 2025

A 2.5-hour session yielded another 17 meteors of which 1 Lyrid and 1 Antihelion. The latter was a +1 ANT in the constellation Lynx.

April 27–28, 2025

Another 2.5 hours of observations. 20 meteors were counted of which 1 Lyrid and 3 from the Antihelion region. Finally, some more bright meteors: 0^h36^m UT a long +1 sporadic meteor in the Big Dipper, 01^h26^m UT a +1 Antihelion in Cancer low west and the nicest at 01^h53^m UT: a 0 sporadioc meteor low in the northwest. Furthermore at 2^h36^m UT the ISS became visible in Ophiuchus and moving east.

April 30–May 1, 2025

This was once again a 2.5-hour session, yielding 19 meteors of which 1 late Lyrid and 3 Antihelion meteors. Two sporadic meteors of +1 were the most beautiful apparitions. Also, a bright ISS passage was seen around 1^h47^m UT moving from Boötes to Pegasus.

Table 2 – Meteor counts April 18–19, 19–20, 26–27, 28, and 30–1 May, 2025.

Date	Period UT		$T_{eff.}$ hr.	*Lm*	*K*	Meteorshowers			
Start	Start	End				LYR	ANT	SPO	Total
18/04/2025	23:10	23:55	0.750	6.35	1.00	2	1	8	11
18/04/2025	23:55	00:40	0.750	6.35	1.00	2	3	5	10
19/04/2025	00:40	01:25	0.750	6.25	1.00	2	1	6	9
19/04/2025	23:46	00:34	0.800	6.30	1.00	1	2	5	8
20/04/2025	00:34	01:30	0.933	6.24	1.05	1	0	7	8
26/04/2025	23:45	00:30	0.750	6.30	1.00	0	0	5	5
27/04/2025	00:30	01:16	0.750	6.30	1.00	1	0	4	5
27/04/2025	01:16	02:21	1.000	6.20	1.00	0	1	6	7
28/03/2025	00:15	01:01	0.750	6.30	1.00	1	1	4	6
28/03/2025	01:01	01:46	0.750	6.30	1.00	0	1	5	6
28/03/2025	01:46	02:32	0.750	6.20	1.00	0	1	7	8
30/04/2025	23:45	00:30	0.750	6.32	1.03	0	2	4	6
01/05/2025	00:30	01:20	0.817	6.30	1.03	1	1	4	6
01/05/2025	01:20	02:20	1.000	6.23	1.03	0	0	7	7

After the moonlight period of May 5–14, observations started again.

May 15–16, 2025

A two-hour evening session yielded 12 meteors of which one late eta Lyrid (ELY) of +2 and 2 meteors from the Antihelion region.

May 18–19, 2025

A three-hour session resulted in 21 meteors. No bright meteors.

May 20–21, 2025

Unfortunately, this session ended after a one hour with fog and cirrus. 8 meteors were counted. One of them a meteor from the Antihelion region. However, the most beautiful meteor was a medium fast sporadic of magnitude –2 which had a path from the Ursa Major to Canes Venatici. Unfortunately, this was the last session during Spring 2025, as a period of more unstable weather began.

Table 3 – Meteor counts May 15, 18–19 and 20–21, 2025.

Date	Period UT		$T_{eff.}$ hr.	*Lm*	*K*	Meteor showers			
Start	Start	End				ELY	ANT	SPO	Total
15/05/2025	21:25	22:30	1.083	6.19	1.03	1	0	5	6
15/05/2025	22:30	23:18	0.800	6.22	1.03	0	2	4	6
18/05/2025	22:00	23:01	1.000	6.25	1.06	0	0	5	5
18/05/2025	23:01	00:02	1.000	6.28	1.06	0	3	6	9
19/05/2025	00:03	01:03	1.000	6.26	1.03	0	0	7	7
20/05/2025	22:50	23:52	1.033	6.25	1.04		1	7	8

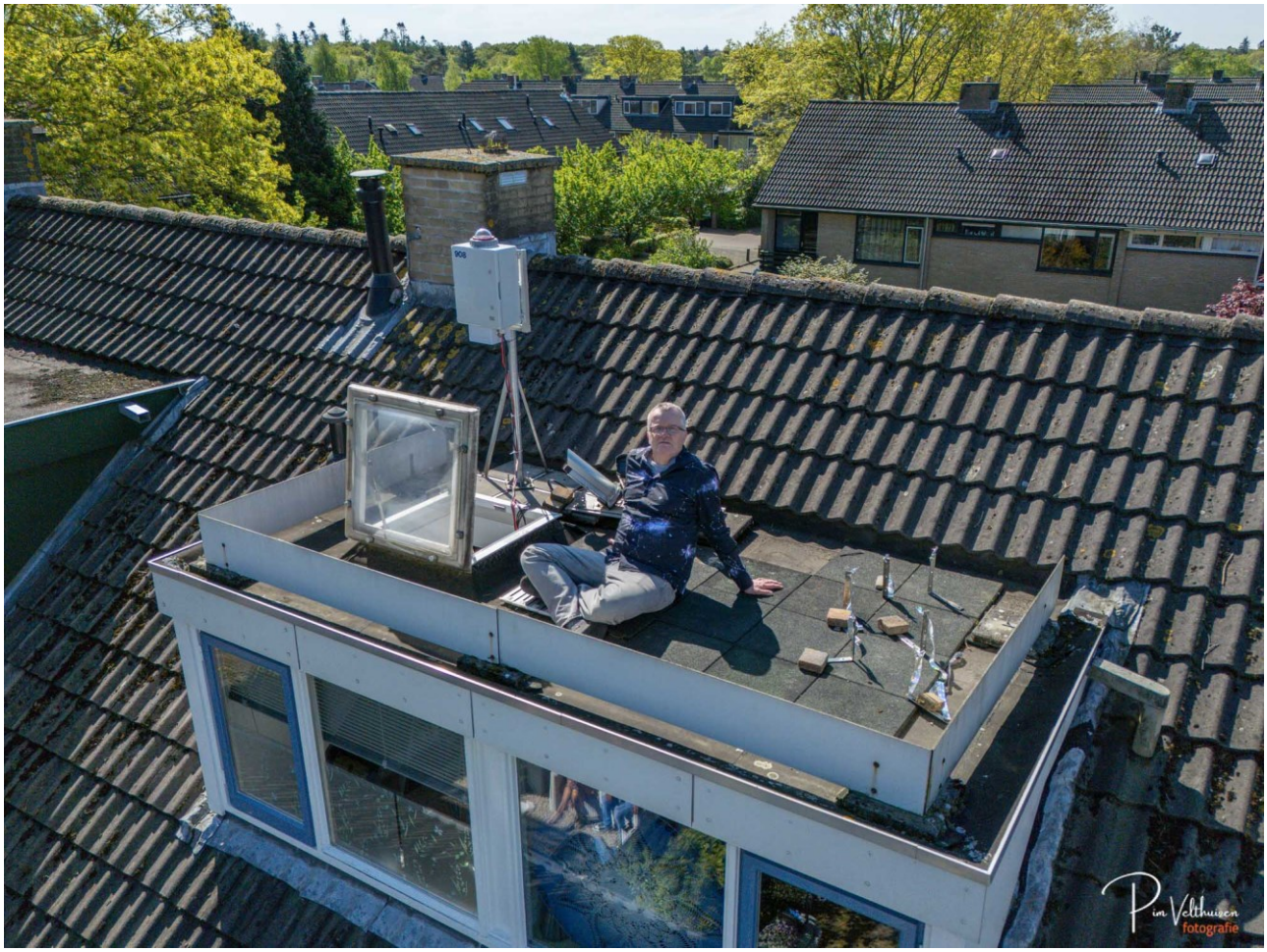

Figure 2 – The author on the flat roof of the dormer with four CAMS systems and all-sky camera EN908. The ribbons on the right are to keep the jackdaws away from the flat roof © Pim van Velthuizen photography[25].

[25] http://pimvelthuizen.nl/

3 New “home” for all-sky camera EN908 Ermelo.

With the old box of the all-sky camera there were some problems with moisture. This was not so much due to the box but more to the wish to work as much as possible without front glass, in order to obtain higher quality of the recordings. The new larger box is now equipped with adjustable lens heating; on hot days a Peltier element ensures that the box remains around 22 degrees Celsius. The control of the camera (a Canon 6D with a Sigma 8 mm F 4.0 fish eye lens) is done with a Linux PC that uses software from the Czech all-sky network. Also new is the control of the Liquid Crystal Shutter. Previously the shutter was set to 16 breaks per second. The new control makes 15 breaks and then skips one. This is done by means of a GPS receiver and always happens exactly to the second. The device was built by Hans Betlem in collaboration with Felix Bettonvil and Marc de Lignie.

Figure 3 – A new box for the all-sky camera EN908 Ermelo. A plastic dome is protecting the lens against dew and rain.

Figure 4 – Inside of the new all-sky housing EN908 Ermelo. During periods without rain the camera can operate without the plastic dome. This gives much better measuring results, especially with fireballs appearing low above the horizon.

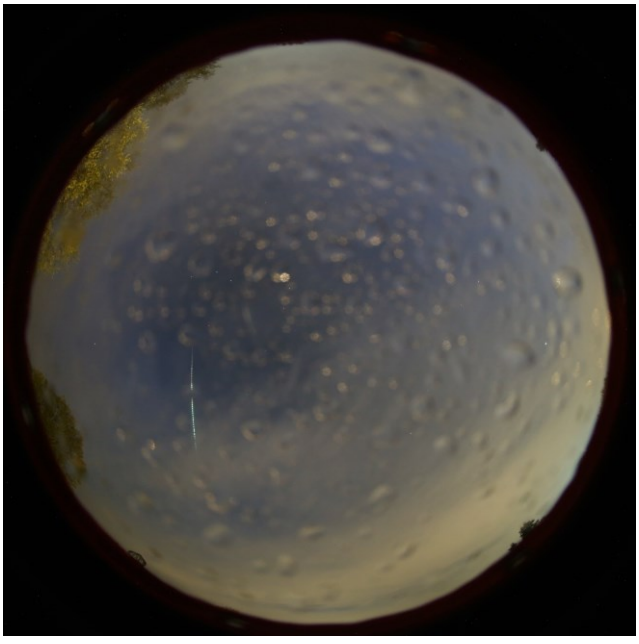

Figure 5 – After an evening with rainshowers the sky cleared: a bright fireball was captured between clouds on April 15, 2025 at $19^{h}55^{m}44^{s}$ UT.

Figure 6 – Close up of the previous image. Clearly visible are the longer breaks for exact time markers in the meteor trail.

Figure 7 – A much sharper image from a fireball without the plastic dome. This fireball appeared on May 16, 2025 at $01^h27^m53^s$ UT.

Figure 8 – Fireball with a terminal flare on May 19, 2025 at $01^h06^m53^s$ UT.

Figure 9 – Also on the meteor roof: 4 CAMS systems.

4 Summary

All in all, a good spring season for visual meteor, CAMS and all-sky observations, despite missing the Lyrid maximum. Again, hoping that this will be a trend for 2025…

References

Miskotte K. (2025). “Visual meteor observations winter 2025”. *eMetN Meteor Journal*, **10**, 301–303.

June 2025 CARMELO report

Mariasole Maglione[1], **Lorenzo Barbieri**[2]

[1] **Gruppo Astrofili Vicentini, Italy**
mariasole@astrofilivicentini.it

[2] **CARMELO network and AAB: Associazione Astrofili Bolognesi, Italy**
carmelometeor@gmail.com

The CARMELO network (Cheap Amateur Radio Meteor Echoes LOgger) is a collaboration of SDR radio receivers aimed at detecting meteor echoes. This report presents the data for June 2025.

1 Introduction

In June, the CARMELO network recorded increasing meteoric activity, and in the first half of the month detected activity consistent with the daytime shower of the Arietids (171 ARI).

2 Methods

The CARMELO network consists of SDR radio receivers. In them, a microprocessor (Raspberry) performs three functions simultaneously:

- By driving a dongle, it tunes the frequency on which the transmitter transmits and tunes like a radio, samples the radio signal and through the FFT (Fast Fourier Transform) measures frequency and received power.
- By analyzing the received data for each packet, it detects meteor echoes and discards false positives and interference.
- It compiles a file containing the event log and sends it to a server.

The data are all generated by the same standard, and are therefore homogeneous and comparable. A single receiver can be assembled with a few devices whose total current cost is about 210 euros.

To participate in the network read the instructions on this page[26].

3 June data

In the plots that follow, all available at this page[27], the abscissae represent time, which is expressed in UT (Universal Time) or in solar longitude (Solar Long), and the ordinates represent the hourly rate, calculated as the total number of events recorded by the network in an hour divided by the number of operating receivers.

In *Figure 1*, the trend of signals detected by the receivers for the month of June.

4 Arietids

Arietids (171 ARI) are a meteor shower active from mid-May to mid-June. It is the most intense diurnal meteor shower (daytime shower) of the year: its maximum occurs when the Sun is already high in the sky, making visual observation extremely difficult, with less than one meteor visible per hour. However, Arietids are well detectable with radio instrumentation.

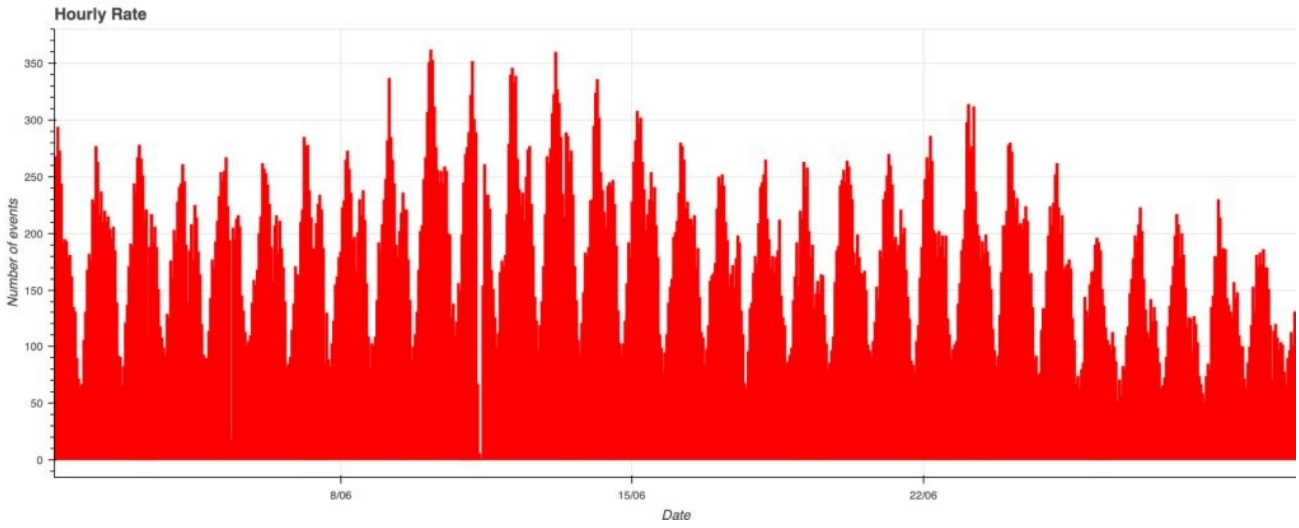

Figure 1 – June 2025 data trend.

[26] http://www.astrofiliabologna.it/about_carmelo

[27] http://www.astrofiliabologna.it/graficocarmelohr

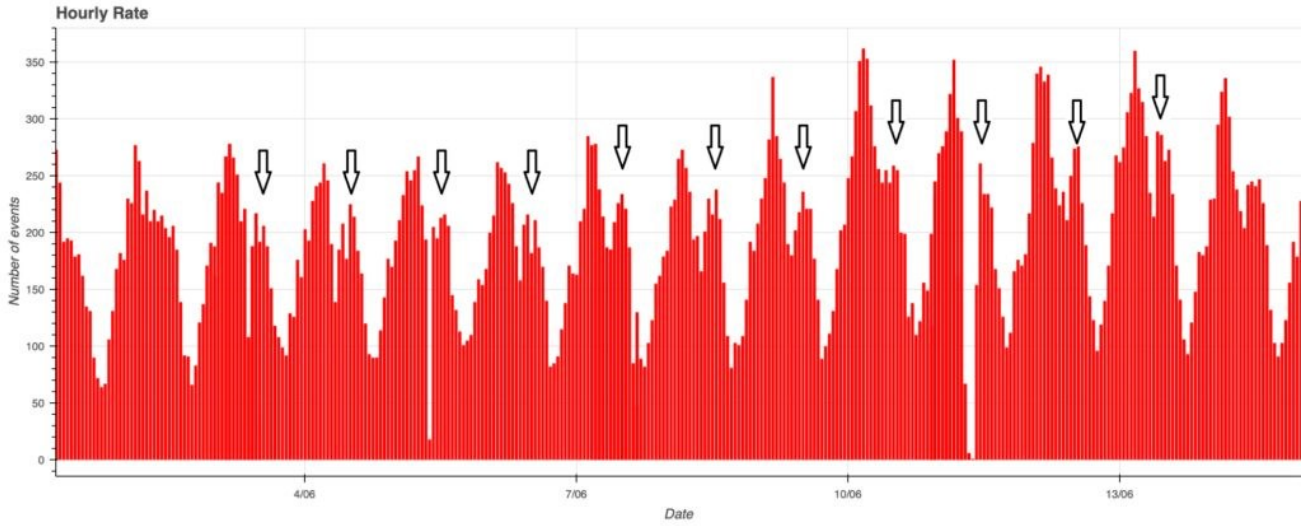

Figure 2 – Hourly rate between June 1 and June 15, 2025, with activity consistent with tracking of the Arietids shower.

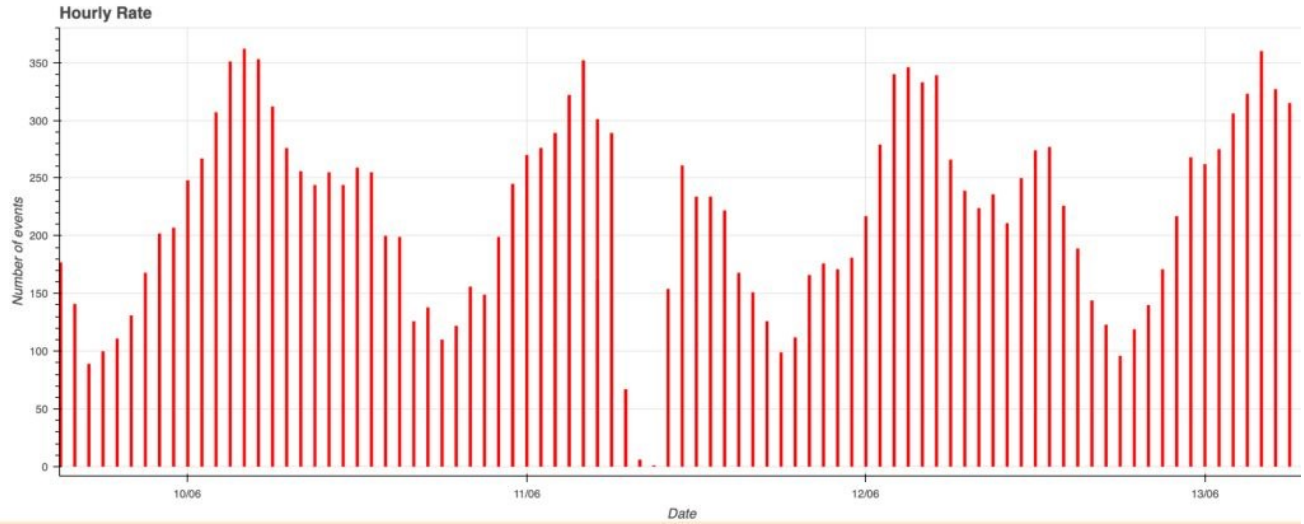

Figure 3 – In the center of the hourly rate chart is the June 11 interruption.

The radiant of the swarm is located in the constellation Aries, at a position about 4 degrees southeast of the star 41 Arietis. The meteors are generally rapid, with an entry velocity into the atmosphere of about 42 km/s, corresponding to an average velocity compared with other showers, which is not high[28].

In 2025, the Arietids meteor shower displayed increasing activity between June 3 and June 13, and the CARMELO network also detected an hourly rate consistent with a daily peak of the shower between 11^h00^m and 12^h00^m UT (*Figure 2*).

5 Graves radar shutdown

From *Figure 1*, which shows the trend of the hourly rate of meteors detected by the CARMELO network, the interruption on June 11, between 7^h00^m UT and 10^h00^m UT, i.e., between solar longitudes 80.28° and 80.40° (see *Figure 3*), jumps out. It corresponds to a shutdown of the Graves radar in France, probably caused by station maintenance.

During the shutdown, which lasted about three hours, CARMELO network receivers recorded only 4 events, all of which were clearly identifiable as false positives. Under normal conditions, in the same time interval, the system records more than 1000 events on average. This comparison leads to an interesting consideration: if in the absence of the radar signal we receive only 4 spurious events, it means that, under standard conditions, about 99.6% of the recordings are actually meteors. A result that confirms the reliability of CARMELO's automatic detection system.

6 The CARMELO network

The network currently consists of 14 receivers, 13 of which are operational, located in Italy, the UK, Croatia and the USA. The European receivers are tuned to the Graves radar

[28] https://www.emeteornews.net/2025/06/12/meteor-activity-outlook-for-14-20-june-2025/

station frequency in France, which is 143.050 MHz. Participating in the network are:

- Lorenzo Barbieri, Budrio (BO) ITA;
- Associazione Astrofili Bolognesi, Bologna ITA;
- Associazione Astrofili Bolognesi, Medelana (BO) ITA;
- Paolo Fontana, Castenaso (BO) ITA;
- Paolo Fontana, Belluno (BL) ITA;
- Associazione Astrofili Pisani, Orciatico (PI) ITA;
- Gruppo Astrofili Persicetani, San Giovanni in Persiceto (BO) ITA;
- Roberto Nesci, Foligno (PG) ITA;
- MarSEC, Marana di Crespadoro (VI) ITA;
- Gruppo Astrofili Vicentini, Arcugnano (VI) ITA;
- Associazione Ravennate Astrofili Theyta, Ravenna (RA) ITA;
- Akademsko Astronomsko Društvo, Rijeka CRO;
- Mike German a Hayfield, Derbyshire UK;
- Mike Otte, Pearl City, Illinois USA.

The authors' hope is that the network can expand both quantitatively and geographically, thus allowing the production of better-quality data.

July 2025 CARMELO report

Mariasole Maglione[1], Lorenzo Barbieri[2], William Rivato[3]

[1] **Gruppo Astrofili Vicentini, Italy**
mariasole@astrofilivicentini.it

[2] **CARMELO network and AAB: Associazione Astrofili Bolognesi, Italy**
carmelometeor@gmail.com

[3] **MarSEC, Marana Space Explorer Center, Italy**

The CARMELO network (Cheap Amateur Radio Meteor Echoes LOgger) is a collaboration of SDR radio receivers aimed at detecting meteor echoes. This report presents the data for July 2025.

1 Introduction

In the first half of July, meteor activity was moderate, mainly dominated by the psi Cassiopeiids meteor shower (187 PCA).

2 Methods

The CARMELO network consists of SDR radio receivers. In them, a microprocessor (Raspberry) performs three functions simultaneously:

- By driving a dongle, it tunes the frequency on which the transmitter transmits and tunes like a radio, samples the radio signal and through the FFT (Fast Fourier Transform) measures frequency and received power.
- By analyzing the received data for each packet, it detects meteor echoes and discards false positives and interference.
- It compiles a file containing the event log and sends it to a server.

The data are all generated by the same standard, and are therefore homogeneous and comparable. A single receiver can be assembled with a few devices whose total current cost is about 210 euros.

To participate in the network read the instructions on this page[29].

3 July data

In the plots that follow, all available at this page[30], the abscissae represent time, which is expressed in UT (Universal Time) or in solar longitude (Solar Long), and the ordinates represent the hourly rate, calculated as the total number of events recorded by the network in an hour divided by the number of operating receivers.

In *Figure 1*, the trend of signals detected by the receivers for the month of July.

4 Psi Cassiopeiids

Psi Cassiopeiids (187 PCA) are a meteor shower active during the first half of July, with a peak around mid-month.

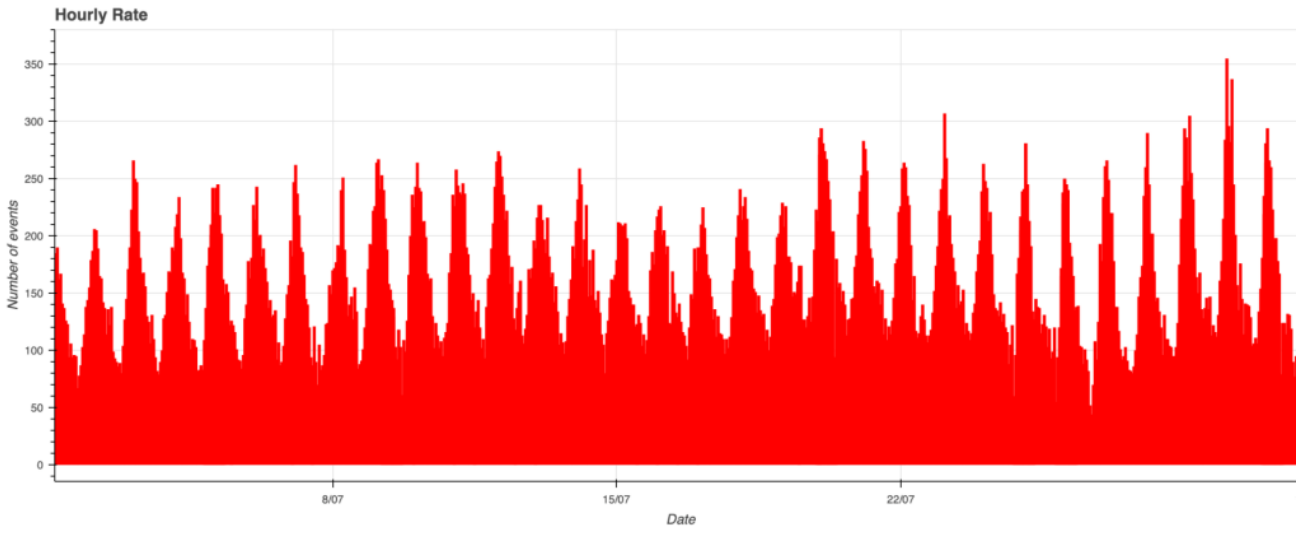

Figure 1 – July 2025 data trend.

[29] http://www.astrofiliabologna.it/about_carmelo

[30] http://www.astrofiliabologna.it/graficocarmelohr

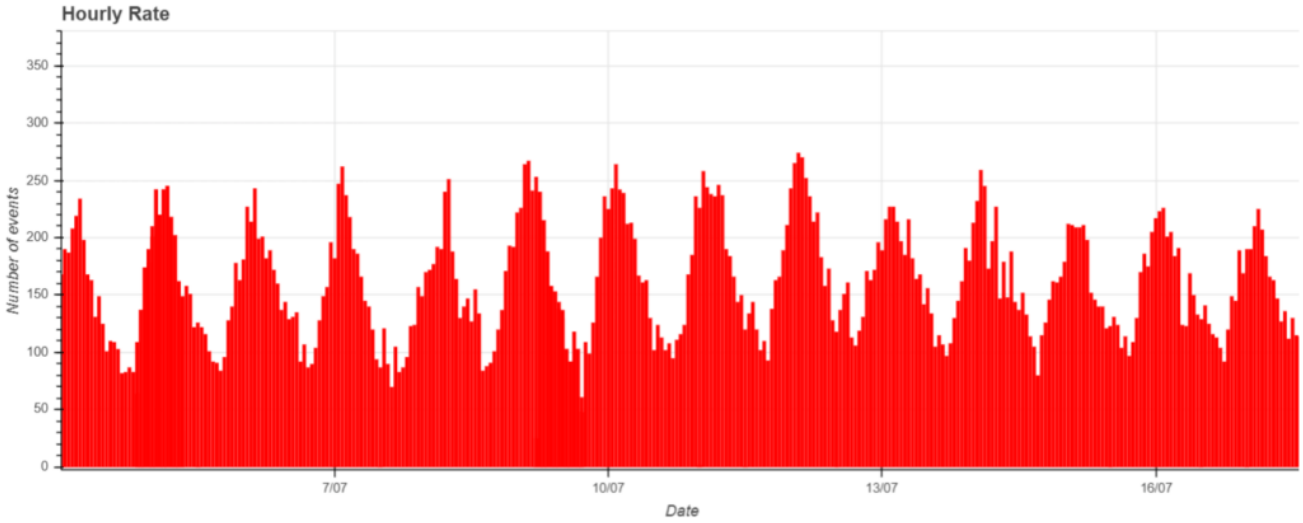

Figure 2 – Hourly rate between July 4 and 18, 2025, showing activity consistent with the tracking of the psi Cassiopeiids meteor shower.

It is a minor shower, not easily visible to the naked eye but detectable through radio observation systems, thanks to the speed and frequency of the meteors, especially during twilight hours. It is not associated with any known parent body (Jenniskens, 2006).

The radiant of the shower is located in the Cassiopeia constellation, near the star psi Cassiopeiae, from which it takes its name. The psi Cassiopeiids are fast meteors, entering Earth's atmosphere at about 58 km/s, and they produce short, intense radio echoes.

In 2025, the psi Cassiopeiids showed increasing activity in the first half of July, and the CARMELO network recorded an hourly rate consistent with the shower's tracking (*Figure. 2*).

5 The CARMELO network

The network currently consists of 14 receivers, 13 of which are operational, located in Italy, the UK, Croatia and the USA. The European receivers are tuned to the Graves radar station frequency in France, which is 143.050 MHz. Participating in the network are:

- Lorenzo Barbieri, Budrio (BO) ITA;
- Associazione Astrofili Bolognesi, Bologna ITA;
- Associazione Astrofili Bolognesi, Medelana (BO) ITA;
- Paolo Fontana, Castenaso (BO) ITA;
- Paolo Fontana, Belluno (BL) ITA;
- Associazione Astrofili Pisani, Orciatico (PI) ITA;
- Gruppo Astrofili Persicetani, San Giovanni in Persiceto (BO) ITA;
- Roberto Nesci, Foligno (PG) ITA;
- MarSEC, Marana di Crespadoro (VI) ITA;
- Gruppo Astrofili Vicentini, Arcugnano (VI) ITA;
- Associazione Ravennate Astrofili Theyta, Ravenna (RA) ITA;
- Akademsko Astronomsko Društvo, Rijeka CRO;
- Mike German a Hayfield, Derbyshire UK;
- Mike Otte, Pearl City, Illinois USA.

The authors' hope is that the network can expand both quantitatively and geographically, thus allowing the production of better-quality data.

Reference

Jenniskens P. (2006). Meteor showers and their parent comets, Cambridge University Press.

Radio meteors June 2025

Felix Verbelen

Vereniging voor Sterrenkunde & Volkssterrenwacht MIRA, Grimbergen, Belgium
felix.verbelen@gmail.com

An overview of the radio observations during June is given.

1 Introduction

The graphs show both the daily totals (*Figure 1 and 2*) and the hourly numbers (*Figure 3 and 4*) of "all" reflections counted automatically, and of manually counted "overdense" reflections, overdense reflections longer than 10 seconds and longer than 1 minute, as observed here at Kampenhout (BE) on the frequency of our VVS-beacon (49.99 MHz) during the month of June 2025.

The hourly numbers, for echoes shorter than 1 minute, are weighted averages derived from:

$$N(h) = \frac{n(h-1)}{4} + \frac{n(h)}{2} + \frac{n(h+1)}{4}$$

Local interference and unidentified noise remained quite limited, with lightning activity recorded on only four days. However, strong solar flares, mostly Type III, occurred almost daily (*Figure 5*).

This month, the well-known daylight showers were particularly dominant, primarily the Arietids (ARI). Other showers were also active, although the number of reflections appeared to be lower than in previous years.

7 reflections lasting longer than one minute were observed this month.

A selection of these, along with a few other interesting recordings is included (*Figures 6 to 18*).

In addition to the usual graphs, you will also find the raw counts in cvs-format[31] from which the graphs are derived. The table contains the following columns: day of the month, hour of the day, day + decimals, solar longitude (epoch J2000), counts of "all" reflections, overdense reflections, reflections longer than 10 seconds and reflections longer than 1 minute, the numbers being the observed reflections of the past hour.

[31] https://www.emeteornews.net/wp-content/uploads/2025/07/202506_49990_FV_rawcounts.csv

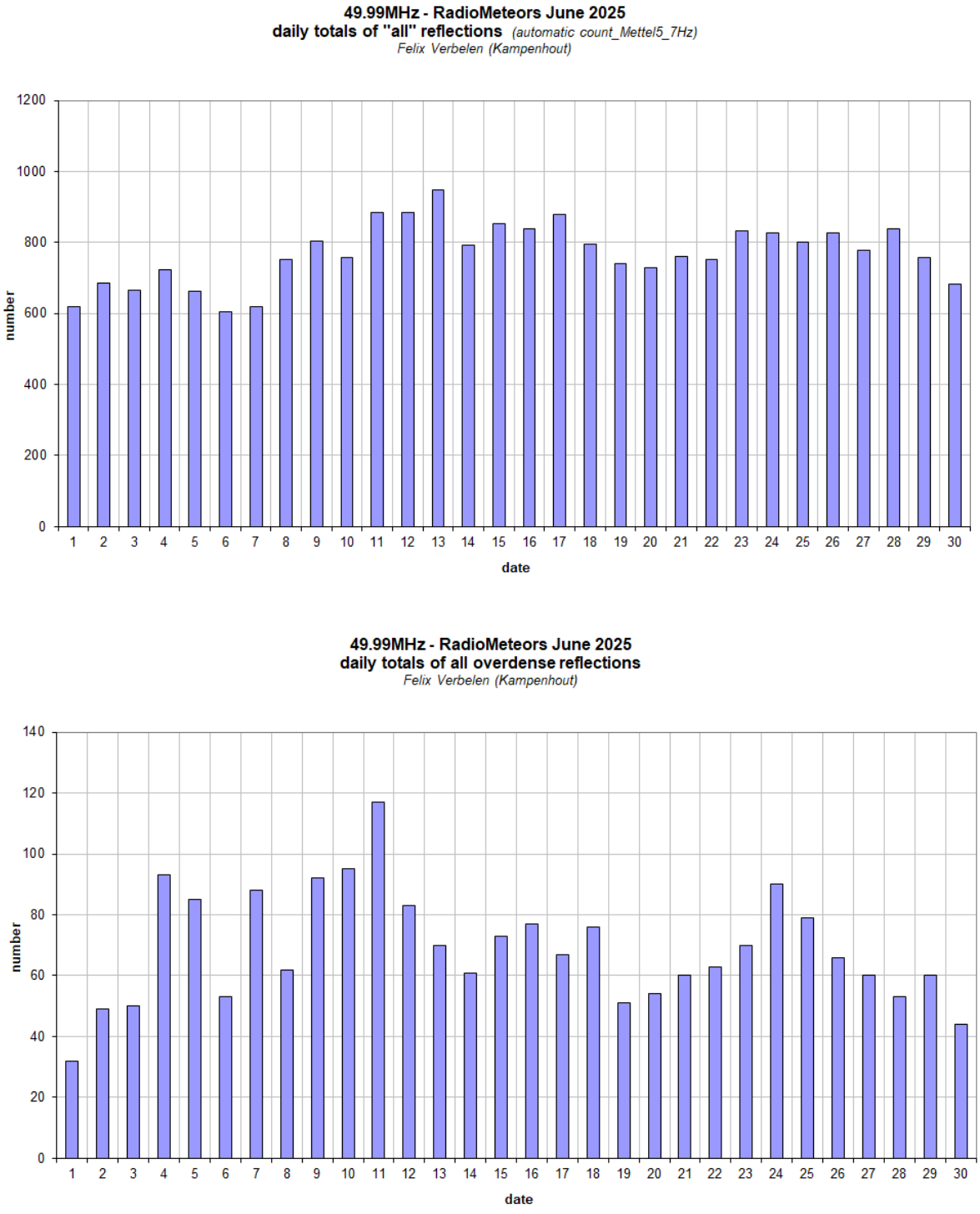

Figure 1 – The daily totals of "all" reflections counted automatically, and of manually counted "overdense" reflections, as observed here at Kampenhout (BE) on the frequency of our VVS-beacon (49.99 MHz) during June 2025.

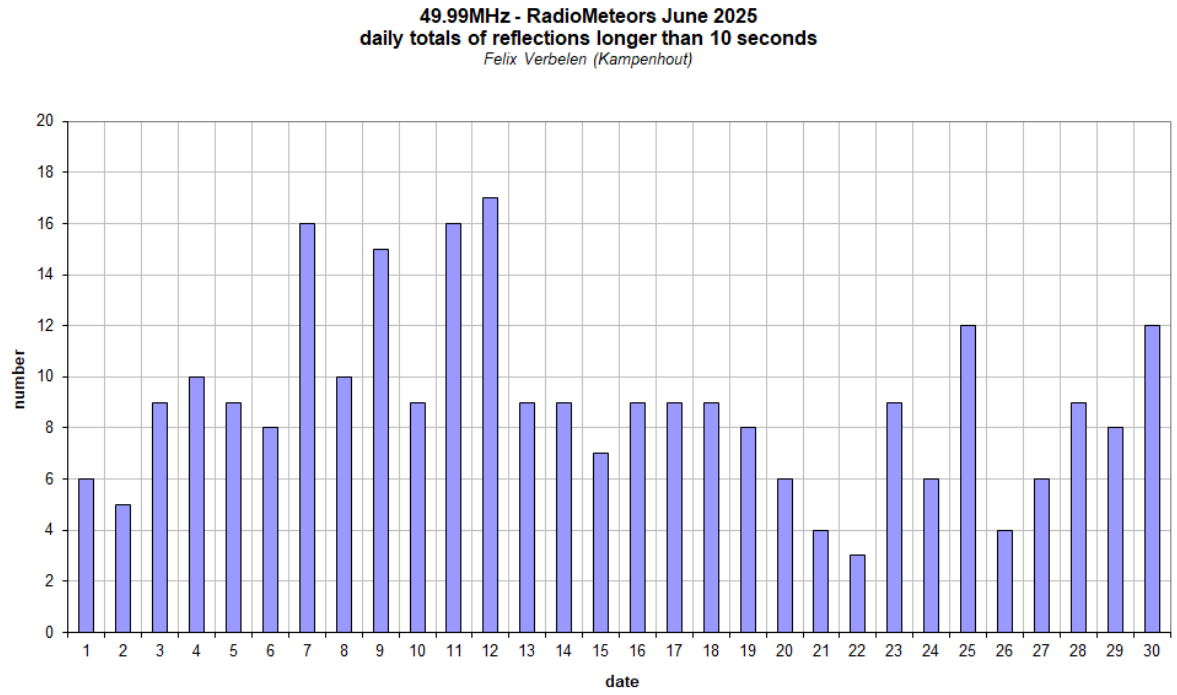

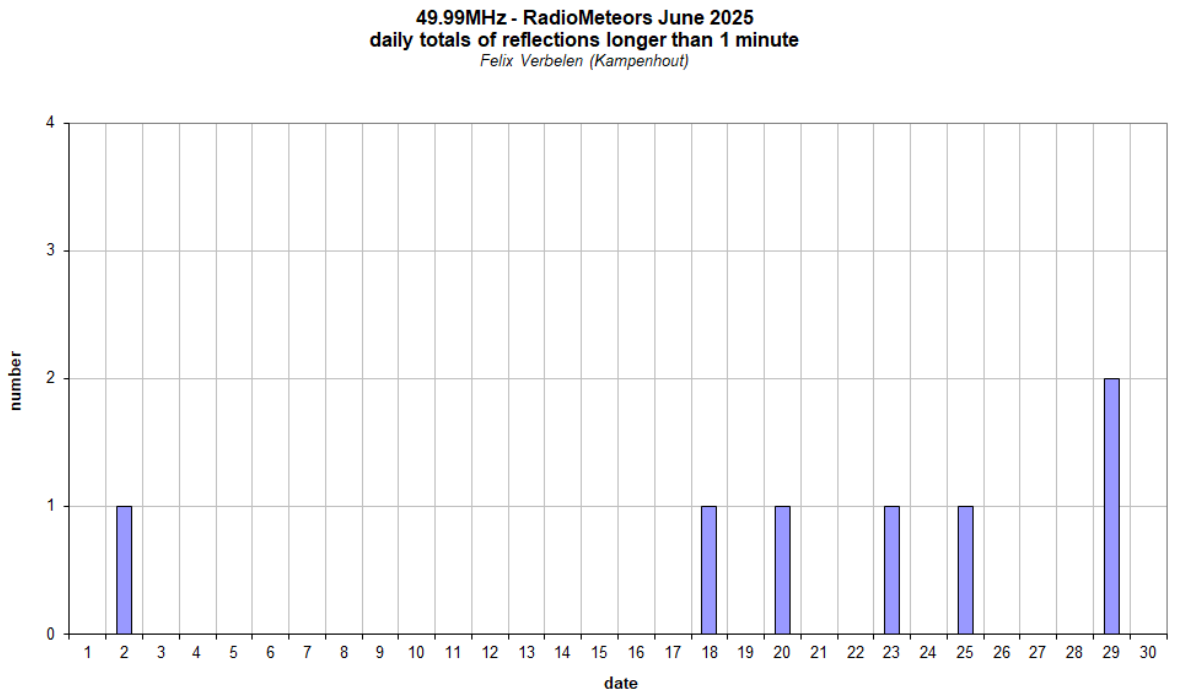

Figure 2 – The daily totals of overdense reflections longer than 10 seconds and longer than 1 minute, as observed here at Kampenhout (BE) on the frequency of our VVS-beacon (49.99 MHz) during June 2025.

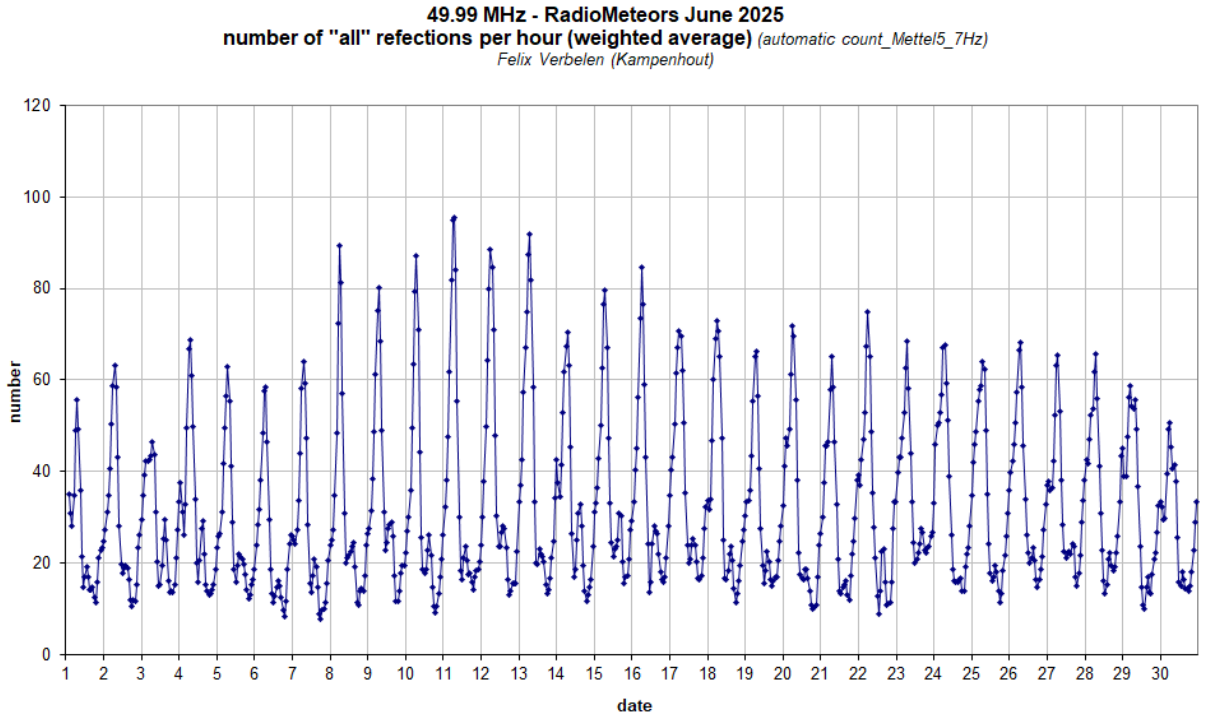

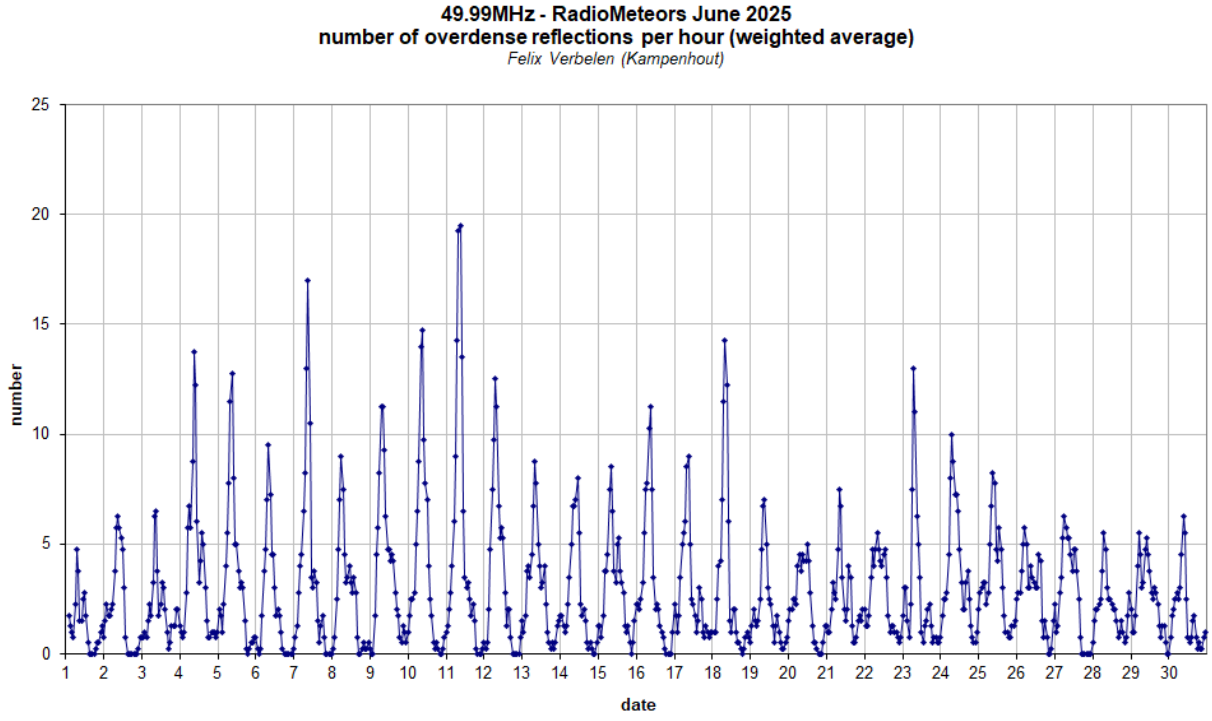

Figure 3 – The hourly numbers of "all" reflections counted automatically, and of manually counted "overdense" reflections, as observed here at Kampenhout (BE) on the frequency of our VVS-beacon (49.99 MHz) during June 2025.

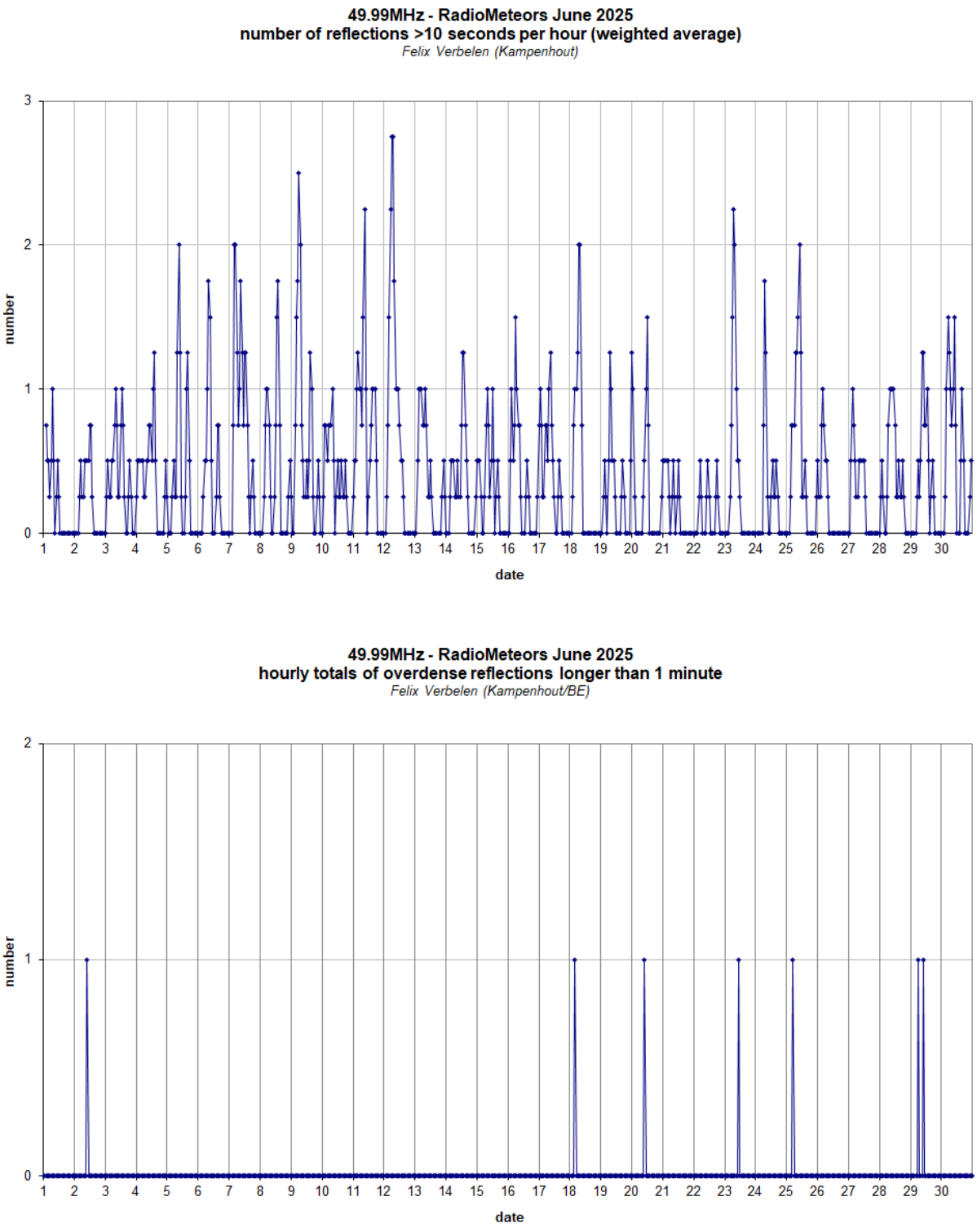

Figure 4 – The hourly numbers of overdense reflections longer than 10 seconds and longer than 1 minute, as observed here at Kampenhout (BE) on the frequency of our VVS-beacon (49.99 MHz) during June 2025.

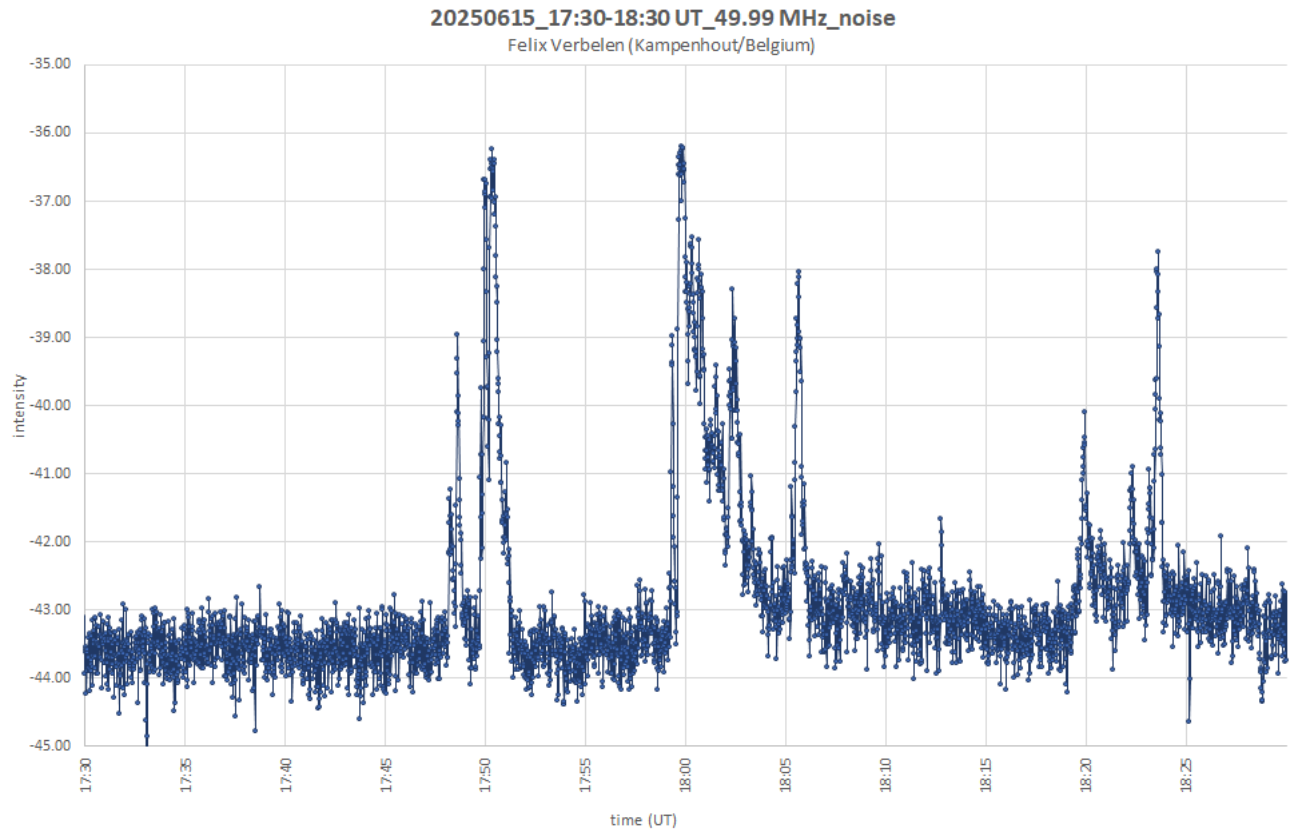

Figure 5 – Strong solar flares, mostly Type III, occurred almost daily.

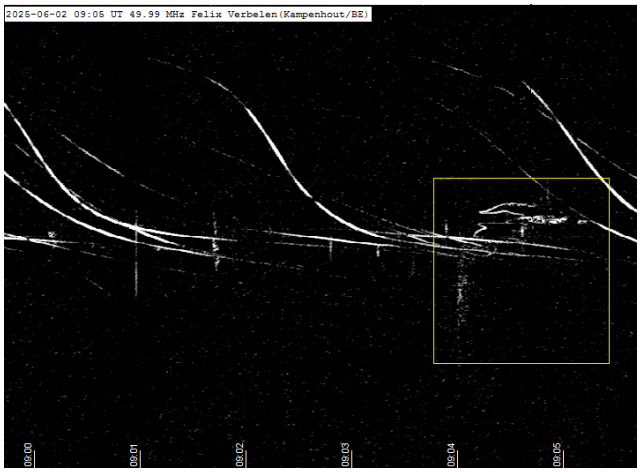

Figure 6 – Meteor echoes June 2, 9^h05^m UT.

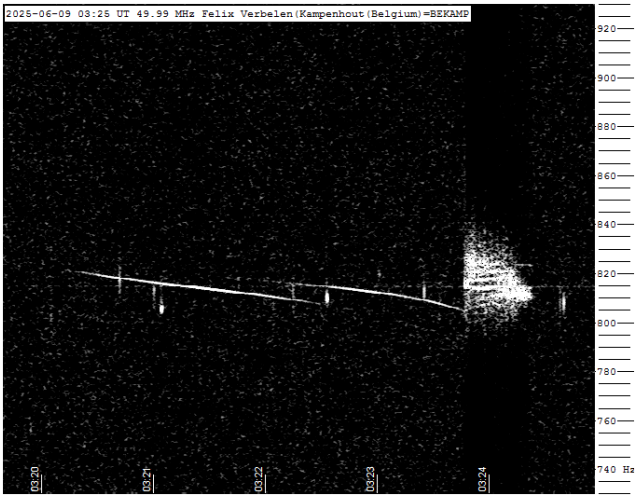

Figure 7 – Meteor echoes June 9, 3^h25^m UT.

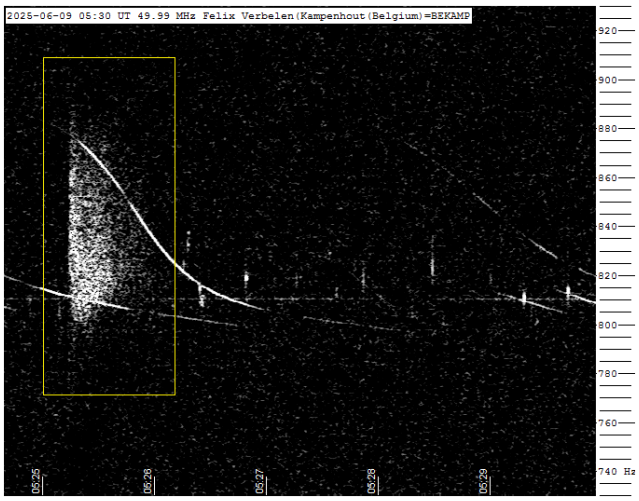

Figure 8 – Meteor echoes June 9, 5^h30^m UT.

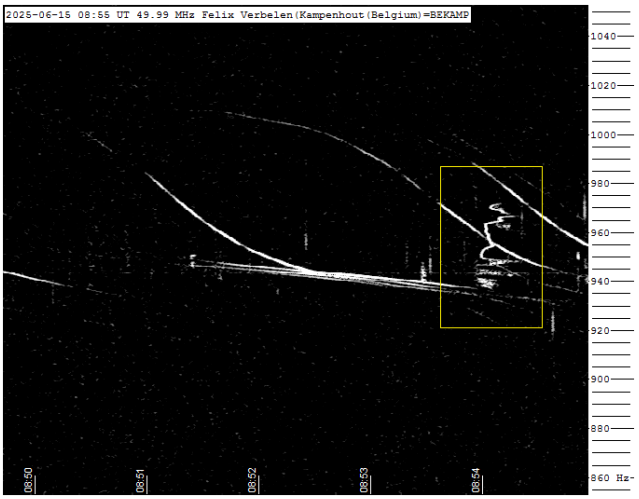

Figure 9 – Meteor echoes June 15, 8^h55^m UT.

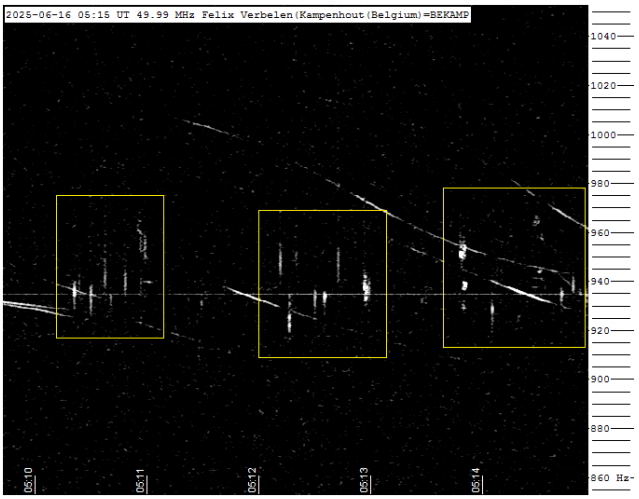

Figure 10 – Meteor echoes June 16, 5^h15^m UT.

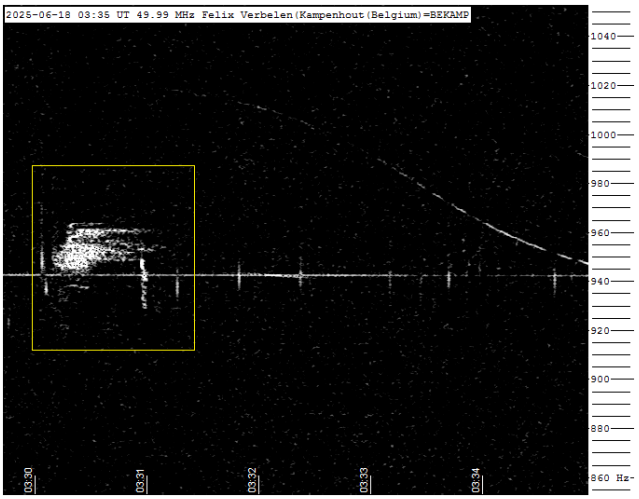

Figure 11 – Meteor echoes June 18, 3^h35^m UT.

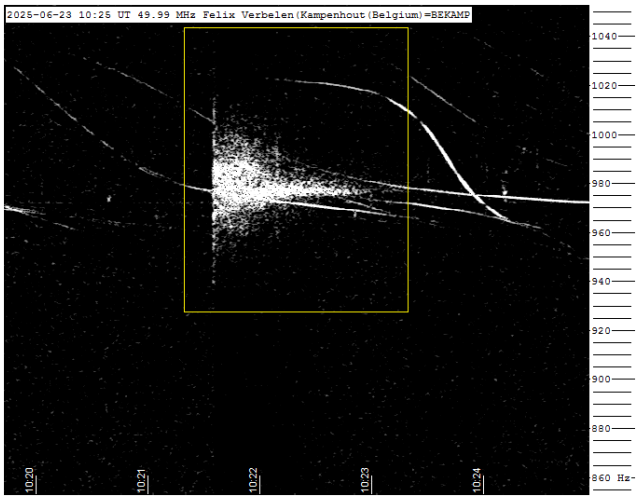

Figure 12 – Meteor echoes June 23, 10^h25^m UT.

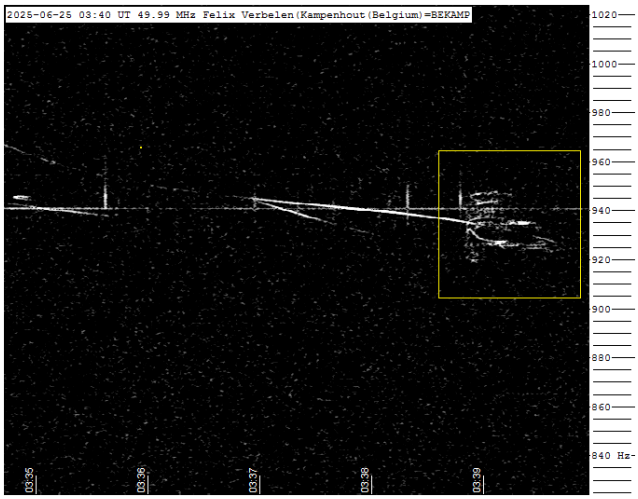

Figure 13 – Meteor echoes June 25, 3^h40^m UT.

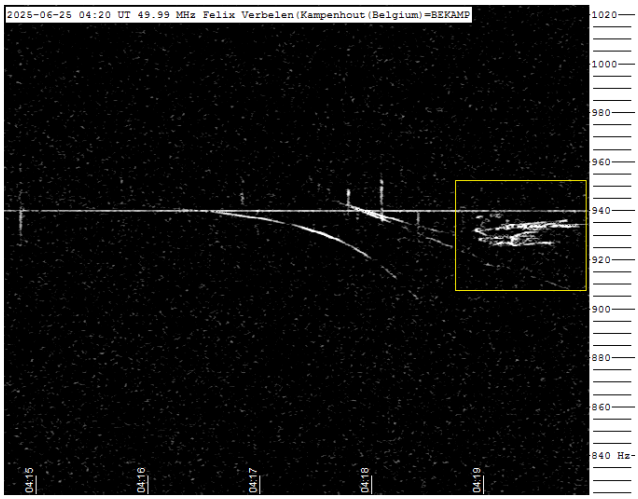

Figure 14 – Meteor echoes June 25, 4^h20^m UT.

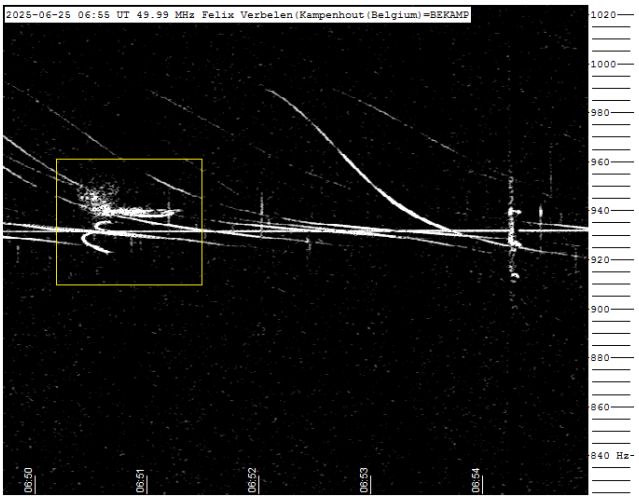

Figure 15 – Meteor echoes June 25, 6^h55^m UT.

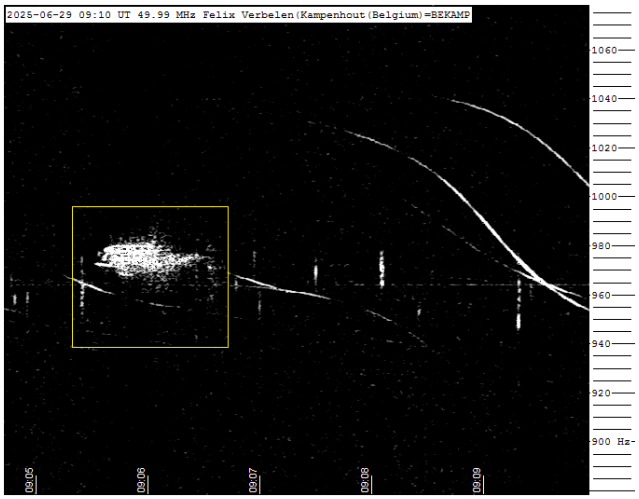

Figure 17 – Meteor echoes June 29, 9^h10^m UT.

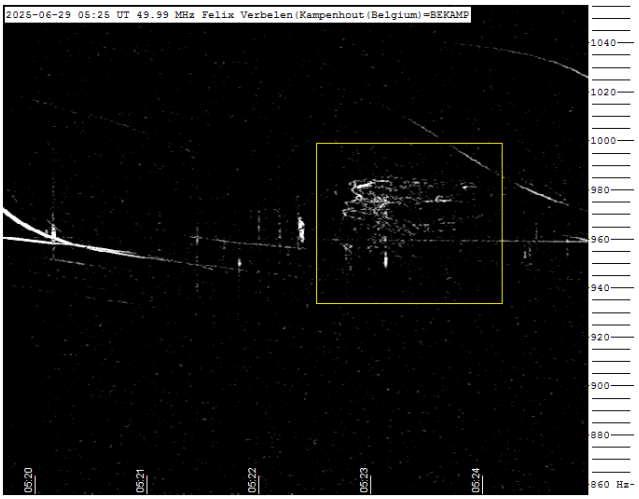

Figure 16 – Meteor echoes June 29, 5^h25^m UT.

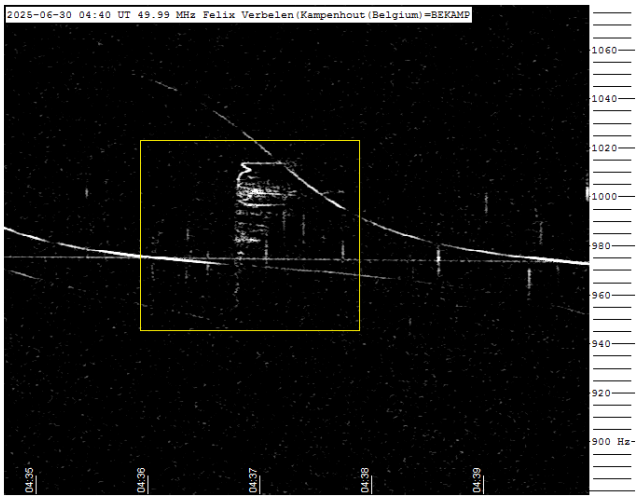

Figure 18 – Meteor echoes June 30, 4^h40^m UT.

Radio meteors July 2025

Felix Verbelen

Vereniging voor Sterrenkunde & Volkssterrenwacht MIRA, Grimbergen, Belgium
felix.verbelen@gmail.com

An overview of the radio observations during July is given.

1 Introduction

The graphs show both the daily totals (*Figure 1 and 2*) and the hourly numbers (*Figure 3 and 4*) of "all" reflections counted automatically, and of manually counted "overdense" reflections, overdense reflections longer than 10 seconds and longer than 1 minute, as observed here at Kampenhout (BE) on the frequency of our VVS-beacon (49.99 MHz) during the month of July 2025.

The hourly numbers, for echoes shorter than 1 minute, are weighted averages derived from:

$$N(h) = \frac{n(h-1)}{4} + \frac{n(h)}{2} + \frac{n(h+1)}{4}$$

Weak to moderate lightning activity was detected on 7 days, and strong solar flares, mostly of type III, occurred almost daily.

Several showers were active this month, with a notable increase in long-duration reflections, especially during the last few days of the month. A total of 14 reflections lasting more than 1 minute were observed, 7 of which occurred from July 27th to 30th. A selection of these, along with a few other interesting recordings is included (*Figures 5 to 22*).

In addition to the usual graphs, you will also find the raw counts in cvs-format[32] from which the graphs are derived. The table contains the following columns: day of the month, hour of the day, day + decimals, solar longitude (epoch J2000), counts of "all" reflections, overdense reflections, reflections longer than 10 seconds and reflections longer than 1 minute, the numbers being the observed reflections of the past hour.

[32] https://www.emeteornews.net/wp-content/uploads/2025/08/202507_49990_FV_rawcounts.csv

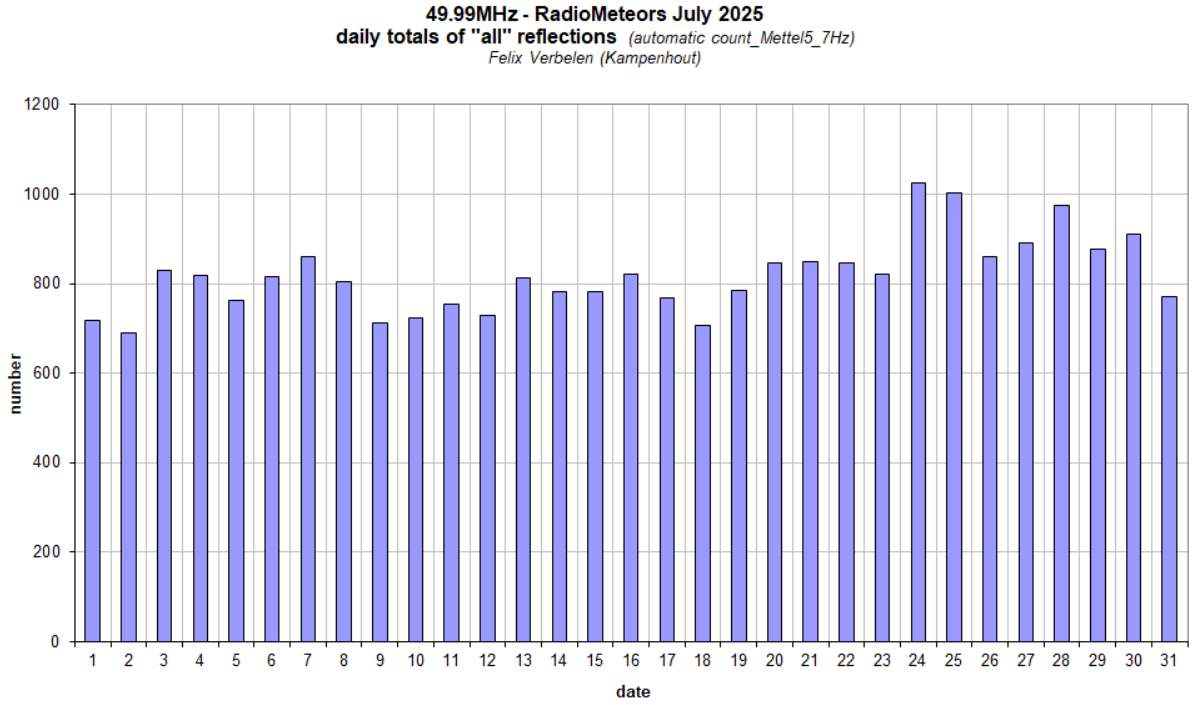

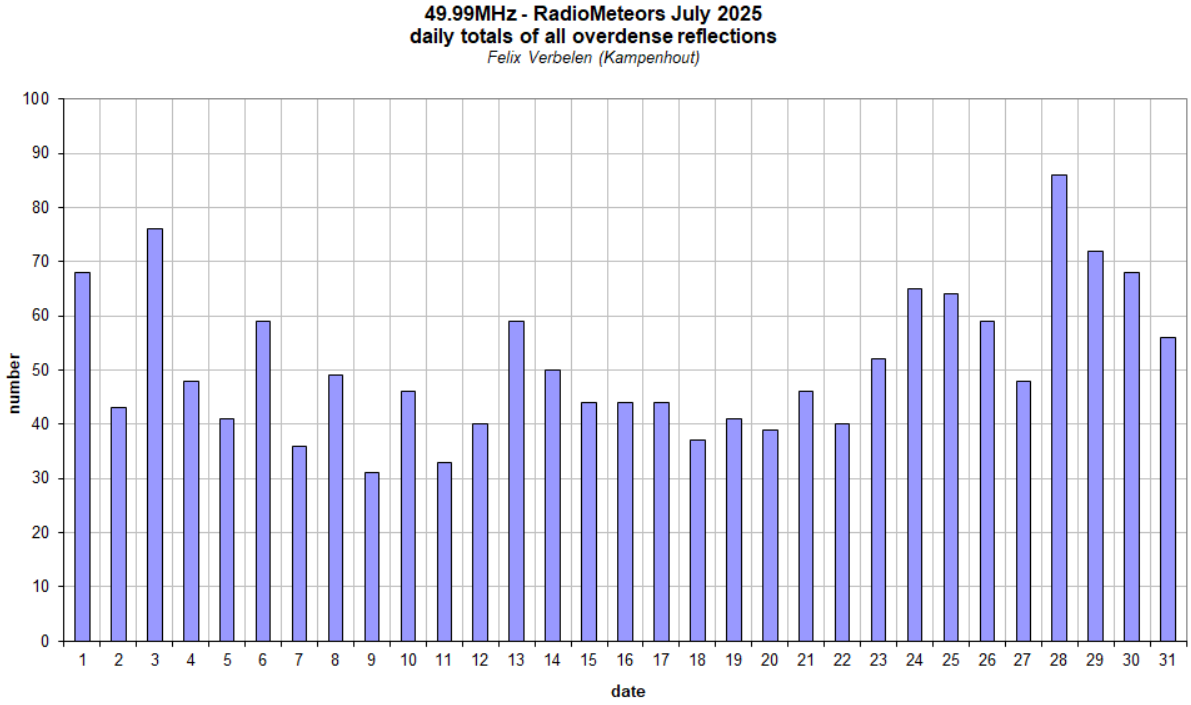

Figure 1 – The daily totals of "all" reflections counted automatically, and of manually counted "overdense" reflections, as observed here at Kampenhout (BE) on the frequency of our VVS-beacon (49.99 MHz) during July 2025.

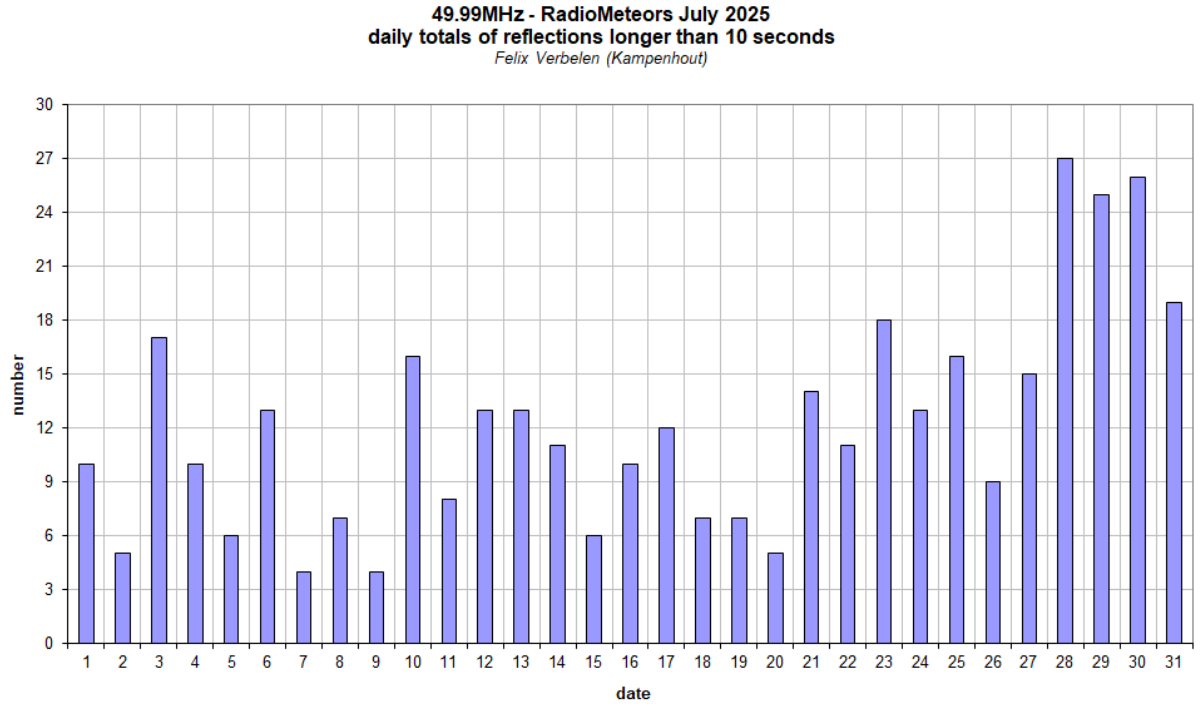

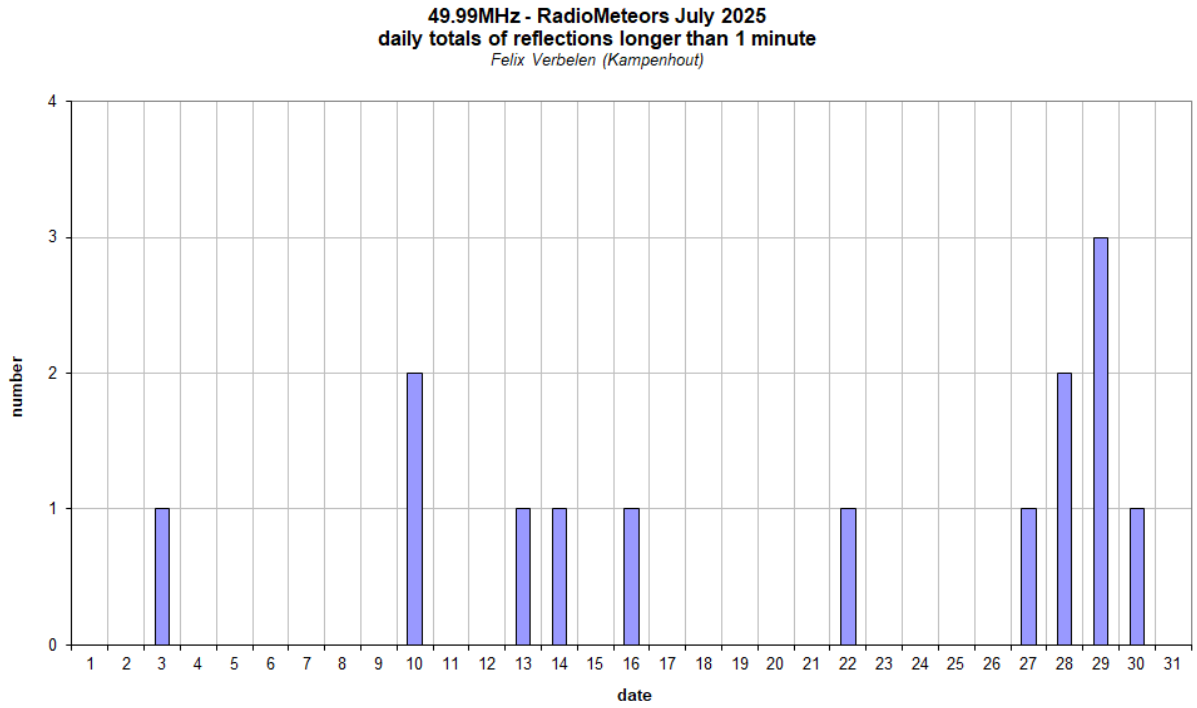

Figure 2 – The daily totals of overdense reflections longer than 10 seconds and longer than 1 minute, as observed here at Kampenhout (BE) on the frequency of our VVS-beacon (49.99 MHz) during July 2025.

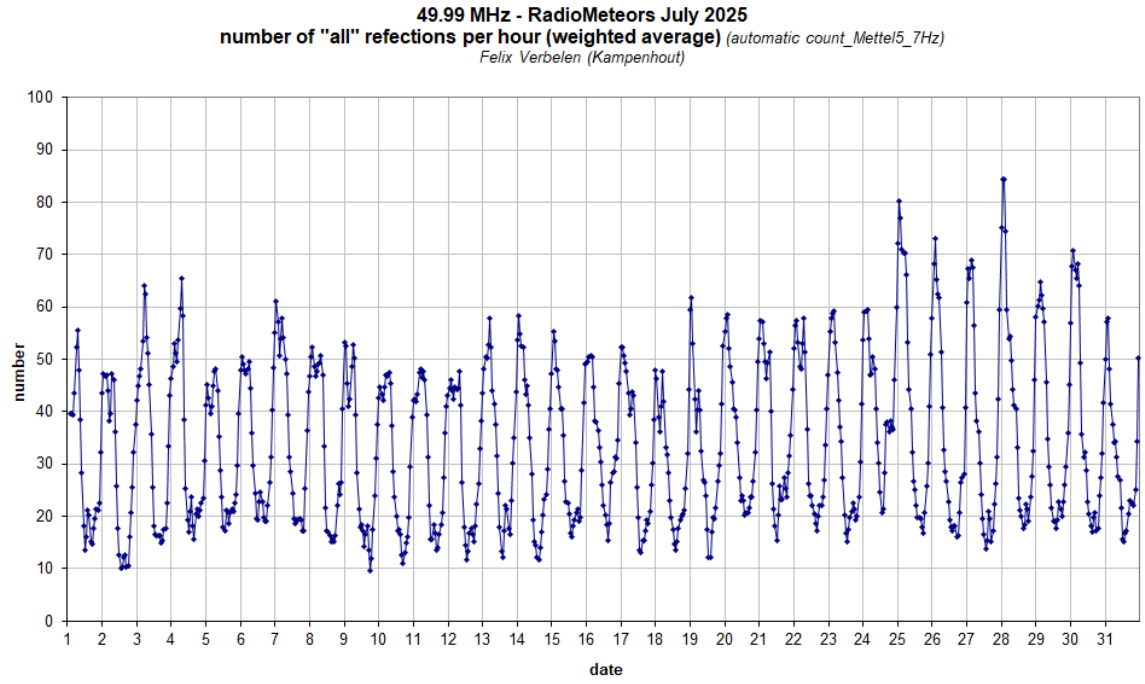

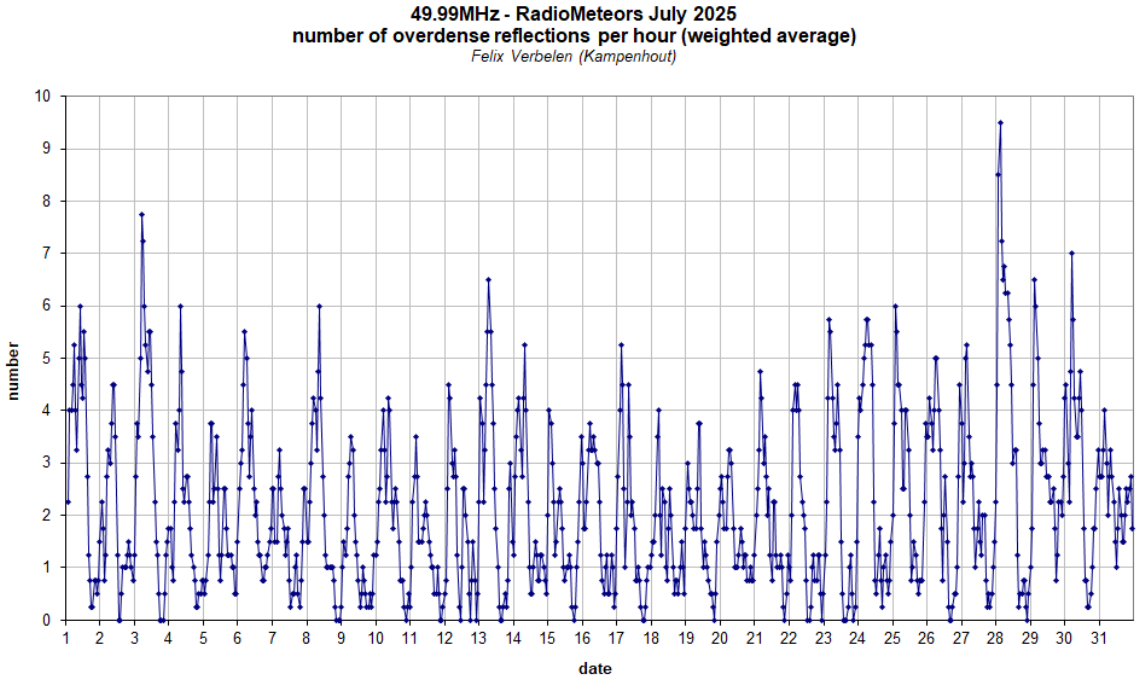

Figure 3 – The hourly numbers of "all" reflections counted automatically, and of manually counted "overdense" reflections, as observed here at Kampenhout (BE) on the frequency of our VVS-beacon (49.99 MHz) during July 2025.

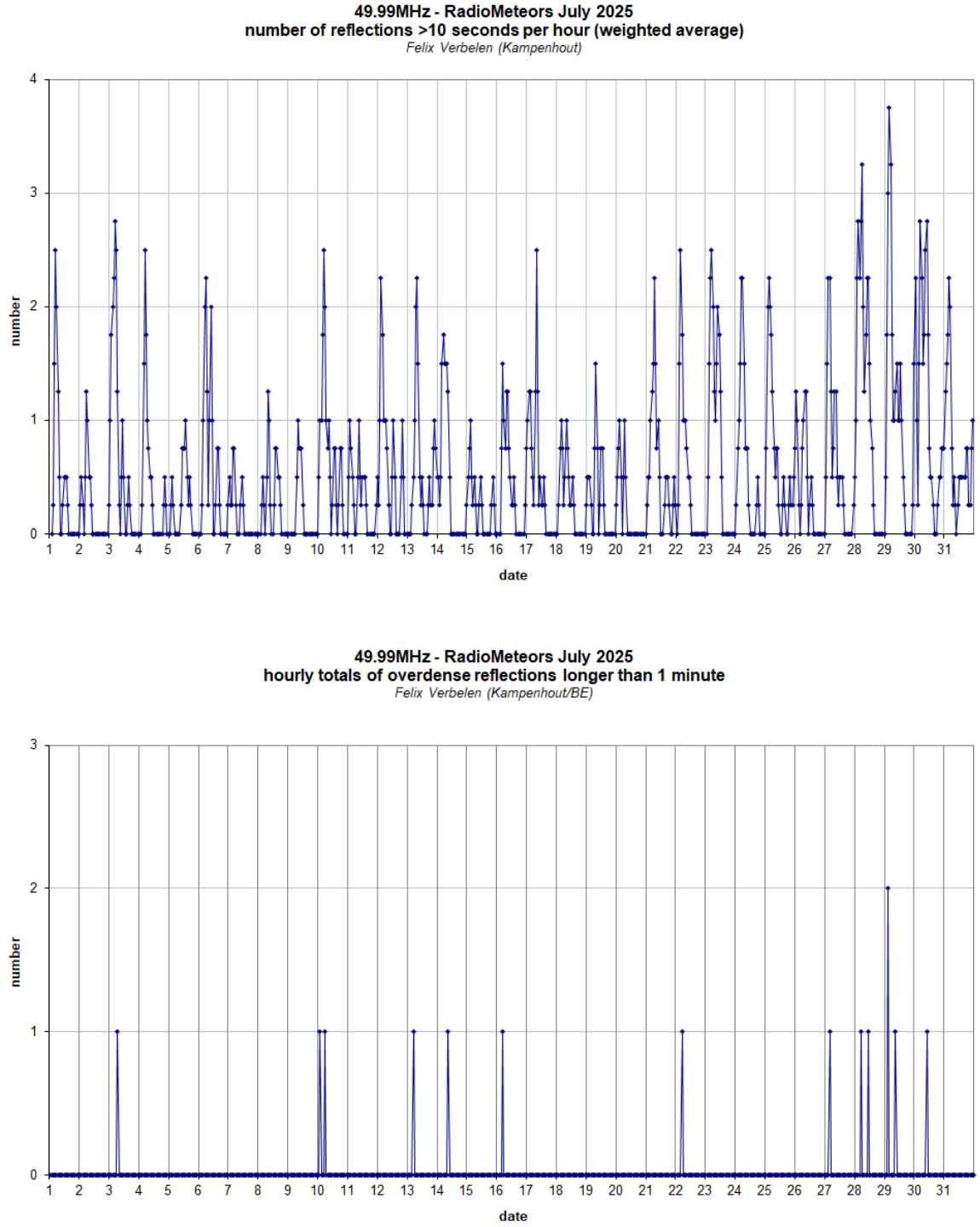

Figure 4 – The hourly numbers of overdense reflections longer than 10 seconds and longer than 1 minute, as observed here at Kampenhout (BE) on the frequency of our VVS-beacon (49.99 MHz) during July 2025.

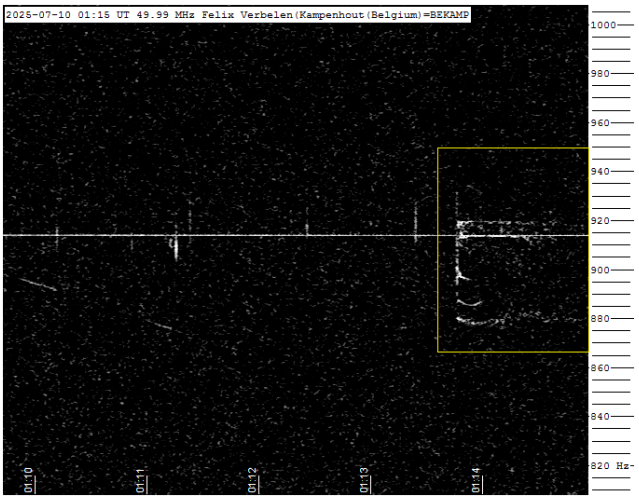

Figure 5 – Meteor echoes July 10, 1^{h}15^{m} UT.

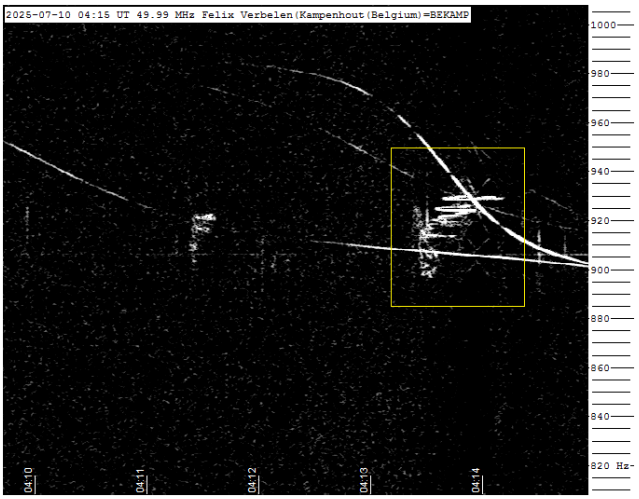

Figure 6 – Meteor echoes July 10, 4^{h}15^{m} UT.

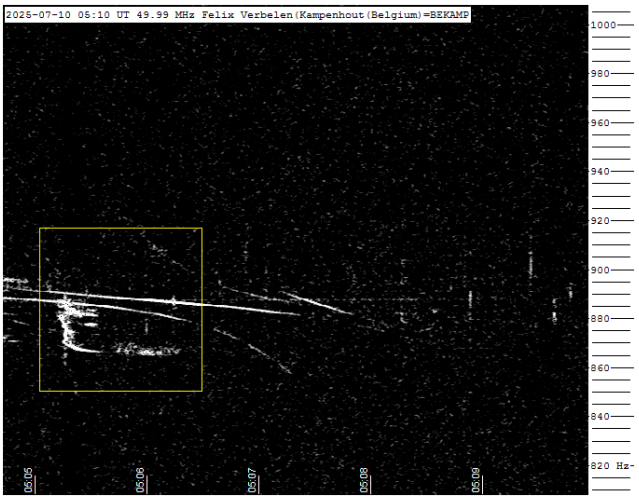

Figure 7 – Meteor echoes July 10, 5^{h}10^{m} UT.

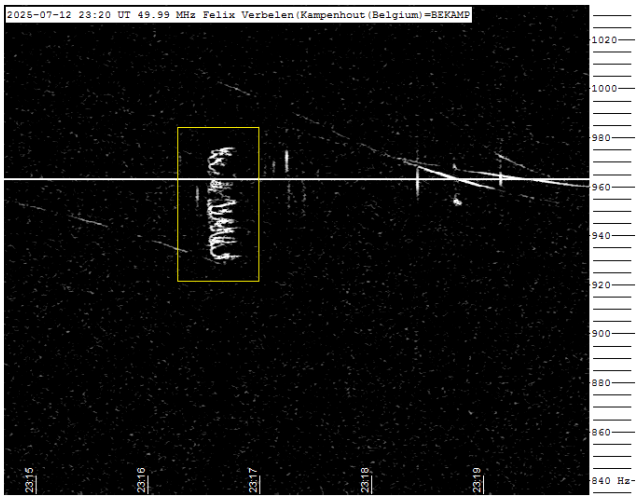

Figure 8 – Meteor echoes July 12, 23^{h}20^{m} UT.

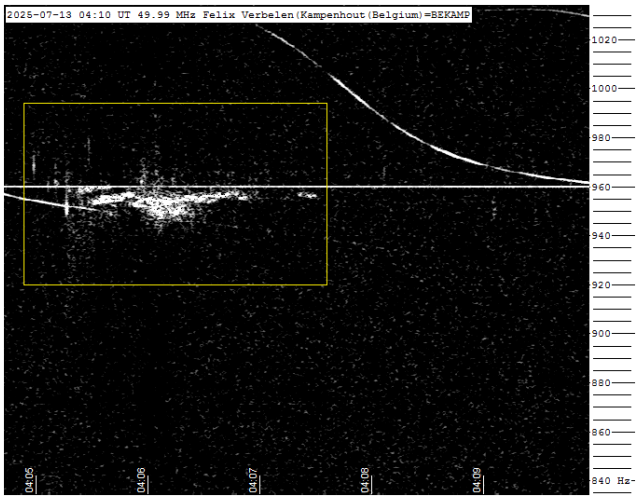

Figure 9 – Meteor echoes July 13, 4^{h}10^{m} UT.

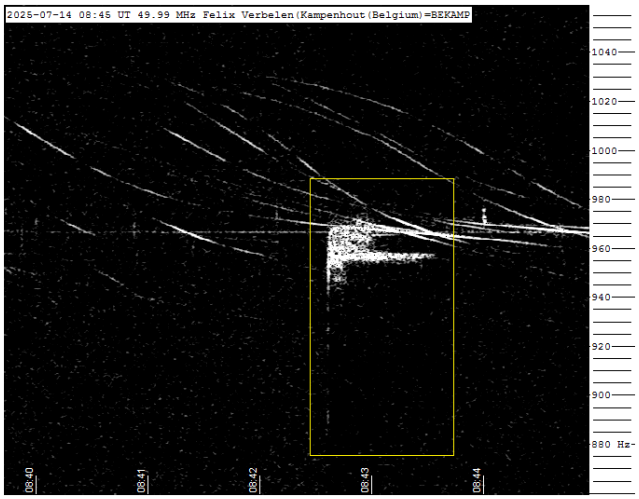

Figure 10 – Meteor echoes July 14, 8^{h}45^{m} UT.

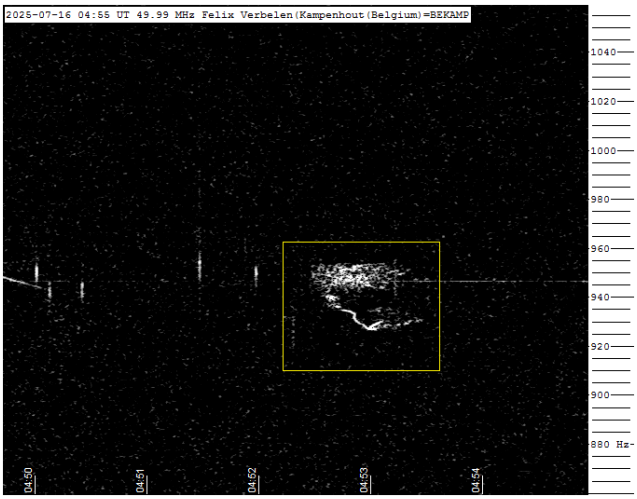

Figure 11 – Meteor echoes July 16, 4^h55^m UT.

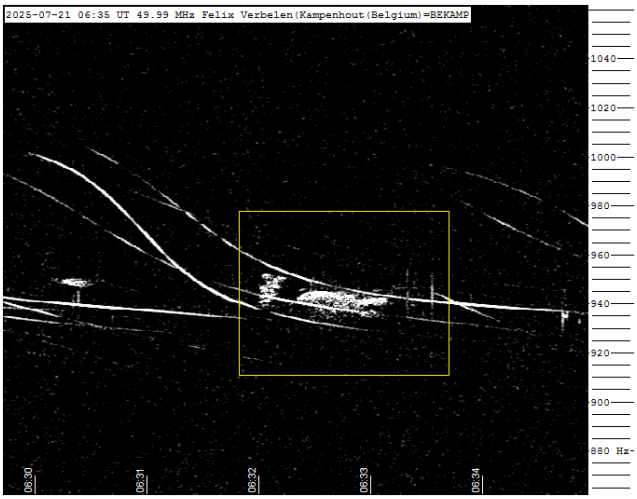

Figure 12 – Meteor echoes July 21, 6^h35^m UT.

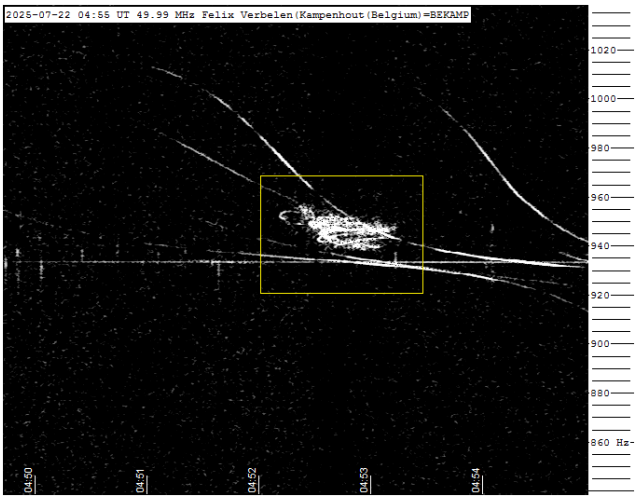

Figure 13 – Meteor echoes July 22, 4^h55^m UT.

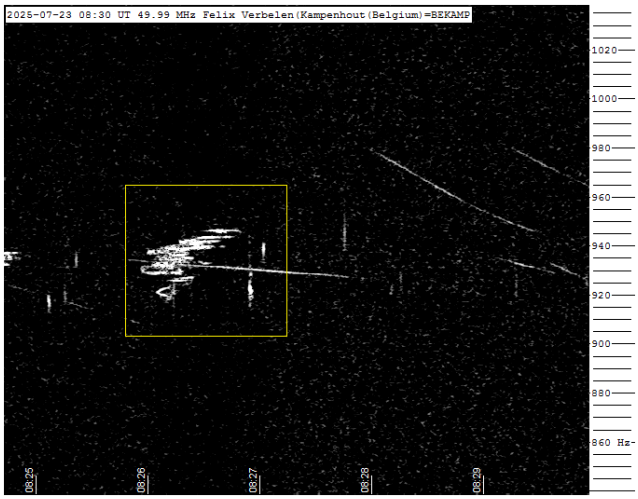

Figure 14 – Meteor echoes July 23, 8^h30^m UT.

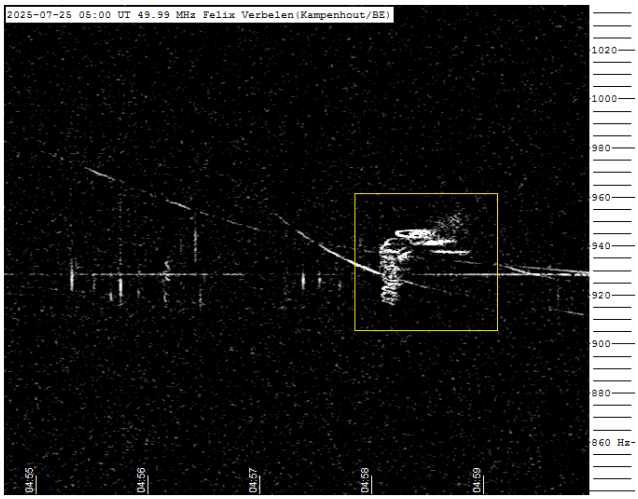

Figure 15 – Meteor echoes July 25, 5^h00^m UT.

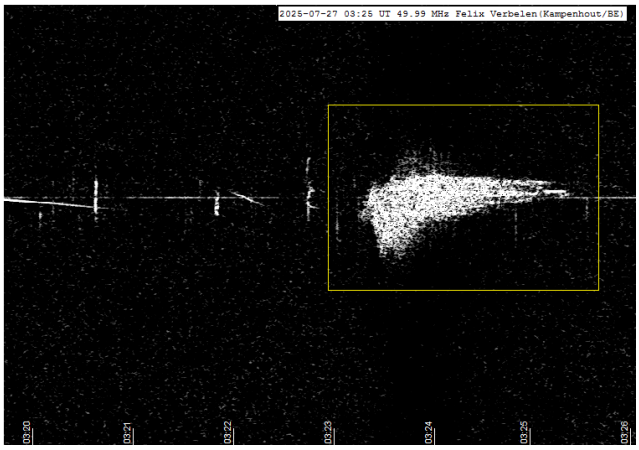

Figure 16 – Meteor echoes July 27, 3^h25^m UT.

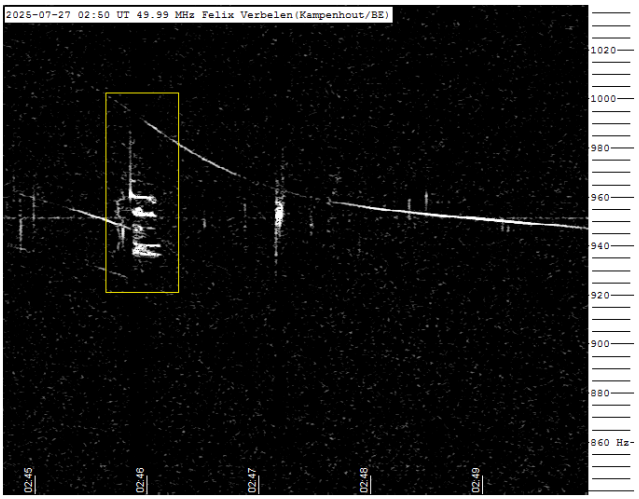

Figure 17 – Meteor echoes July 27, 2^h50^m UT.

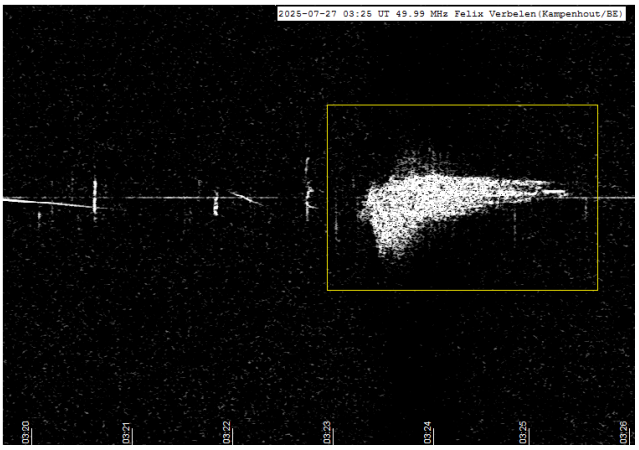

Figure 18 – Meteor echoes July 27, 3^h25^m UT.

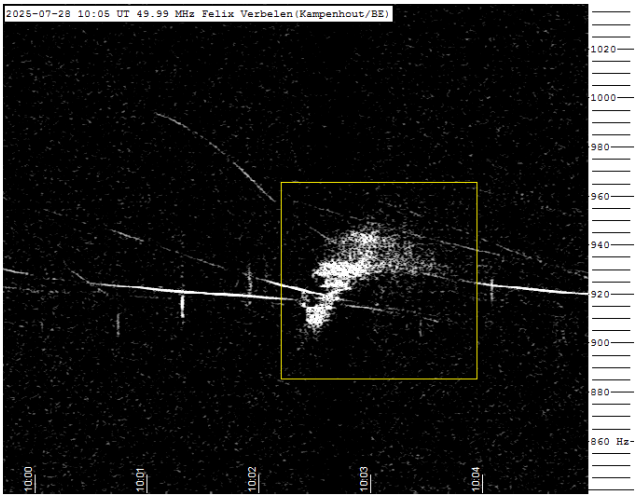

Figure 19 – Meteor echoes July 28, 10^h05^m UT.

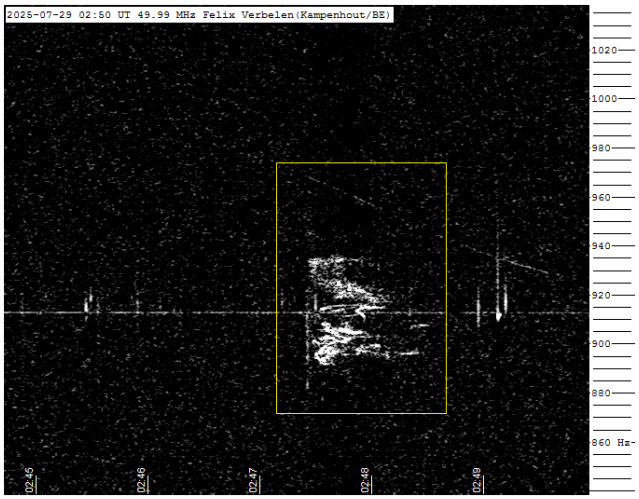

Figure 20 – Meteor echoes July 29, 2^h50^m UT.

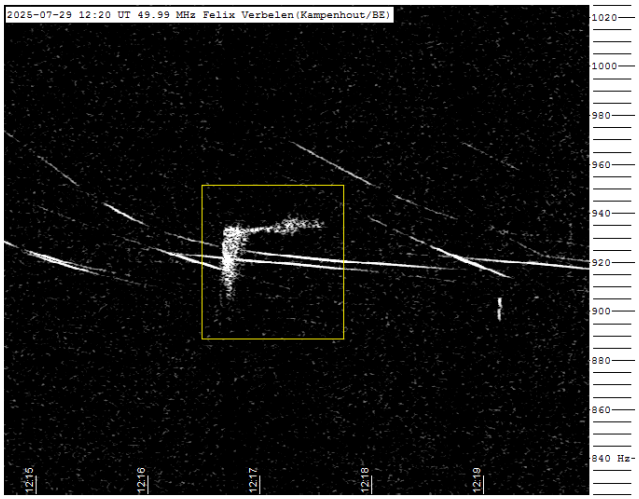

Figure 21 – Meteor echoes July 29, 12^h20^m UT.

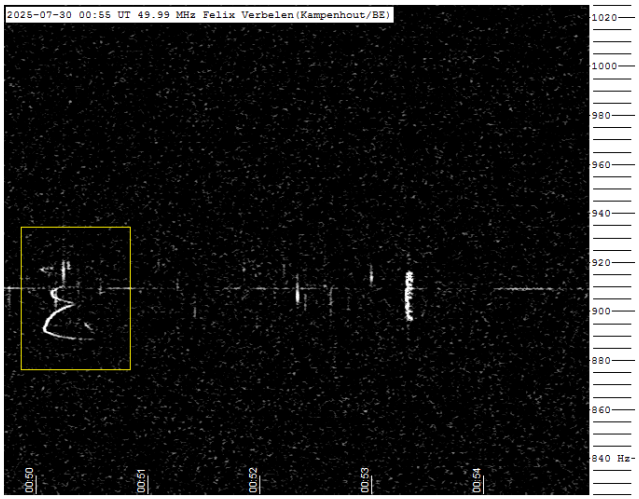

Figure 22 – Meteor echoes July 30, 0^h55^m UT.

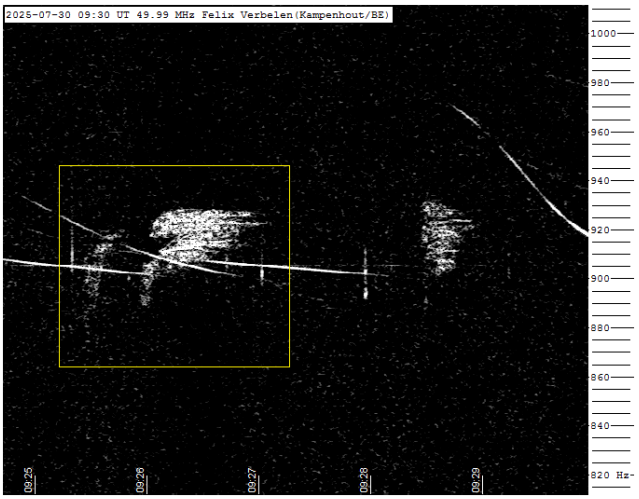

Figure 23 – Meteor echoes July 30, 9^h30^m UT.

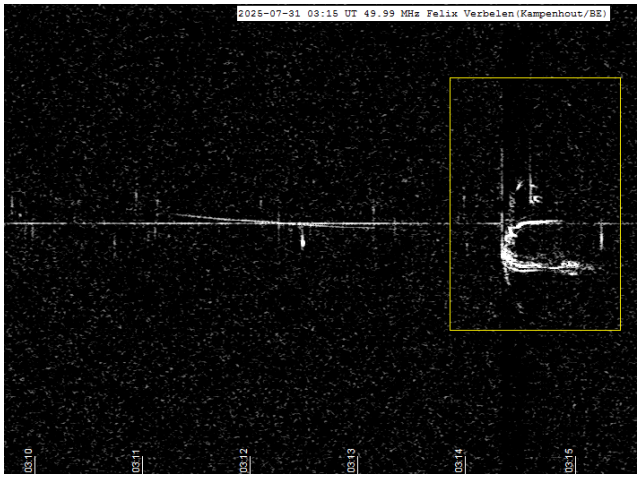

Figure 24 – Meteor echoes July 31, 9^h30^m UT.

Bright fireball observed over Brazil in July 2024

Lauriston de Sousa Trindade[1], Alfredo Dal'Ava Jr.[1], Marcelo Domingues[1], Marcelo Zurita[1,2], Gabriel Gonçalves Silva[1,3]

[1] **Brazilian Meteor Observation Network, Nhandeara, Brazil**
bramon@bramonmeteor.org

[2] **Associação Paraibana de Astronomia, João Pessoa, Brazil**
marcelozurita@gmail.com

[3] **Instituto de Química, Universidade de São Paulo, São Paulo, Brazil**
gabrielg@iq.usp.br

The Brazilian Meteor Observation Network, BRAMON, reports a bright bolide observed over Brazil on July 13, 2024.

1 Introduction

The Brazilian Meteor Observation Network (BRAMON) conducts a citizen science project, which began operations in 2014 to observe and analyze the physical properties of meteoroids, meteors, and meteorites in Brazil (Amaral et al., 2018). For this purpose, we employ an array of automated cameras. The BRAMON also provides important information about the paths of meteors and the orbits of their original meteoroids. This report describes the preliminary analysis of a bright meteor observed over Brazil at 03^h10^m UT on July 13, 2024.

2 Equipment and methods

The event presented here was recorded by multiple security cameras. None of them had initial astrometric calibration. The fields of view varied from camera to camera. We selected videos that showed the meteor's trajectory for a longer duration and where we could accurately determine the cameras' geographical locations. Part of the work was facilitated by BRAMON's partnership with the "Clima Ao Vivo" weather monitoring network, which also had several cameras in the region and captured the event. Additionally, using "Clima Ao Vivo"'s footage, we were able to work on the meteor's light curve.

3 Analysis of the 2024 July 13 event

This giant fireball was observed on July 13, 2024, at $03^h10^m36.0^s$ UT and was analyzed using videos from two cameras in the "Clima ao Vivo" weather monitoring network. Neither of the cameras had prior astrometric calibration and were located in the cities of Olindina, Bahia, and Guamaré, Rio Grande do Norte. The BRAMON was responsible for performing the astrometric calibration of the cameras' fields of view and determining the azimuths, elevations, and duration of the meteor to establish its atmospheric trajectory, light curve, and orbit before its collision with Earth (*Figures 1 and 2*).

Figure 1 – View of the bolide from the city of Olindina, BA. Image: Clima ao Vivo.

The peak brightness corresponded to an absolute magnitude of –19.0 ± 1.0. The frame of maximum brightness can be seen in *Figure 3*. An image of the Moon on March 20, 2024, with 84% illumination can be seen in *Figure 4*. None of the several videos clearly shows whether there was fragmentation along its atmospheric path. The following code was assigned for our internal control: 20240713_031036, and generally and popularly, we are referring to the event as the "Piauí Bolide". A publication containing a compilation of videos showing parts of the trajectory and intensity of the brightness can be viewed on YouTube[33]. There were hundreds of eyewitnesses to the event, mainly in the states of Piauí, Ceará, Pernambuco, and Bahia.

Figure 2 – View of the bolide from the city of Guamaré, RN. Image: Clima ao Vivo.

Figure 3 – Frame from the video recorded from the city of Olindina, BA, showing the peak brightness of the bolide.

Figure 4 – Image of the moon, 84% illuminated, as seen from the Olindina, BA. Image: Clima ao Vivo.

3.1 Atmospheric trajectory and orbital data

The meteor appeared over the city of Caridade do Piauí, at coordinates: latitude = –7.861893° and longitude = –40.976162°, at an altitude of 90.7 ± 0.5 km. The beginning of the dark flight occurred over the city of Padre Marcos, at coordinates: latitude = –7.443764 and longitude = –40.928661, at an altitude of 28.8 ± 0.5 km. The observed radiant had the following coordinates: $\alpha = 292.72°$ and $\delta = –44.51°$. The meteoroid had a speed of 13.3 km/s upon entering Earth's atmosphere. The atmospheric path of the bright trajectory can be seen in *Figure 5*.

Figure 5 – Atmospheric path of the Piauí Bolide and its ground projection.

After determining the trajectory and geocentric velocity, we were able to calculate the preliminary orbit. The orbital elements can be seen in *Table 1*. The Tisserand's parameter with respect to Jupiter $T_J = 4.58$ indicates most likely asteroidal origin.

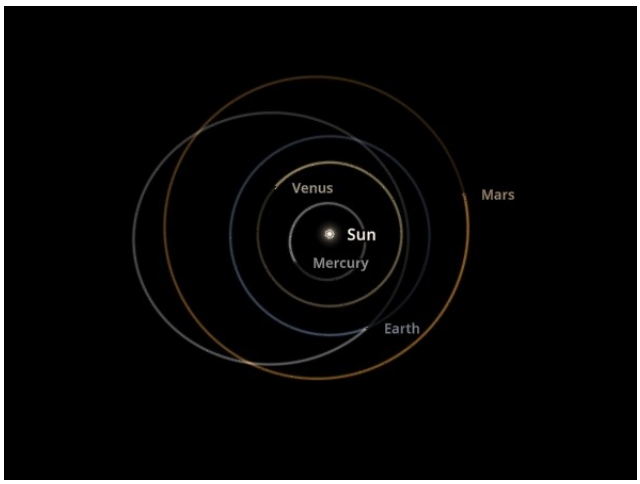

Figure 6 – Representation of the inner Solar System at the time of the Piauí Bolide event.

[33] https://www.youtube.com/watch?v=t6f2KBBbIRA

Figure 6 shows the representation of the inner solar system and the calculated orbit of the meteoroid that generated the Piauí Bolide at the moment of its collision with Earth's atmosphere.

Table 1 – Orbital data (J2000) for the meteor during its encounter with the Earth's atmosphere.

Event	20240713_031036
a (A.U.)	1.42
e	0.45
i (°)	11.0
ω (°)	73.43
Ω (°)	290.90
T_J	4.58

3.2 Comparison with the Meteor Data Center database

Based on the orbital elements, a search was conducted to verify if the Bolide's orbit matched any meteor showers already cataloged in the Meteor Data Center (MDC) database. The verification was done using three dissimilarity criteria: Southworth and Hawkins (1963), Drummond (1981), and Jopek (1993). The following thresholds were used: $D_D = 0.09$; $D_{SH} = 0.15$; and $D_H = 0.15$. No meteor showers from the MDC list showed sufficient similarity. Thus, we declare the Piauí Bolide to be part of the sporadic background.

3.3 Comparison with the JPL asteroid and comet database

The list of comets and asteroids maintained by NASA's Jet Propulsion Laboratory (JPL) was used to search for orbital similarities with the bolide recorded in Brazil. We compared the orbit of the meteoroid that generated the Piauí Bolide with 30509 interplanetary objects. The following thresholds were used for the search: $D_{SH} < 0.1$; $D_D < 0.05$; and $D_H < 0.1$. *Table 2* shows the results of the objects with at least one criterion being met.

Table 2 – Objects with at least one dissimilarity criterion met in comparison with the Piauí Bolide, the Tisserand's parameter with respect to Jupiter is listed too.

Object	D_{SH}	D_D	D_H	Tj
2006 OK3	0.087	–	0.086	4.05
2021 NY3	0.091	0.043	0.082	4.45
2019 NK2	–	0.043	–	4.55
2005 XA8	–	0.045	–	4.60
2014 YW34	–	0.047	–	4.63
2023 XN16	–	0.047	–	4.52
2010 AK	–	–	0.078	4.00
2023 N2	–	–	0.080	4.53
2019 OX44	–	–	0.092	4.02
2012 XF133	–	–	0.098	4.41

3.4 Satellite image

The Geostationary Lightning Mapper (GLM) is a satellite-based detector designed for near-infrared optical transients. It is positioned aboard the GOES-16 satellite in geostationary orbit, enabling continuous monitoring of a specific area, including Brazil. This setup allows GLM to achieve unprecedented lightning detection rates from space. Operating day and night, GLM detects all types of lightning with high spatial resolution and efficiency. *Figure 7* shows the frame where we have the record of the flash generated by the bolide (meteor flare 20240713_031036).

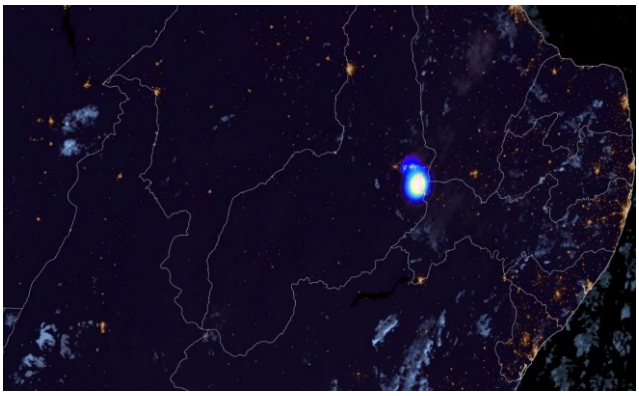

Figure 7 – Detail of the GOES-16 GLM system image, on July 13th at 03^h10^m UT, showing detection of the meteor flare 20240713_031036.

3.5 Impact energy

The CNEOS catalog includes the geocentric velocity components and geographic coordinates for bolides detected by U.S. government sensors. The event 20240713_031036 is recorded with the following peak brightness timestamp: 2024–07–13 $03^h10^m41^s$, with geographic coordinates: 7.4°S and 41.0°W. No disclosure was made regarding the calculation of the velocity vector components. The energy calculated by CNEOS for the event was equivalent to 1.5 kt. Considering the calculated velocity of 13.3 km/s, the meteoroid that generated the bolide would have had an initial mass of approximately 62 tons. *Figure 8* shows the event's location on the CNEOS Fireball infrasound recording map.

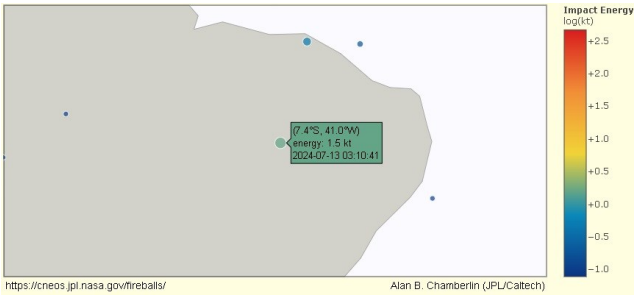

Figure 8 – CNEOS map with the marking of the Piauí Bolide event.

4 Conclusion

The bolide from Piauí was recorded by several security cameras in various states of northeastern Brazil. None of them provided astrometric calibration. All astrometry work was done based on the georeferencing of these cameras and

analysis of the recorded landscapes. We can estimate that the bolide was generated by a small asteroid, weighing approximately 62 tons and with a diameter of just under 3 meters. It entered the atmosphere at a speed of 13.3 km/s and traveled 55 km before the dark flight. Dissimilarity tests did not indicate equivalence with already cataloged meteor showers. Other asteroids that have some orbital similarities were indicated based on D_D, D_{SH}, and D_H tests. However, such similarities are not conclusive. Since fireball reports were implemented by the monitoring system of the United States of America, the Piauí Bolide has been the most energetic event recorded over Brazilian soil. With hundreds of witnesses, the bolide sparked the interest of thousands of Brazilians about meteorites and motivated several expeditions of meteorite hunters to the city of Padre Marcos, in the state of Piauí. Today, one year after the event, no meteorite associated with this event has been located.

References

Amaral L. S., Trindade L. S., Bella C. A. P. B., Zurita M. L. P. V., Poltronieri R. C., Silva G. G., Faria C. J. L., Jung C. F., and Koukal J. A. (2018). "Brazilian Meteor Observation Network: History of creation and first developments". In Gyssens M. and Rault J.-L., editors, *Proceedings of the International Meteor Conference*, Petnica, Serbia, 21–24 September, 2017. IMO, pages 171–175.

Drummond J. D. (1981). "A test of comet and meteor shower associations". *Icarus*, **45**, 545–553.

Jopek T. J. (1993). "Remarks on the meteor orbital similarity D-criterion". *Icarus*, **106**, 603–607.

Southworth R. R. and Hawkins G. S. (1963). "Statistics of meteor streams". *Smithson. Contrib. Astrophys*., **7**, 261–286.

eMetN METEOR JOURNAL

Since 2016 the mission of eMetN Meteor Journal is to offer meteor news to a global audience and to provide a swift exchange of information in all fields of active amateur meteor work. eMetN Meteor Journal is freely available without any fees. eMetN Meteor Journal is independent from any country, society, observatory or institute. Articles are abstracted and archived with ADS Abstract Service: https://ui.adsabs.harvard.edu/search/q=eMetN

You are welcome to contribute to eMetN Meteor Journal on a regular or casual basis, if you wish to. Anyone can become an author or editor, for more info read: https://www.emeteornews.net/writing-content-for-emeteornews/

Articles for eMetN Meteor Journal should be submitted to: paul.roggemans@gmail.com

Contact: info@emeteornews.net

Contributors:

- Aitov A.
- Barbieri L.
- Campell-Burns P.
- Dal'Ava Jr. A.
- de Sousa Trindade L.
- Domingues M.
- Gonçalves Silva G.
- Harachka Y.
- Madiedo J.
- Maglione M.
- Miskotte K.
- Rivato W.
- Roggemans P.
- Šegon D.
- Verbelen F.
- Vida D.
- Wood J.
- Zurita M.

Online publication https://www.emeteornews.net and https://www.emetn.net
ISSN 3041-4261, publisher: Paul Roggemans, Pijnboomstraat 25, 2800 Mechelen, Belgium